THE UNIVERSITY OF QUEENSLAND

SCHOOL OF CIVIL ENGINEERING

REPORT CH86/12

AIR ENTRAINMENT AND ENERGY DISSIPATION ON A 8.9° SLOPE STEPPED SPILLWAY WITH FLAT AND POOLED STEPS

AUTHORS: Stefan FELDER, Christopher FROMM and Hubert CHANSON

HYDRAULIC MODEL REPORTS

This report is published by the School of Civil Engineering at the University of Queensland. Lists of recently-published titles of this series and of other publications are provided at the end of this report. Requests for copies of any of these documents should be addressed to the Civil Engineering Secretary.

School of Civil Engineering
The University of Queensland
Brisbane QLD 4072
AUSTRALIA

Telephone: (61 7) 3365 4163
Fax: (61 7) 3365 4599

URL: http://www.eng.uq.edu.au/civil/

First published in 2012 by
School of Civil Engineering
The University of Queensland, Brisbane QLD 4072, Australia

ISBN No. 9781742720531

The University of Queensland, St Lucia QLD

Air Entrainment and Energy Dissipation on a 8.9° Slope Stepped Spillway with Flat and Pooled Steps

by

Stefan FELDER

PhD student, The University of Queensland, School of Civil Engineering, Brisbane QLD 4072, Australia

Christopher FROMM

Student, RWTH Aachen University, Institute of Hydraulic Engineering and Water Resources Management, Aachen 52056, Germany

and

Hubert CHANSON

Professor, The University of Queensland, School of Civil Engineering, Brisbane QLD 4072, Australia, Email: h.chanson@uq.edu.au

REPORT No. CH86/12

ISBN 9781742720531

School of Civil Engineering, The University of Queensland, May 2012

Pooled stepped storm waterway besides to a railway bridge - Dimensions: 1:1 slope, h = 0.7 to 1 m, w =0.4 m - Note the concrete wall at downstream end to protect nearby road from splashing

Abstract

Stepped spillways were investigated experimentally in the last few decades. Although some recent research focused on the air-water flow properties, there is a knowledge gap for an optimum stepped spillway design in terms of energy dissipation and aeration performances. To date the flat stepped spillway design was tested, although only a few studies investigated the air-water flows on flat pooled stepped spillways. Herein a physical study was performed on a stepped spillway model with a 8.9° slope and step heights of 0.05 m. Three stepped configurations were tested: a flat stepped chute, a pooled step chute (w/h=1) and a chute with an alternation of flat and pooled steps. Detailed air-water flow measurements were conducted for all three stepped configurations for a broad range of discharges 0.02 $m^3/s \leq Q \leq 0.117$ m^3/s corresponding to Reynolds numbers between 1.4×10^5 and 9.3×10^5. The visual observations showed some typical flow pattern on the flat stepped spillway with nappe, transition and skimming flows depending upon the flow rate. On the pooled stepped spillway configurations, some strong instabilities were observed in the transition flow regime. These self-induced instabilities were associated with unsteady cavity recirculation and ejection processes as well as some strong jump waves propagating downstream. For the stepped spillway with combination of flat and pooled steps, no skimming flow regime was achieved within the investigated flow conditions. A comparison of air-water flow properties showed some basic differences between the three configurations in terms of void fraction, bubble count rate, interfacial velocity, turbulence intensity and chord size distributions. The results in terms of the rate of energy dissipation and residual head showed the largest rate of energy dissipation and the smallest residual head for the stepped spillway with combination of flat and pooled steps. The Darcy-Weisbach friction factor was the smallest for the flat stepped spillway and the largest for the pooled stepped spillway configurations. While the stepped chute configuration with an alternation of flat and pooled steps yielded the largest rate of energy dissipation, the geometry must not be regarded as an optimum design because this configuration was characterised by some strong flow instabilities and unsteady flow processes which are unsuitable for a safe operation of the spillway system.

Keywords: Air-water flows, Self-induced instabilities, Pooled stepped spillway, Stepped spillway, Energy dissipation, Residual head, Flow resistance, Turbulence.

TABLE OF CONTENTS

LIST OF SYMBOLS

The following symbols are used in this report:

C	void fraction defined as the volume of air per unit volume of air and water; it is also called air concentration or local air content;
C_{mean}	depth-average void fraction defined in terms of Y_{90}: $C_{mean} = 1 - d/Y_{90}$;
D_H	hydraulic diameter (m);
D_o	dimensionless constant;
d	equivalent clear water flow depth (m);
$\bar{d}$	average equivalent clear water flow depth (m) for stepped spillway with combination of flat and pooled steps;
d_c	critical flow depth (m): $d_c = \sqrt[3]{q_w^2 / g}$;
F	air bubble count rate or bubble frequency (Hz) defined as the number of detected air bubbles per unit time;
F_{max}	maximum bubble count rate in a cross-section (Hz);
f_e	equivalent Darcy-Weisbach friction factor in air-water flows;
$\bar{f}_e$	average equivalent Darcy-Weisbach friction factor for stepped spillway with combination of flat and pooled steps;
g	gravity constant (m/s^2);
H	total head (m);
H_{dam}	dam height (m);
H_{max}	maximum upstream head (m) above chute toe: $H_{max} = H_{dam} + 3/2 \times d_c$;
H_{res}	residual head (m);
h	vertical step height (m);
K'	dimensionless integration constant;
k_s	step cavity roughness height (m): $k_s = (h+w) \times \cos\theta$;
L_I	longitudinal distance (m) measured from the weir crest to the inception point of free-surface aeration;
l	horizontal step length (m);
l_w	pool weir length (m);
N	power law exponent;
Q	water discharge (m^3/s);
q_w	water discharge per unit width (m^2/s);
Re	Reynolds number defined in terms of the hydraulic diameter: $Re = \rho_w \times U_w \times D_H / \mu_w$;
R_{xx}	normalised auto-correlation function (reference) probe;
R_{xy}	normalised cross-correlation function between two probe output signals;
$(R_{xy})_{max}$	maximum cross-correlation between two probe output signals;
S_f	friction slope: $S_f = - \partial H / \partial x$;
$\bar{S}_f$	average friction slope for stepped spillway with combination of flat and pooled steps;
T	time lag (s) for which $R_{xy} = (R_{xy})_{max}$;

Tu	turbulence intensity;
Tu_{max}	maximum turbulence intensity in a cross-section;
$T_{0.5}$	characteristic time lag τ for which $R_{xx} = 0.5$;
t	time (s);
U_w	mean flow velocity (m/s): $U_w = q_w/d$;
$\overline{U}_w$	average mean flow velocity (m/s) for stepped spillway with combination of flat and pooled steps;
V	interfacial velocity (m/s);
V_c	critical flow velocity (m/s);
V_{90}	characteristic interfacial velocity (m/s) where the void fraction is 90%;
W	channel width (m);
w	weir height in pooled stepped spillway configuration (m), also called pool height;
x	distance along the channel bottom (m);
Y_{90}	characteristic depth (m) where the void fraction is 90%;
y	distance (m) measured normal to the invert (or channel bed);
ΔH	total head loss (m): $\Delta H = H_{max} - H_{res}$;
Δx	streamwise separation distance (m) between probe sensors;
Δz	transverse separation distance (m) between probe sensors;
Δz_o	height (m) to the weir crest from the calculated step edge;
ρ	density (kg/m^3);
θ	angle between pseudo-bottom formed by the step edges and the horizontal;
τ	time lag (s);
$\tau_{0.5}$	characteristic time lag τ for which $R_{xy} = 0.5 \times (R_{xy})_{max}$;
Ø	probe sensor diameter (m);
μ	dynamic viscosity (Pa.s);

Subscript

c	critical flow conditions;
max	maximum value;
mean	mean signal component;
xx	auto-correlation of reference probe signal;
xz	cross-correlation;
w	water properties;

Abbreviations

IWW	Institute of Hydraulic Engineering and Water Resources Management, RWTH Aachen University, Germany;
PDF	probability density function;
RWTH	Rheinisch-Westfaelische Technische Hochschule (University of Aachen), Germany;
SK	skimming flow regime;

TRA	transition flow regime;
UQ	The University of Queensland, Australia.

1. INTRODUCTION

1.1 AIR-WATER FLOWS ON STEPPED SPILLWAYS

Air-water flows on stepped spillways were investigated experimentally in the last few decades (e.g. HORNER 1969; PEYRAS et al 1992; CHANSON 1995,2001; OHTSU & YASUDA 1997; CHAMANI & RAJARATNAM 1999; BOES 2000; MATOS 2001; TOOMBES 2002). The research provided design guidelines for stepped spillway channels with various channel geometries and slopes. Most recent research focused on the air-water flow properties and energy dissipation performances, including some more detailed air-water flow properties such as bubble count rate, turbulence and microscopic air-water properties (e.g. CHANSON & TOOMBES 2002; GONZALEZ 2005; CHANSON & CAROSI 2007; TOOMBES and CHANSON 2008a,b; FELDER & CHANSON 2009b,2011a). Numerical modelling of stepped spillway flows has not been successful yet despite some studies in the clear water flow region (CHENG et al. 2006; QIAN et al. 2009; MEIRELES et al. 2009). There is a knowledge gap for an optimum stepped spillway design in terms of energy dissipation and aeration performances.

To date the stepped spillway design with flat steps was extensively tested, and only a few studies investigated the air-water flows on pooled stepped spillways (Fig. 1-1) (Table 1-1). Table 1-1 lists a number studies on pooled stepped spillways encompassing detailed air-water flow measurements. KÖKPINAR (2004) conducted experiments on a stepped spillway with 30° with three different configurations: flat, pooled and combination of flat and pooled steps. A similar study was conducted by ANDRÉ (2004) who investigated further modifications of the pooled stepped spillway design with two channel slopes. A study of self-induced instabilities on pooled stepped spillways with slopes of 8.9° and 14.6° was conducted by THORWARTH & KOENGETER (2006) and THORWARTH (2008). All the studies provided some new insights into the flow processes on pooled stepped spillways although limited.

1.2 OUTLINE OF THE REPORT

The present study investigated systematically the air-water flow properties and the energy dissipation performances down a 8.9° slope stepped chute with three stepped spillway configurations: flat, pooled and combination of flat and pooled steps (Table 1-1). The flow patterns were observed for all configurations. A comparative study was conducted in terms of the air-water flow properties, i.e. void fraction, bubble count rate, interfacial velocity, turbulence intensity and chord sizes, as well as energy dissipation and flow resistance. The study aimed to provide some novel details on the pooled stepped spillway design and its energy dissipation performance and flow resistance capabilities in comparison to a flat stepped spillway on a moderate slope.

In Section 2, the experimental facility, the instrumentation and the flow conditions are introduced. Section 3 focuses upon the presentation of the air-water flow pattern including the instationary processes on the pooled stepped spillway configurations. A comparative study of flow properties is presented in Section 4. Section 5 shows the performance of the investigated configurations in terms of energy dissipation, residual head and flow resistance. A brief conclusion is given in Section 6. Some additional data sets are presented in the Appendices.

Table 1-1 – Experimental studies of air-water flow properties on pooled stepped spillway configurations

Reference (1)	θ (°) (2)	Step geometry (3)	Flow conditions (4)	Instrumentation (5)	Comment (6)
KÖKPINAR (2004)	30	Flat steps: h = 6 cm, l = 10.4 cm Pooled steps: h = 6 cm, l = 10.4 cm, w = 3 cm Combination of flat/pooled steps: h = 6 cm, l = 10.4 cm, w = 3 cm	Q = 0.03 – 0.100 m^3/s, Re =2.4×10^5 – 8.0×10^5	Double-tip fibre-optical probe (Ø = 0.08 mm)	W = 0.5 m, 64 steps, l_w = 2.6 cm
ANDRÉ (2004)	18.6	Flat steps: h = 6 cm, l = 17.8 cm Pooled steps: h = 6 cm, l = 17.8 cm, w = 3 cm Combination of flat/pooled steps: h = 6 cm, l = 17.8 cm, w = 3 cm	Q = 0.02 – 0.130 m^3/s, Re =1.6×10^5 – 1.0×10^6	Double-tip fibre-optical probe (Ø = 0.08 mm)	W = 0.5 m, 42/64 steps, l_w = 2.6 cm
	30	Flat steps: h = 6 cm, l = 10.4 cm Pooled steps: h = 6 cm, l = 10.4 cm, w = 3 cm Combination of flat/pooled steps: h = 6 cm, l = 10.4 cm, w = 3 cm			
THORWARTH (2008)	8.9	Pooled steps: h = 5 cm, l = 31.9 cm, w = 0 – 5 cm	Q = 0.025 – 0.117 m^3/s, Re =2.0×10^5 - 9.3×10^5	Double-tip conductivity probe (Ø = 0.13 mm)	W = 0.5 m, 22/26 steps, l_w = 1.5 cm
	14.6	Pooled steps: h = 5 cm, l = 19.2 cm, w = 0 – 5 cm			
Present study	8.9	Flat steps: h = 5 cm, l = 31.9 cm	Q = 0.018 – 0.117 m^3/s, Re =1.4×10^5 - 9.3×10^5	Double-tip conductivity probe (Ø = 0.25 mm)	W = 0.5 m, 21 steps, l_w = 1.5 cm
		Pooled steps: h = w = 5 cm, l = 31.9 cm	Q = 0.027 – 0.117 m^3/s, Re =2.2×10^5 - 9.3×10^5		
		Combination of flat/pooled steps: h = w = 5 cm, l = 31.9 cm	Q = 0.027 – 0.117 m^3/s, Re =2.2×10^5 - 9.3×10^5		

Notes: θ: channel slope; h: step height; l: step length; w: weir height; l_w: pool weir length; W: Channel width; Q: water discharge; Re: Reynolds number defined in terms of the hydraulic diameter.

Fig. 1-1 - Photographs of pooled stepped spillways and cascades

(A) Sorpe dam stepped spillway - Construction: 1926-1935, H_{dam} = 69 m, design discharge: 46 m^3/s (Left) Looking downstream on 31 Mar. 2004 (Photograph Hubert CHANSON); (Right) Cascade operation at low flow during the early 2000s (Courtesy of Ruhrverband, Essen, Germany)

(B) Pooled stepped storm waterway besides to a railway bridge near Avignon (France) on 20 Sept. 2000 - Dimensions: 1:1 slope, h = 0.7 to 1 m, w =0.4 m - Note the concrete wall at downstream end to protect nearby road from splashing

(C) Pooled stepped cascade of the Bosquet des Rocailles, Jardins du Château de Versailles (France) on 27 July 2008 (Shutter speed: 1/500s)

2. EXPERIMENTAL FACILITY, INSTRUMENTATION AND SIGNAL PROCESSING

2.1 EXPERIMENTAL FACILITY

The experimental study was conducted on a large size stepped spillway model at the Institute of Hydraulic Engineering and Water Resources Management (IWW) of the RWTH Aachen (Germany). The facility had a length of 12 m and consisted of an intake tank which provided a constant upstream water head. The water entered the experimental test section through an uncontrolled broad-crested weir of 0.5 m width (Fig. 2-1). Fig. 2-1 illustrates the broad-crested weir at the upstream end of the stepped spillway test section. The test section consisted of 21 steps made out of PVC with step heights h = 0.05 m, step width W = 0.50 m and of step length l = 0.319 m (i.e. channel slope $\theta = 8.9°$). At the downstream end of the stepped chute, a hydraulic jump dissipated the energy in a long channel. The discharge was measured at the end of the downstream channel using an ultrasonic range finder and a sharp-crested weir. More details about the experimented facility were described by THORWARTH & KOENGETER (2006) and by THORWARTH (2008) who conducted a detailed study of self-induced instabilities on the pooled stepped spillway model at IWW.

Three different stepped spillway configurations were investigated (Fig. 2-2). Figure 2-2 illustrates the experimental configurations including a stepped spillway equipped with flat steps (Fig. 2-2A) and a pooled stepped spillway with weir height of w = 5 cm and pool weir thickness l_w = 1.5 cm (Fig. 2-2B). The third configuration was a stepped spillway with a combination of flat and pooled steps (Fig. 2-2C).

Fig. 2-1 - Broad crested weir at the upstream end: looking downstream - Configuration with flat steps: $\theta = 8.9°$, $d_c/h = 0.95$, $Q = 0.016$ m^3/s, $Re = 1.28 \times 10^5$

Fig. 2-2 – Stepped spillway configurations in the present study (θ = 8.9°)

(A) Flat stepped spillway

(B) Pooled stepped spillway

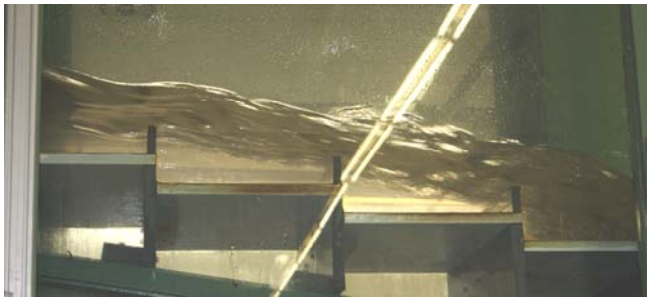

(C) Combination of flat and pooled steps

2.2 PHASE DETECTION INTRUSIVE PROBE AND SIGNAL PROCESSING

An extensive set of experiments was conducted with all three configurations for a wide range of discharges 0.018 $m^3/s < Q < 0.117$ m^3/s. The measurements were performed using a double-tip conductivity probe (Fig. 2-3). The probe was typically located at step edges in the air-water flow region. Figure 2-3 shows the double-tip conductivity probe. The probe had an inner diameter Ø = 0.13 mm for both tips which were separated in the streamwise direction Δx = 5.1 mm and in transverse direction Δz = 1 mm. The probe was designed at IWW and successfully used by THORWATH (2008) and BUNG (2009,2011). The translation of the conductivity probe in the vertical direction was controlled by a trolley system equipped with an (isel®) control device.

Fig. 2-3 – Double-tip conductivity probe (Ø = 0.13 mm); Flow from right to left

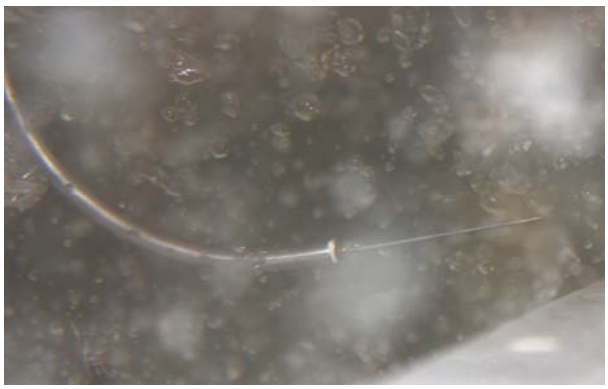

All measurements were conducted for 45 s at a sampling rate of 20 kHz per probe tip. The raw data were recorded with a LabVIEW^{TM} software. A Fortran program was used to calculate the full set of air-water flow properties from the raw probe signal. The program was developed at UQ and previously used in a number of air-water flow studies on a stepped spillway (FELDER & CHANSON 2011a,b) and in hydraulic jump (CHACHEREAU & CHANSON 2011). The air-water flow calculations included the void fraction C (i.e. air concentration), the bubble count rate F defined as the number of bubbles/droplets detected by a leading probe sensor per unit time, the time-averaged interfacial velocity V calculated by a cross-correlation analysis and the turbulence intensity Tu. Further microscopic properties included the air bubble and water droplet chord sizes which were a measure of the characteristic air/water size in streamwise direction.

2.3 EXPERIMENTAL FLOW CONDITIONS

The experiments were conducted for a broad range of discharges at several step edges downstream of the inception point of free surface aeration. Table 2-1 summarises the experimental flow conditions for the three investigated configurations in the present study.

Table 2-1 - Experimental investigations of the stepped spillway flows for three different configurations at the IWW ($\theta = 8.9°$)

Configuration (1)	d_c/h [-] (2)	Q [m^3/s] (3)	Re [-] (4)	Investigation (5)	Comment (6)
Flat stepped spillway	1.0 – 3.55	0.018 - 0.117	1.4×10^5 - 9.3×10^5	Air-water flow measurements with double-tip conductivity probe	Air-water flow properties
	0.24 – 3.55	0.002 - 0.117	1.6×10^4 - 9.3×10^5	Visual observations	Flow pattern
Pooled stepped spillway	1.35 – 3.55	0.027 - 0.117	2.2×10^5 - 9.3×10^5	Air-water flow measurements with double-tip conductivity probe	Air-water flow properties
	0.39 – 3.55	0.004 - 0.117	3.4×10^4 - 9.3×10^5	Visual observations	Flow pattern
Combination of flat and pooled steps	1.35 – 3.55	0.027 - 0.117	2.2×10^5 - 9.3×10^5	Air-water flow measurements with double-tip conductivity probe	Air-water flow properties
	0.52 – 3.55	0.007 - 0.117	5.2×10^4 - 9.3×10^5	Visual observations	Flow patterns

Note: d_c: critical flow depth ($d_c = \sqrt[3]{q_w^2 / g}$).

3. FLOW PATTERNS ON THE STEPPED SPILLWAYS

3.1 AIR-WATER FLOW PATTERN ON STEPPED SPILLWAYS

For the three stepped spillway configurations, some detailed visual observations of the flow pattern were conducted. The observations included the flow processes in nappe, transition and skimming flow regimes for a wide range of discharges 0.002 $m^3/s \leq Q \leq 0.117$ m^3/s. Some instabilities were seen in the configurations with pooled steps and with a combination of flat and pooled steps. Details about the self-induced instabilities on pooled stepped spillways with slopes of 8.9° and 14.6° were reported by THORWARTH (2008). FELDER & CHANSON (2012) identified some characteristic recirculation and ejection frequencies of the instabilities on the pooled stepped spillway with 8.9° slope. They investigated also the location of the inception point for all three flow configurations and the changes of flow regimes (FELDER & CHANSON 2012). In this section, some typical flow patterns for the stepped spillways with flat, pooled and combination of flat and pooled steps are presented. The self-induced instabilities observed on the pooled stepped spillway and combination of flat and pooled steps are discussed.

3.1.1 Air-water flow pattern on flat stepped spillway

Some air-water flow patterns for the flat stepped spillway are shown in Figure 3-1 for three typical discharges in the nappe, transition and skimming flow regimes. For the nappe flow regime, the flow propagated in a succession of free-falling jet and small hydraulic jump on each step (Fig. 3-1A). The flow was aerated from the first step edge and all along the stepped spillway. Most kinetic energy was dissipated along the stepped spillway. The present observations were typical of nappe flow on flat stepped spillways with comparable channel slope (CHANSON and TOOMBES 1997, TOOMBES 2002, TOOMBES and CHANSON 2008a). For dimensionless flow rates $0.95 < d_c/h < 1.69$, a transition flow regime was observed. Key flow features included some strong droplet splashing and irregular flow motion (Fig. 3-1B). The observations highlighted some typical flow motions with strong energy dissipation and turbulent fluctuations as seen in earlier studies (CHANSON & TOOMBES 2004). For the largest flow rates, a skimming flow regime took place (Fig. 3-1C). At the upstream end, the flow was a clear water flow. Once the outer edge of the turbulent boundary layer reached the free surface, the air entrainment process started at the inception point (left hand side of Fig. 3-1C). Further downstream, an air-water flow mixture was seen while the pseudo free surface was basically parallel to the pseudo-bottom formed by the step edges. Some recirculation was present in the step cavities and some water droplets were ejected above the flow (right hand side of Fig. 3-1C). Overall, the findings of the current study were consistent with observations by THORWATH (2008) on the same stepped spillway model.

Fig. 3-1 – Air-water flow pattern for different flow regimes on the flat stepped spillway ($\theta = 8.9°$)

(A) Nappe/transition flow regime: $d_c/h = 0.95$, $Q = 0.016$ m^3/s, $Re = 1.28 \times 10^5$

(B) Transition flow regime: $d_c/h = 1.59$, $Q = 0.035$ m^3/s, $Re = 2.78 \times 10^5$

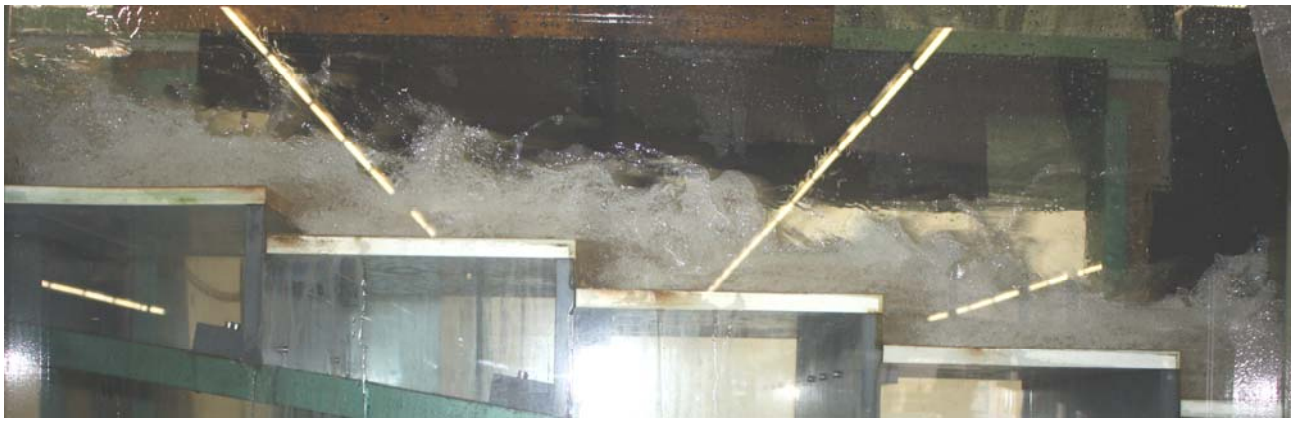

(C) Skimming flow regime: $d_c/h = 2.56$, $Q = 0.072$ m^3/s, $Re = 5.71 \times 10^5$

3.1.2 Air-water flow pattern on pooled stepped spillway

The flow observations on the pooled stepped spillway showed some typical flow characteristics close to those reported by KOENGETER & THORWATH (2006), THORWATH (2008) and FELDER & CHANSON (2012). For the lowest flow rates, a nappe flow regime took place (Fig. 3-

2). In Figure 3-2, some characteristic features of the nappe flow are visible including a free falling jet from one step cavity into the following water-filled pool. Air was entrained at the plunge point and some recirculation motion was seen for the larger flow rates in nappe flows. The air was mostly released to the free-surface before the next overfall. Overall the flow motion was stable (Fig. 3-2).

For dimensionless flow rates $1.08 < d_c/h < 1.76$, the flow became instable in a transition flow regime (Fig. 3-3). Some flow instabilities were present including some self-induced jump waves (THORWARTH 2008). The jump waves were accompanied by some irregular appearance of hydraulic jump at the downstream end of the pool and some irregular cavity ejection processes. Some more details about the self-induced instabilities are discussed in section 3.2.

For the largest discharges $d_c/h > 1.76$, a skimming flow regime was observed. At the upstream end of the channel, a mono-phase flow existed with a free-surface parallel to the pseudo-bottom (Fig. 3-4). Visually the free-surface appeared to be less stable than in a skimming flow on the flat stepped spillway (Fig. 3-1C). Some strong free-surface fluctuations were visible upstream of the inception point of free-surface aeration (Fig. 3-4). The fluctuation seemed to be linked with the increased step roughness induced by the weir pools. Downstream of the inception point, a two-phase flow mixture was consistently seen with a surface roughly parallel to the pseudo-bottom formed by the step edges (Fig. 3-5). Some instable cavity recirculation and ejection processes were seen for all skimming flow discharges in the present study. Further details about the characteristic frequencies of these instabilities were investigated by FELDER & CHANSON (2012).

Fig. 3-2 – Nappe flow regime on the pooled stepped spillway ($\theta = 8.9°$, $h = w = 5$ cm): $d_c/h = 1.02$, $Q = 0.018$ m^3/s, $Re = 1.43 \times 10^5$

Fig. 3-3 – Transition flow regime on the pooled stepped spillway (θ = 8.9°, h = w = 5 cm) d_c/h = 1.39, Q = 0.029 m^3/s, Re = 2.27×10^5

Fig. 3-4 – Clear water flows just upstream of the inception point of air entrainment in a skimming flow regime on the pooled stepped spillway (θ = 8.9°, h = w = 5 cm): d_c/h = 2.28, Q = 0.060 m^3/s, Re = 4.78×10^5

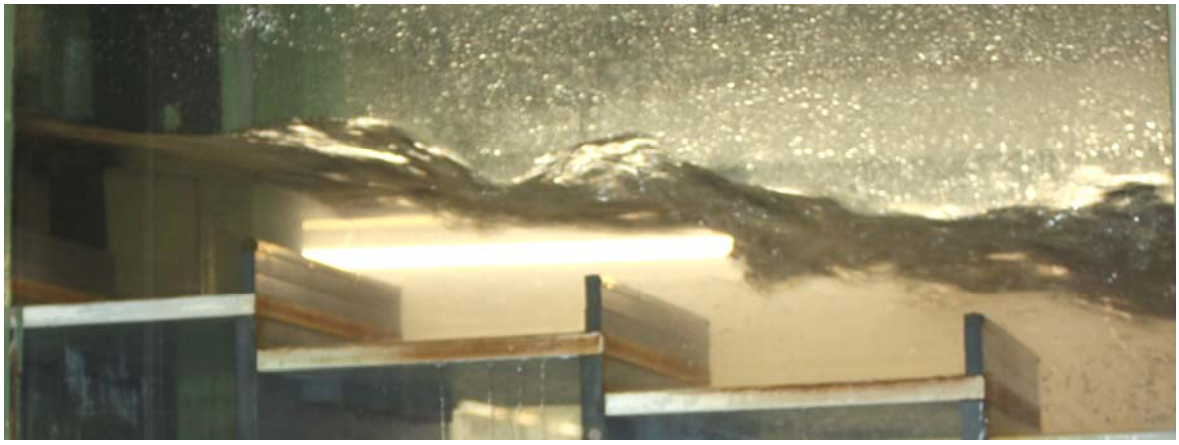

Fig. 3-5 – Skimming flow regime on the pooled stepped spillway (θ = 8.9°, h = w = 5 cm): d_c/h = 2.66, Q = 0.076 m^3/s, Re = 6.03×10^5

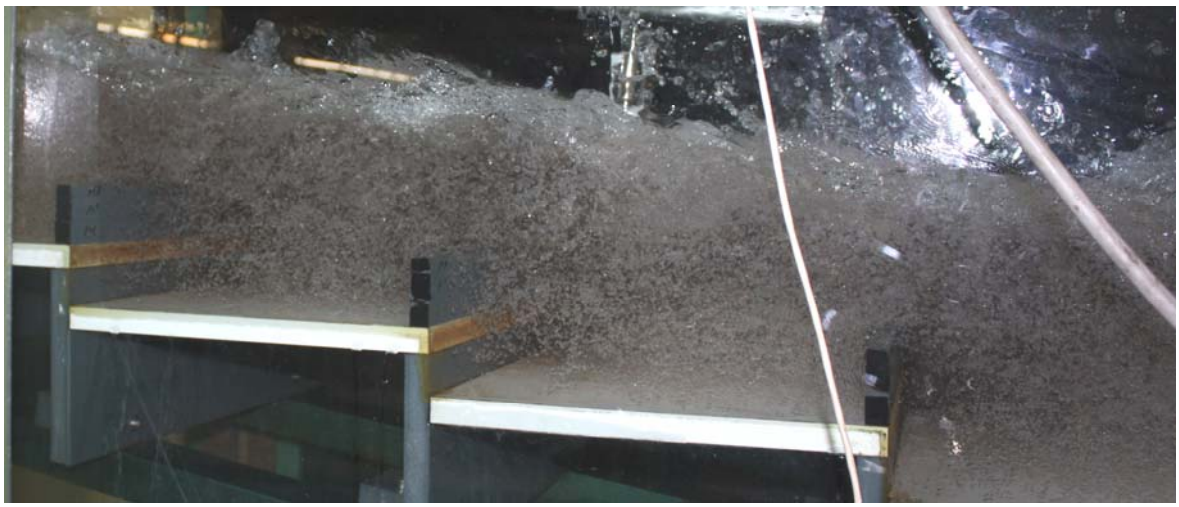

3.1.3 Air-water flow pattern for the combination of flat and pooled stepped spillway

For the stepped spillway configuration with combination of flat and pooled steps, the visual observations showed some characteristic flow features. For dimensionless flow rates $d_c/h < 1.0$, a nappe flow regime was observed (Fig. 3-6). The air-water flow cascaded downstream in a series of free-falling jets. The flow became aerated from the first step edge. A hydraulic jump dissipated most of the flow energy before the next overfall at the pooled weir (Fig. 3-6).

For larger flow rates ($d_c/h > 1.0$), a transition flow was observed (Fig. 3-7). The flow appeared chaotic with some strong droplet splashing at all step edges downstream of the inception point of air entrainment. Some flow instabilities were present for all flow rates, including some irregular cavity ejection and recirculation process as well as some instationary free-surface waves (Fig. 3-7). Within the experimental flow conditions investigated herein, no skimming flow regime was seen. The finding was consistent with the visual observations of KÖKPINAR (2004) down a 30° slope stepped spillway with combined flat and pooled steps. He reported a change from transition to skimming flows for a flow rate significantly larger than that observed on flat and pooled stepped spillways. In the present study, a clear water flow was observed at the upstream end (Fig. 3-8). In Figure 3-8, the inception point and the air entrainment downstream of the inception point are illustrated for two discharges. The entrainment process was linked with a jet flow caused by the first pooled weir. The aeration process at the inception point was therefore completely different compared to typical entrainment processes on flat and pooled stepped spillways.

Fig. 3-6 – Nappe flow regime on the stepped spillway with combination of flat and pooled steps ($\theta = 8.9°$, $h = w = 5$ cm): $d_c/h = 0.73$, $Q = 0.011$ m^3/s, $Re = 8.74 \times 10^4$

Fig. 3-7 – Transition flow regime on the stepped spillway with combination of flat and pooled steps ($\theta = 8.9°$, h = w = 5 cm):

(A) $d_c/h = 1.33$, $Q = 0.027$ m^3/s, $Re = 2.14 \times 10^5$

(B) $d_c/h = 3.34$, $Q = 0.107$ m^3/s, $Re = 8.49 \times 10^5$

Fig. 3-8 – Inception point of air-entrainment for the stepped spillway with combination of flat and pooled steps in transition flow regime ($\theta = 8.9°$, h = w = 5 cm):

(A) $d_c/h = 1.86$, $Q = 0.044$ m^3/s, $Re = 3.53 \times 10^5$ (B) $d_c/h = 2.95$, $Q = 0.089$ m^3/s, $Re = 7.04 \times 10^5$

3.2 SELF-INDUCED INSTABILITIES ON THE POOLED STEPPED SPILLWAY

Some strong self-induced flow instationarities were observed on the pooled stepped spillway. Such instabilities were previously investigated by THORWARTH (2008) showing that the instationarities were associated with some jump wave processes. Figure 3-9 illustrates some typical jump waves observed in the present study for a transition flow discharge. The series of pictures

shows the propagation of the waves (Fig. 3-9). The frequencies of the jump waves were about 0.25-0.4 Hz in the present study.

Some waves were caused by some pulsating clear-water flows in the first step pool downstream of the broad-crested weir (Fig. 3-10). In Figure 3-10, a series of photographs of the pulsations is illustrated. The pulsations initiated jump waves every 6-8 s herein. The flow pattern was observed in the transition flow regime. The pulsations caused every second jump wave to propagate downstream. The other waves seemed to be initiated by further instationaries in the first few stepped pools. The irregular ejection and recirculation processes within each pooled cavity appeared more often with frequencies of 0.5-2Hz as shown by THORWARTH (2008) and FELDER & CHANSON (2012).

Fig. 3-9 – Instabilities in the transition flow regime on the pooled stepped spillway ($\theta = 8.9°$, h = w = 5 cm): $d_c/h = 1.20$, Q = 0.023 m^3/s, Re = 1.83×10^5 - Chronological order from top left corner to bottom right corner

Fig. 3-10 – Pulsating flow in the first step cavity downstream of the broad-crested weir in the transition flow regime on the pooled stepped spillway ($\theta = 8.9°$, $h = w = 5$ cm): $d_c/h = 1.08$, $Q = 0.020$ m^3/s, $Re = 1.56 \times 10^5$ - Chronological order from top left corner to bottom right corner

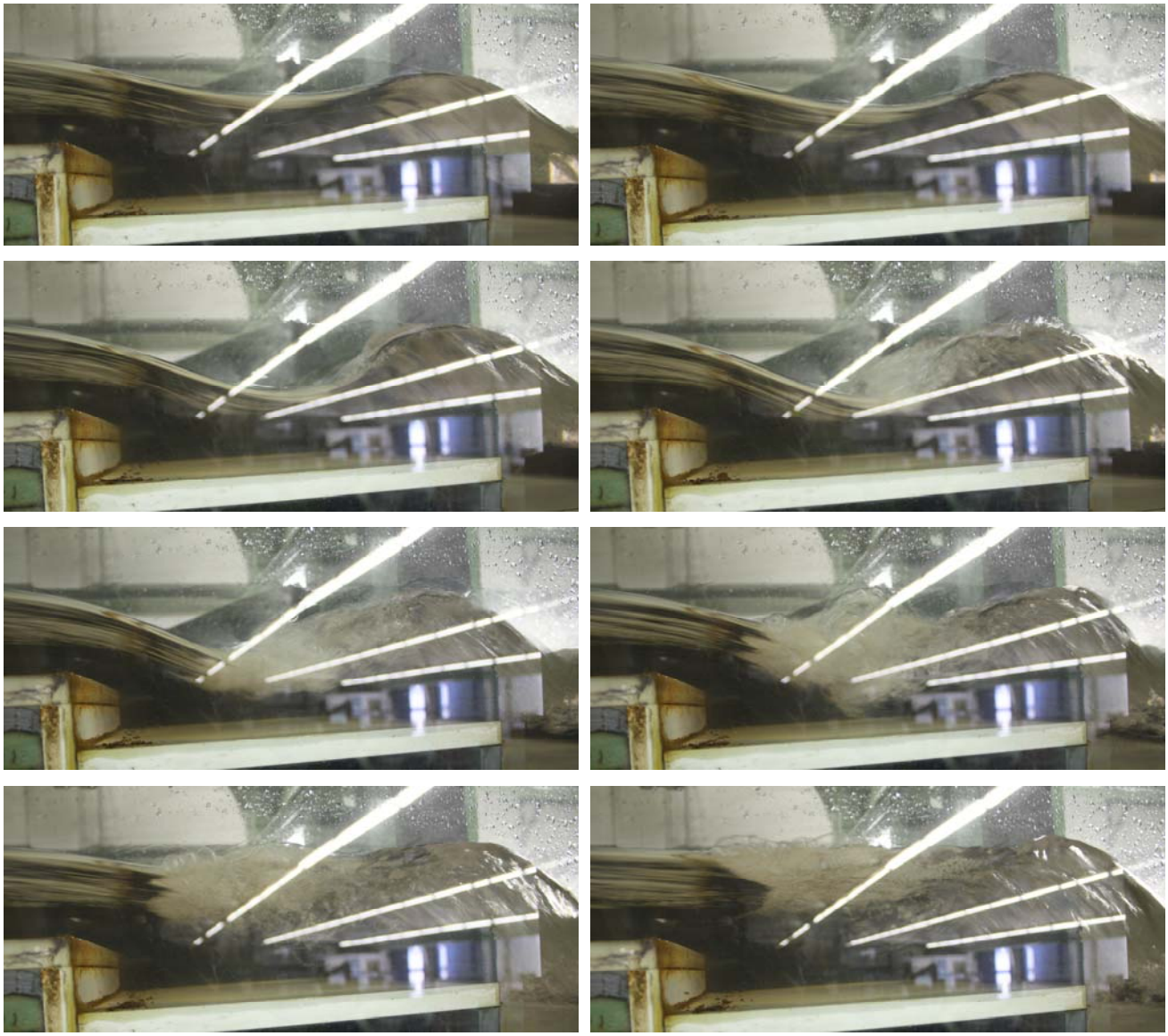

4. AIR-WATER FLOW PROPERTIES ON THE STEPPED SPILLWAYS

4.1 PRESENTATION

The air-water flow properties were measured for all three configurations at several step edges downstream of the inception point of free-surface aeration (Fig. 4-1). Figure 4-1 present a sketch of the three stepped spillway configurations and their geometric dimensions: step height h, step length l, channel width W, pool weir height w, and pooled weir length l_w. The locations of the double-tip conductivity probe measurements on channel centre line are sketched, with y = 0 at the step edge for the flat steps and y = 0 at the pool weir edge for the pooled step. The flow properties were compared for a range of discharges 0.02 $m^3/s \leq Q \leq 0.117$ m^3/s between the three stepped spillway configurations. Table 4-1 summarises the experimental conditions for the air-water flow measurements, while the air-water flow properties were compared in terms of the void fraction, bubble count rate, interfacial velocity, turbulence intensity, and bubble/droplet chord sizes.

Fig. 4-1 – Sketch of stepped spillway configurations in the present study (θ = 8.9°)

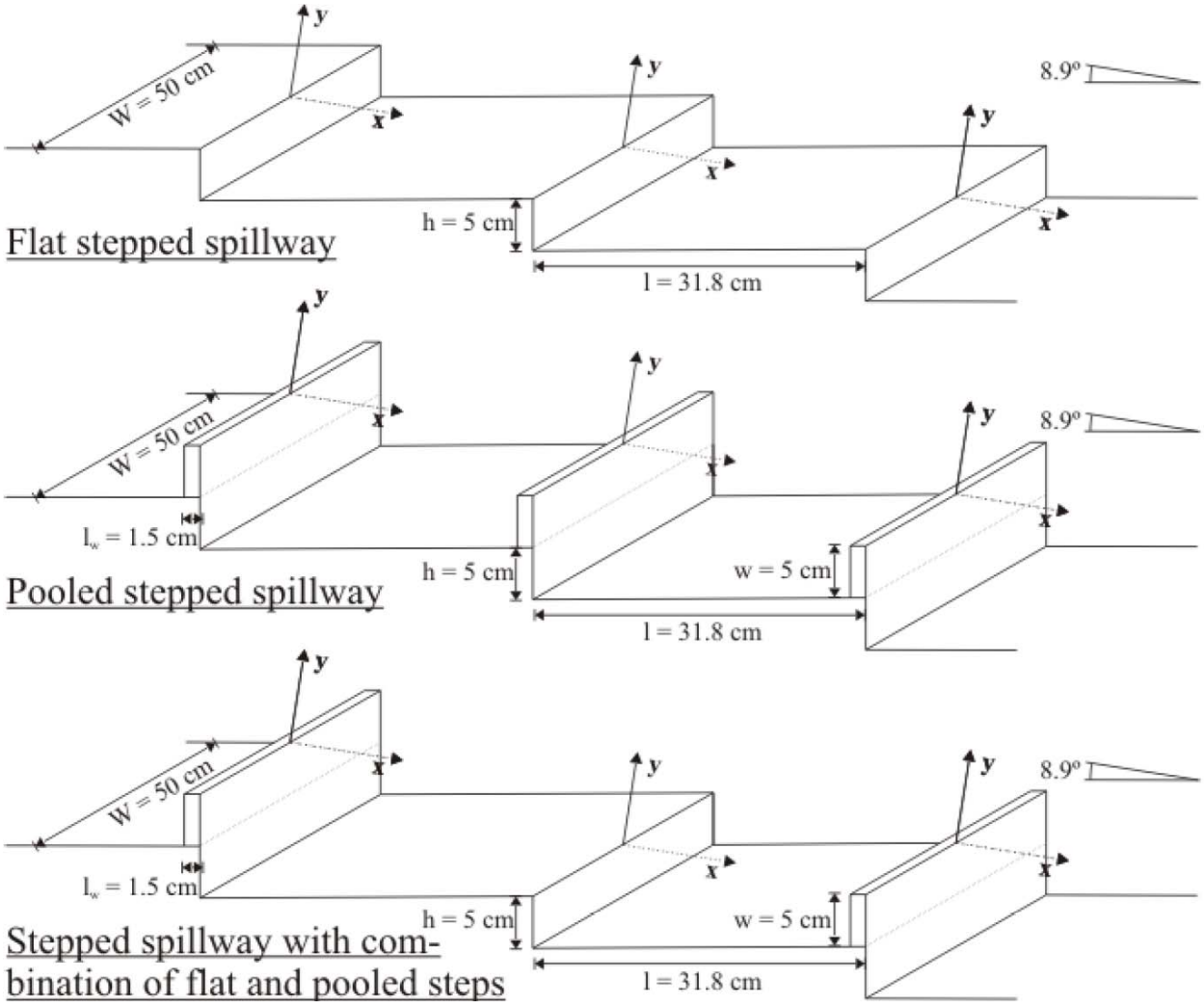

Table 4-1 - Air-water flow measurements with a double-tip conductivity probe for three different stepped spillway configurations at IWW ($\theta = 8.9°$)

Configuration (1)	d_c/h [-] (2)	Q [m^3/s] (3)	Re [-] (4)	Measurement at step edge (5)	Inception point step edge (6)	Flow regime (7)
Flat stepped spillway	1.0	0.018	1.39×10^5	21	4	TRA
	1.35	0.027	2.18×10^5	21	4	TRA
	1.7	0.039	3.10×10^5	16-21	5	SK/TRA
	2.0	0.049	3.93×10^5	21	6	SK
	2.3	0.061	4.85×10^5	21	7	SK
	2.66	0.076	6.03×10^5	16-21	9 to 10	SK
	3.0	0.091	7.23×10^5	21	10 to 11	SK
	3.3	0.105	8.34×10^5	21	13 to 14	SK
	3.55	0.117	9.30×10^5	17-21	14 to 15	SK
Pooled stepped spillway	1.35	0.027	2.18×10^5	14-21	3	TRA
	1.7	0.039	3.10×10^5	14-21	5	SK/TRA
	2.0	0.049	3.93×10^5	20+21	6	SK
	2.3	0.061	4.85×10^5	14-21	7	SK
	2.66	0.076	6.03×10^5	14-21	8	SK
	3.0	0.091	7.23×10^5	20+21	9	SK
	3.3	0.105	8.34×10^5	14-21	10	SK
	3.55	0.117	9.30×10^5	14-21	11	SK
Combination of flat and pooled steps	1.35	0.027	2.18×10^5	20+21	3 to 4	TRA
	1.7	0.039	3.10×10^5	14-21	4	TRA
	2.0	0.049	3.93×10^5	20+21	4 to 5	TRA
	2.3	0.061	4.85×10^5	20+21	4 to 5	TRA
	2.66	0.076	6.03×10^5	14-21	5	TRA
	3.0	0.091	7.23×10^5	20+21	5	TRA
	3.3	0.105	8.34×10^5	20+21	5	TRA
	3.55	0.117	9.30×10^5	14-21	5	TRA

Notes: d_c: critical flow depth; h: vertical step height; Q: water discharge; Re: Reynolds number defined in terms of the hydraulic diameter; SK: skimming flow regime; TRA: transition flow regime.

4.2 AIR-WATER FLOW PROPERTIES

The vertical distributions of void fractions showed some typical S-shape distributions for all experiments (Fig. 4-2). In Figure 4-2, some typical void fraction distributions are shown for the three stepped configurations. In Figures 4-2A and 4-2B, the void fraction is presented as a function of the dimensionless distance from the step edge y/Y_{90}. The vertical elevation y was measured starting from the edge for the flat steps and at the pool weir edge for the pooled steps; Y_{90} is the distance for which C = 90%. For the smaller flow rate, all void fraction distributions were very

close (Fig. 4-2A). For the larger flow rates, the void fraction distributions for the stepped spillway with combination of flat and pooled steps differed from those on both flat and pooled steps (Fig. 4-2B). In Figures 4-2A and 4-2B, the experimental data were also compared with the advective diffusion equation (CHANSON & TOOMBES 2002):

$$C = 1 - \tanh^2\left(K' - \frac{y / Y_{90}}{2 \times D_o} + \frac{(y / Y_{90} - 1/3)^3}{3 \times D_o}\right) \quad (4\text{-}1)$$

where K' is an integration constant and D_o is a function of the depth-averaged void fraction C_{mean} only:

$$K' = 0.32745015 + \frac{1}{2 \times D_o} - \frac{8}{81 \times D_o} \quad (4\text{-}2)$$

$$C_{mean} = 0.7622 \times (1.0434 - \exp(-3.614 \times D_o)) \quad (4\text{-}3)$$

For all data sets in the present study, the advective diffusion equation (Eq. (4-1)) matched well the experimental data as illustrated in Figure 4-2.

Some typical void fraction distributions are also presented in Figures 4-2C and 4-2D for several consecutive step edges as functions of the dimensionless distance from the step edge $(y+w)/d_c$, where w is the weir height and d_c the critical flow depth. Some differences were noted, possibly linked with the different definition of y = 0 for the pooled and flat steps. For the combination of flat and pooled steps, some differences were also observed with the different step types for the larger discharges (Fig. 4-2D). The void fraction distributions at the flat and pooled steps were in agreement for all measured steps. Similarly the shapes of the void fraction distribution at consecutive step edges were unchanged for all experiments for the flat and pooled stepped spillways.

Some typical dimensionless distributions of bubble count rates are illustrated in Figure 4-3 as functions of y/Y_{90} (Fig. 4-3A) and $(y+w)/d_c$ (Fig 4-3B) for several consecutive step edges for all three stepped configurations. For a given step configuration, the bubble count rate distributions changed little for all experiments. Some differences in terms of bubble count rate distributions between flat and pooled steps were observed for the combination of flat and pooled steps. The differences were the largest for the smaller flow rates (Fig. 4-3B), while the bubble count rate distributions for the largest flow rates were close to those for both flat and pooled steps.

The comparison of all three stepped configurations highlighted the largest bubble count rates for the flat stepped spillway for a given flow rate within the experimental flow conditions. For the smallest flow rates, the combination of flat and pooled steps had the smallest bubble count rates while, for the largest discharges, the pooled stepped spillway configuration had the smallest values. With increasing discharge the differences between all configurations became smaller (Fig. 4-3A).

Fig. 4-2 – Comparison of void fraction distributions on the stepped spillways with flat, pooled and combination of flat and pooled steps (θ = 8.9°) - Comparison with Equation (4-1)

(A) $d_c/h = 2.0$, $Q = 0.049$ m^3/s, $Re = 3.93\times10^5$ (B) $d_c/h = 3.3$, $Q = 0.105$ m^3/s, $Re = 8.34\times10^5$

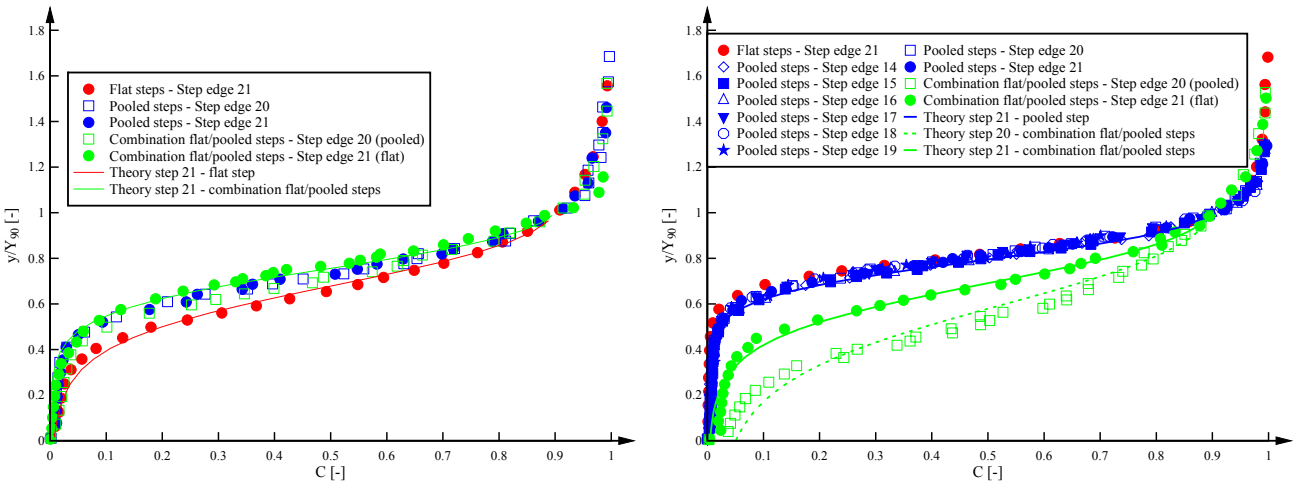

(C) $d_c/h = 2.3$, $Q = 0.061$ m^3/s, $Re = 4.85\times10^5$ (D) $d_c/h = 3.55$, $Q = 0.117$ m^3/s, $Re = 9.30\times10^5$

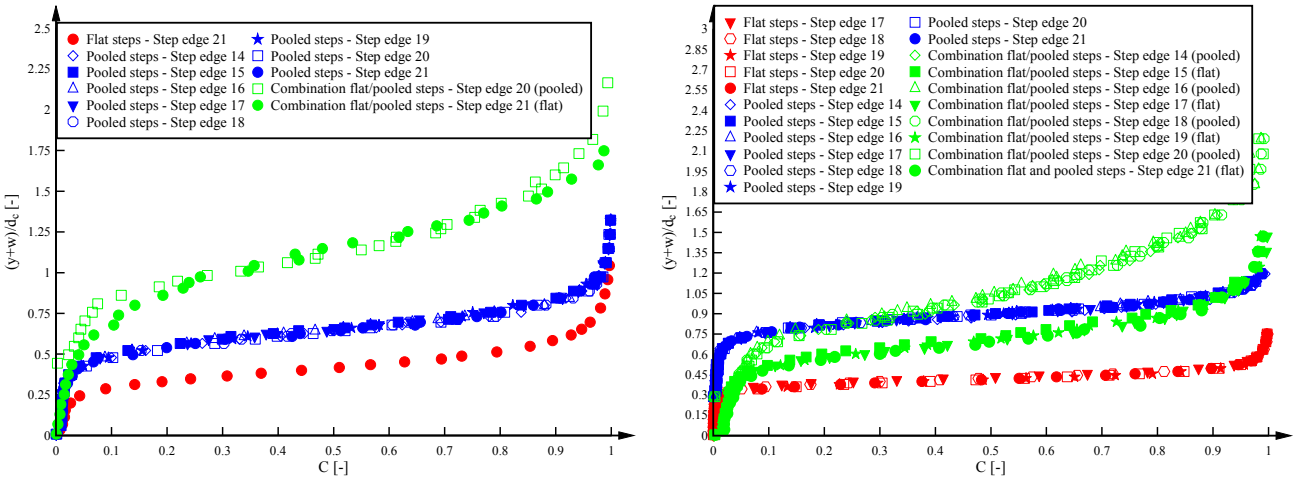

Fig. 4-3 – Comparison of dimensionless bubble count rate distributions on the stepped spillways with flat, pooled and combination of flat and pooled steps (θ = 8.9°)

(A) $d_c/h = 3.55$, $Q = 0.117$ m^3/s, $Re = 9.30\times10^5$ (B) $d_c/h = 1.7$, $Q = 0.039$ m^3/s, $Re = 3.10\times10^5$

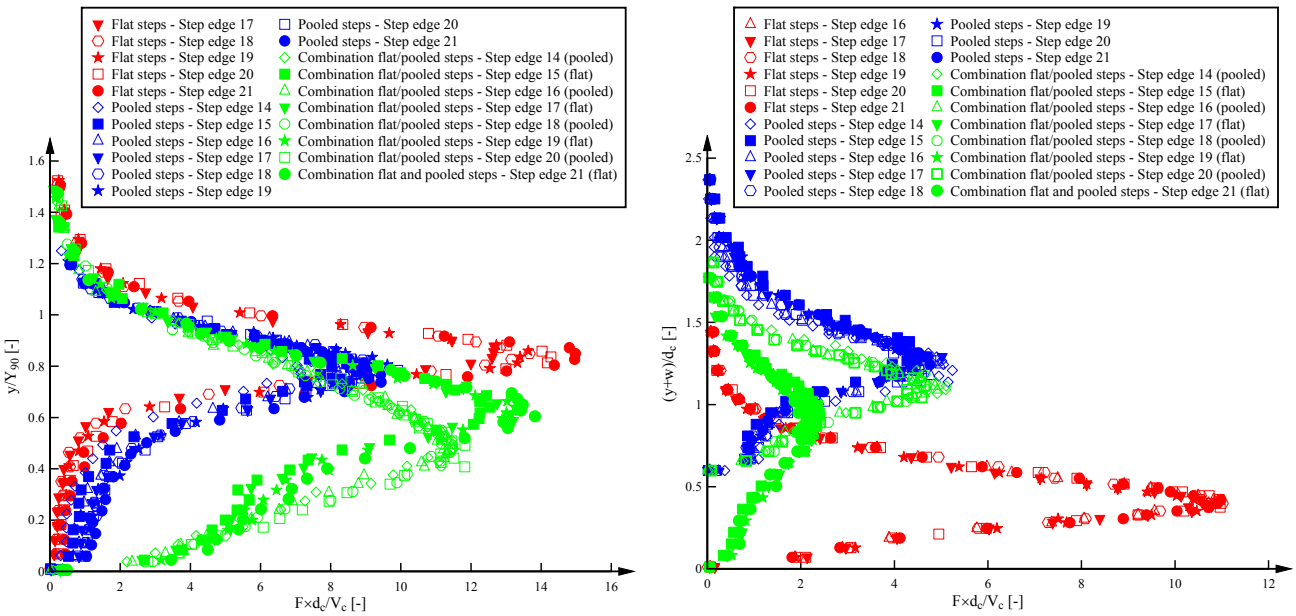

Some typical interfacial velocity distributions are presented in Figure 4-4. Data for all three configurations are presented as functions of y/Y_{90} and $(y+w)/d_c$ respectively in Figure 4-4A and 4-4B respectively. A good agreement was achieved between flat and pooled stepped spillway data in terms of dimensionless interfacial velocity V/V_{90}, as well as for the pooled step data on the stepped spillway configuration with combination of flat and pooled steps (Fig. 4-4A). For all discharges, the data collapsed reasonably well with a power law:

$$\frac{V}{V_{90}} = \left(\frac{y}{Y_{90}}\right)^{1/N} \qquad 0 \leq y/Y_{90} \leq 1 \quad (4\text{-}4)$$

The value of the exponent N may vary from one step edge to the next one for a given flow rate, with on average N = 10. For $y/Y_{90} > 1$, the velocity distributions had a quasi uniform profile :

$$\frac{V}{V_{90}} = 1 \qquad 1 < y/Y_{90} \quad (4\text{-}5)$$

For the flat and pooled stepped spillway configurations, the data were in close agreement with Equations 4-4 and 4-5 (Fig. 4-4A). Some data scatter was seen for the pooled steps on the spillway configuration with combination of flat and pooled steps.

A very different velocity profile shape was observed for the flat steps in the combination of flat and pooled steps in terms of the dimensionless distribution V/V_{90}. The interfacial velocity distribution exhibited a distribution shape similar to those observed at the impact of nappe flow jets and in transition flows (CHANSON and TOOMBES 2004, TOOMBES and CHANSON 2008b) (Fig. 4-

4A).

In Figure 4-4B, the dimensionless interfacial velocity distributions are presented in terms of V/V_c showing distinctive features. The largest interfacial velocities were observed for the flat stepped spillway. The magnitudes of V/V_c for the stepped spillways with pooled steps and with combination of pooled and flat steps were close and about 30% smaller than the flat stepped spillway velocity data (Fig. 4-4B).

Fig. 4-4 – Comparison of dimensionless interfacial velocity distributions on the stepped spillways with flat, pooled and combination of flat and pooled steps (θ = 8.9°)

(A) $d_c/h = 2.66$, $Q = 0.076$ m^3/s, $Re = 6.03\times10^5$ (B) $d_c/h = 3.3$, $Q = 0.105$ m^3/s, $Re = 8.34\times10^5$

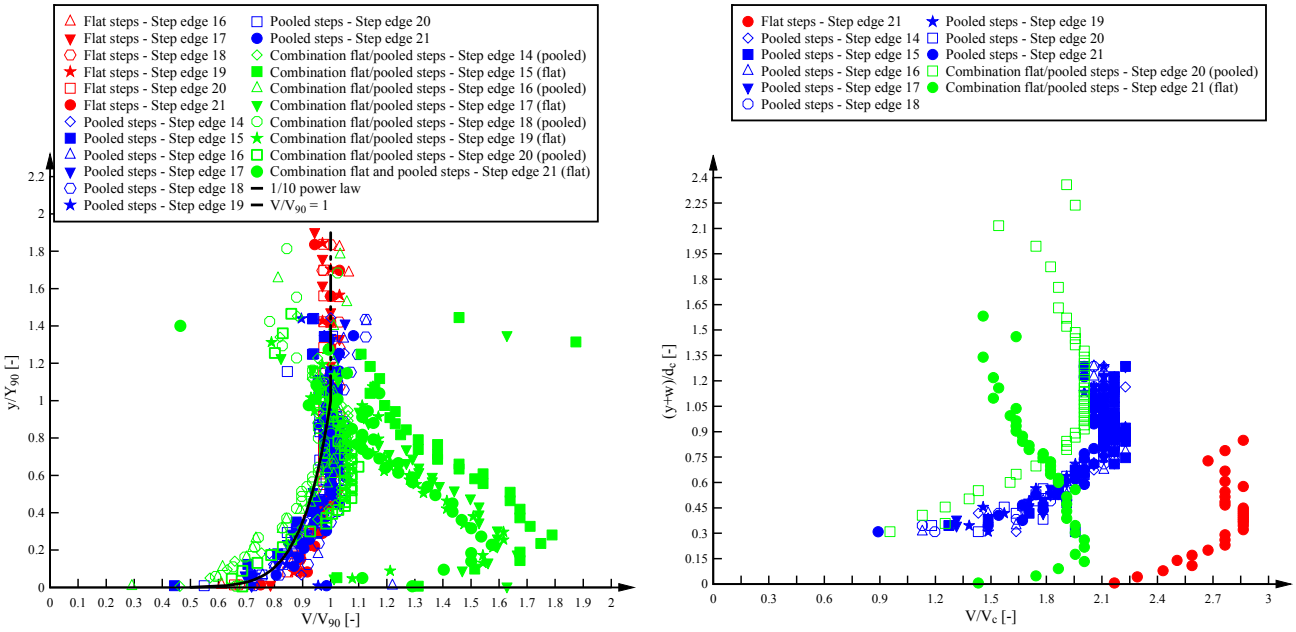

Some typical distributions of turbulence intensity Tu are illustrated in Figure 4-5 for all experimental configurations. The turbulence intensity in air-water flows was calculated from the difference in shapes of the auto- and cross-correlation functions. Tu was a spatial-average quantity characterising the turbulent fluctuations of the interfacial velocity. It was calculated as:

$$Tu = 0.851 \times \frac{\sqrt{\tau_{0.5}^{\ 2} - T_{0.5}^{\ 2}}}{T} \qquad (4\text{-}6)$$

where $\tau_{0.5}$ is the time scale for which the cross-correlation function is half of its maximum value such as: $R_{xy}(T+\tau_{0.5}) = 0.5\times R_{xy}(T)$, R_{xy} is the normalised cross-correlation function and $T_{0.5}$ is the characteristic time for which the normalised auto-correlation function equals: $R_{xx}(T_{0.5}) = 0.5$ (CHANSON and TOOMBES 2002).

The distributions of turbulence intensity showed some very large turbulence levels for the pooled stepped spillway and for the spillway with combination of pooled and flat steps. Maximum values

of up to 500-900% were observed in the intermediate flow region (0.3 < C < 0.7). These turbulence intensity levels were discussed by FELDER & CHANSON (2012). FELDER & CHANSON (2012) showed that the instationary processes on the pooled stepped spillway configurations contributed significantly to the turbulent kinetic energy of the flow. The turbulence levels on the flat stepped spillway showed values of about 150% in the intermediate flow region which were consistent with previous studies on flat stepped spillways (CHANSON and TOOMBES 2002, FELDER and CHANSON 2009b).

Figures 4-6 and 4-7 present some typical bubble and droplet chord size probability distribution functions respectively. Some small differences were observed in terms of the air bubble and water droplet chord sizes. For all configurations, similar chord sizes were seen in both bubbly flow and spray regions for the flat and pooled stepped spillways (Fig. 4-6 & 4-7). Some differences were visible for the stepped spillway configuration with combination of flat and pooled stepped spillways. In Figure 4-6, some typical air bubble chord size distributions are shown for two consecutive step edges for the three configurations. For the smaller flow rate all data collapsed quite well and showed typical log-normal distributions (Fig. 4-6A), but for the larger flow rate for which the combined stepped spillway data showed a larger amount of small air bubble chord sizes (Fig. 4-6B). Further chord size distribution data suggested that there was no clear trend linked with the deviations between the flow configurations (Appendix A).

Fig. 4-5 – Comparison of turbulence intensity distributions on the stepped spillways with flat, pooled and combination of flat and pooled steps (θ = 8.9°)

(A) $d_c/h = 1.7$, $Q = 0.039$ m^3/s, $Re = 3.10\times10^5$ (B) $d_c/h = 2.66$, $Q = 0.076$ m^3/s, $Re = 6.03\times10^5$

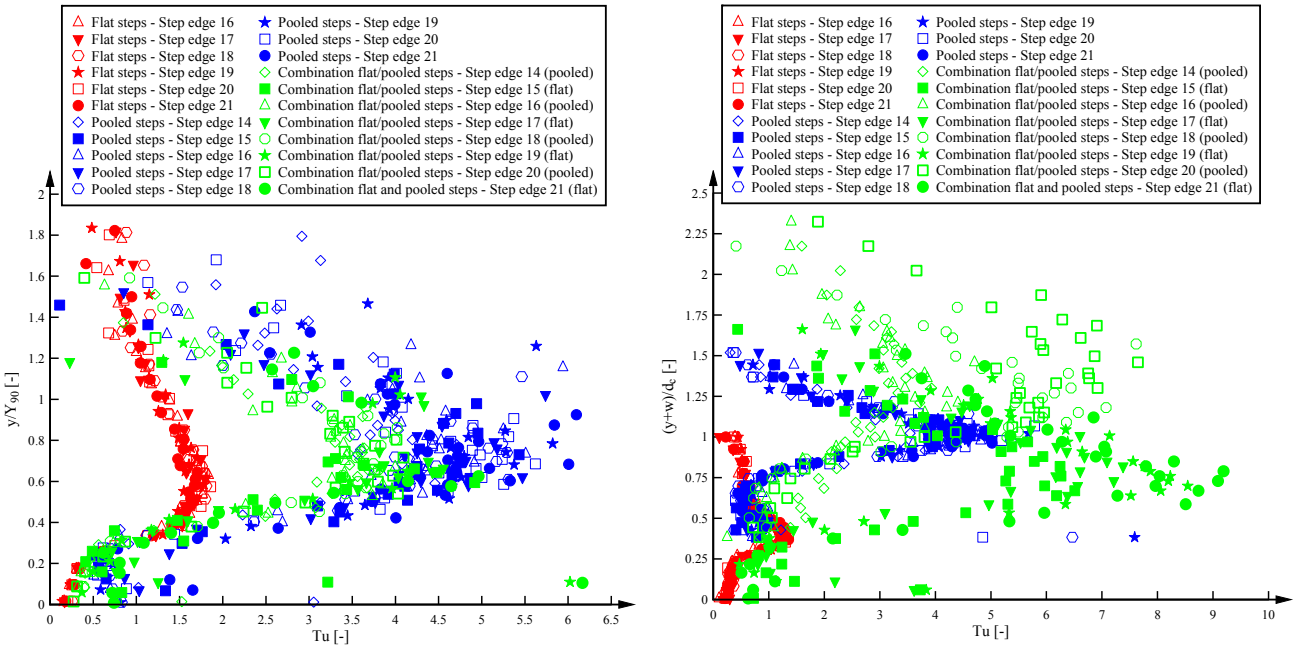

Fig. 4-6 Comparison of probability distribution functions of air bubble chord sizes on stepped spillways with flat, pooled and combination of flat and pooled steps (θ = 8.9°)

(A) d_c/h = 1.7, Q = 0.039 m^3/s, Re = 3.10×10^5; Step edge 20

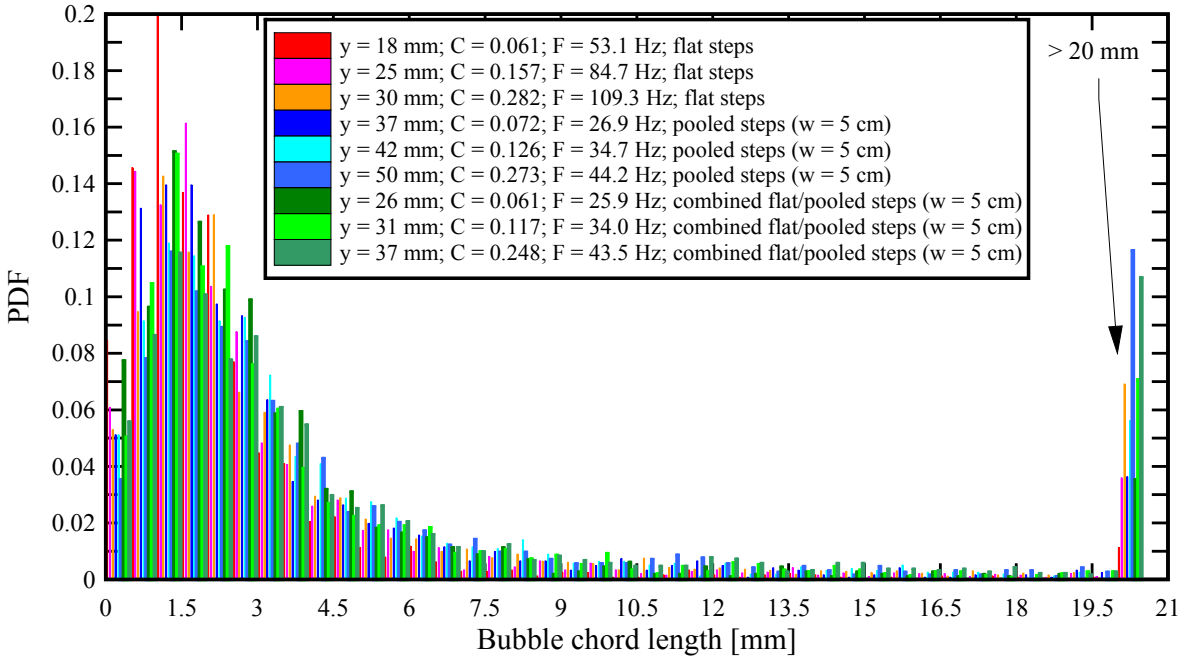

(B) d_c/h = 3.55, Q = 0.117 m^3/s, Re = 9.30×10^5; Step edge 21

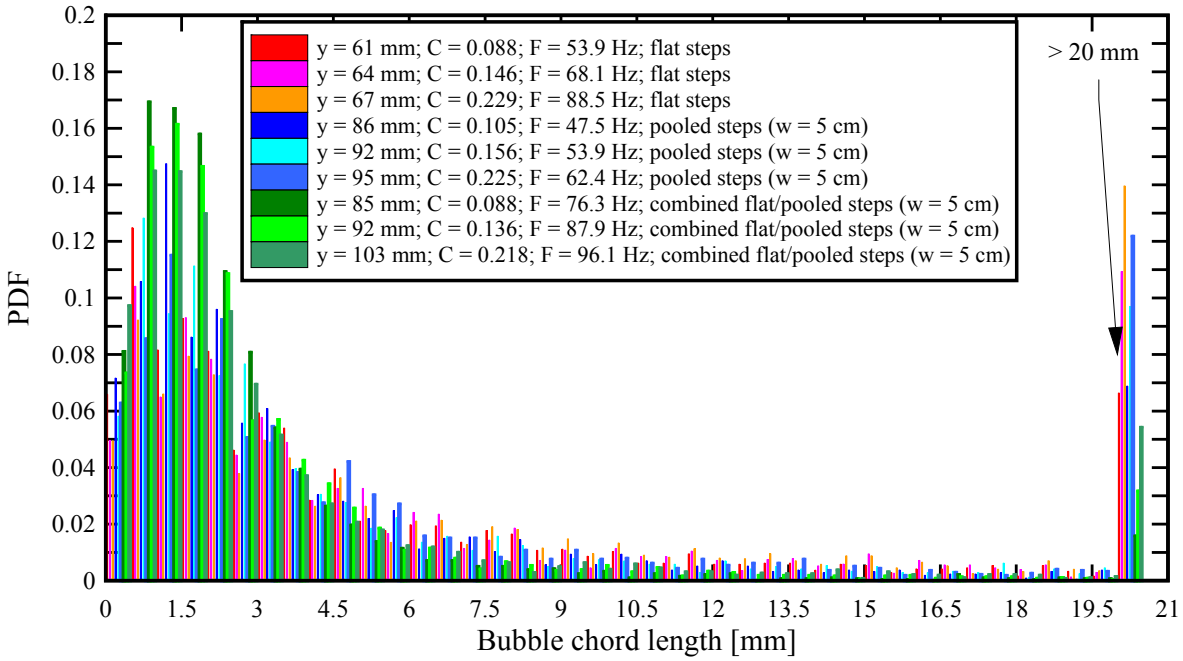

Fig. 4-7 Comparison of probability distribution functions of water droplet chord sizes on stepped spillways with flat, pooled and combination of flat and pooled steps (θ = 8.9°)

(A) $d_c/h = 2.66$, $Q = 0.076$ m^3/s, $Re = 6.03\times10^5$; Step edge 20

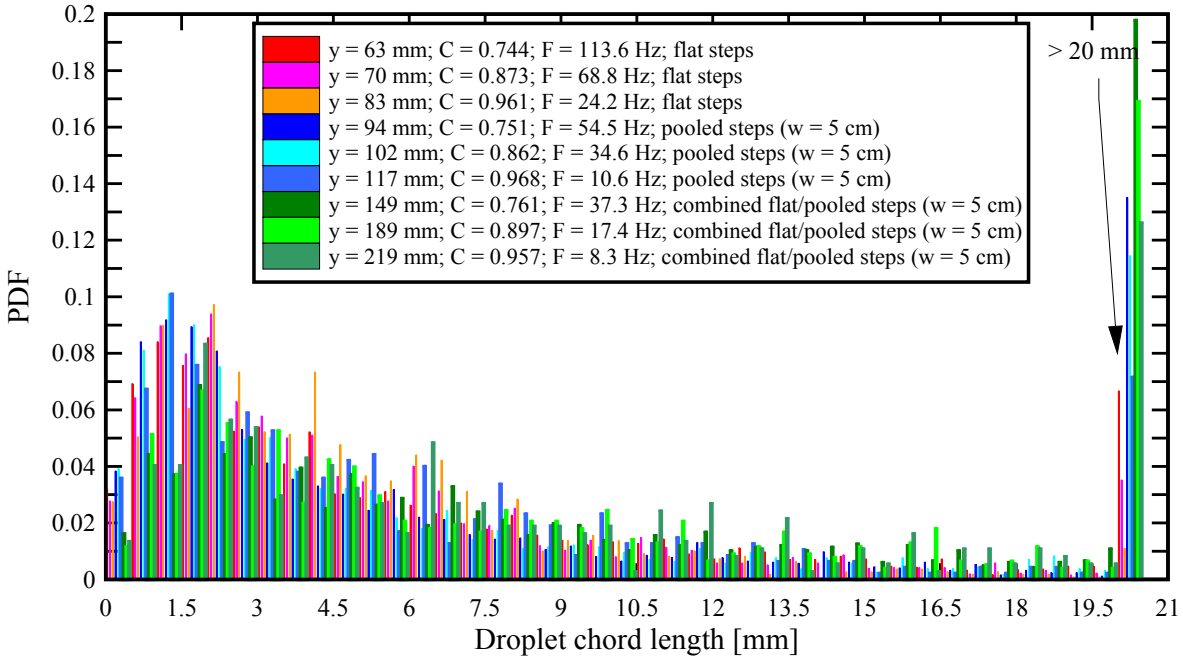

(B) $d_c/h = 2.66$, $Q = 0.076$ m^3/s, $Re = 6.03\times10^5$; Step edge 21

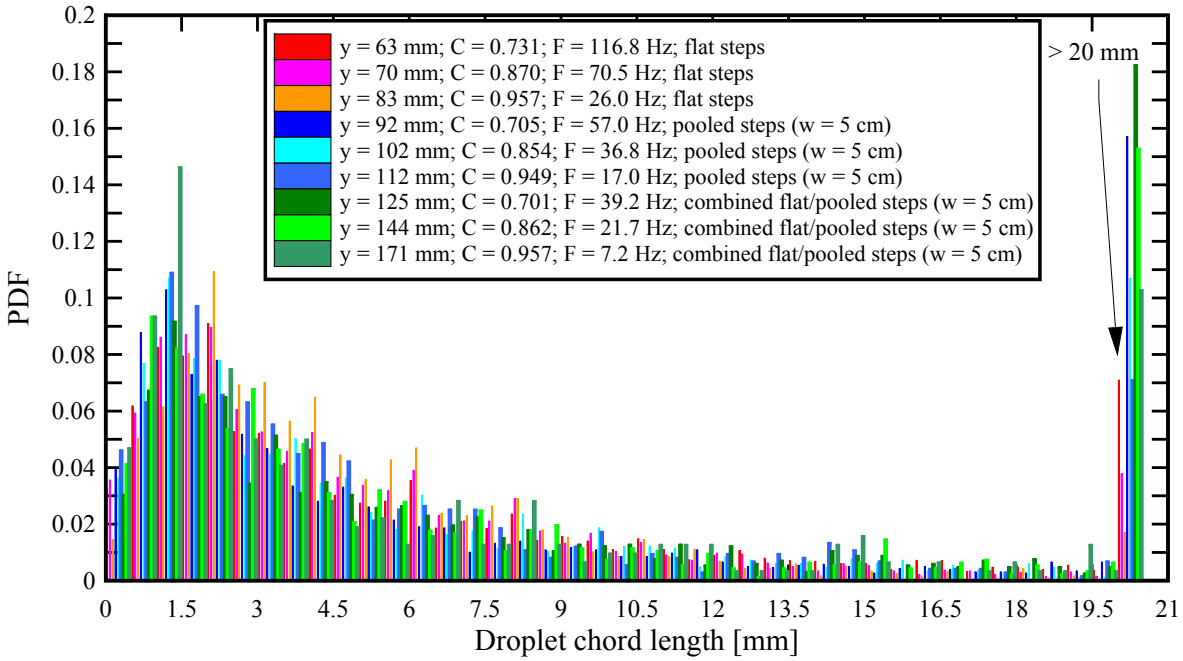

Similar results were found in terms of the water droplet PDF chord sizes (Fig. 4-7). An amount of larger water droplet chord sizes was observed for the configuration with flat and pooled steps, while the chord sizes for the flat and pooled stepped spillways showed similar distributions close to a log-normal distribution shape. Further PDF distribution data are presented in Appendix A showing

close results between all three configurations.

4.3 DISCUSSION

Some basic air-water flow properties were compared between the three configurations highlighting some key differences (see section 4.2). A further comparison of some characteristic parameters confirmed the findings. Namely the depth averaged void fraction C_{mean} and the characteristic air-water velocity V_{90}. The basic results are presented in Figure 4-8 as functions of the dimensionless distance from the inception point of free-surface aeration.

The present data showed that the void fraction distributions were in good agreement between the flat and pooled stepped spillways, but some differences were observed for the stepped spillway configuration with combination of flat and pooled steps. In that configuration, the mean air concentration C_{mean} was larger compared to the other configurations for larger discharges as illustrated in Figure 4-8A. The data highlighted however some large fluctuations in terms of C_{mean} linked with the alternation of flat and pooled steps. The largest aeration was seen on the pooled steps on the combined stepped spillway configuration.

Another key feature is the dimensionless characteristic interfacial velocity V_{90}/V_c (Fig. 4-8B). The largest dimensionless interfacial velocities were observed for the flat stepped spillway configuration as seen in Figure 4-8B. The lowest of V_{90}/V_c were seen for the combination of flat and pooled steps. Some data scatter was noted for the stepped spillway with combination of flat and pooled steps.

Further characteristic parameters are presented in Appendix B. Overall the results were consistent with the observations presented in section 4.2 in terms of maximum bubble count rates and maximum turbulence levels.

Fig. 4-8 Comparison of longitudinal distributions of characteristic parameters for the stepped spillway with flat, pooled and combination of flat and pooled steps (θ = 8.9°)

(A) Mean air-concentration C_{mean}

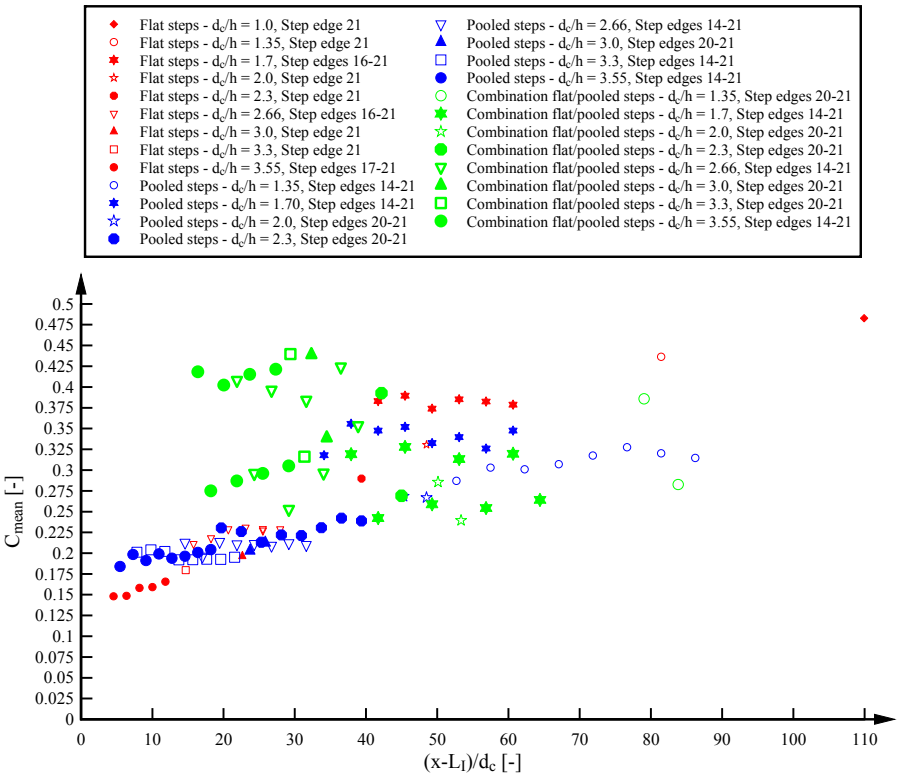

(B) Characteristic dimensionless interfacial velocity V_{90}/V_c

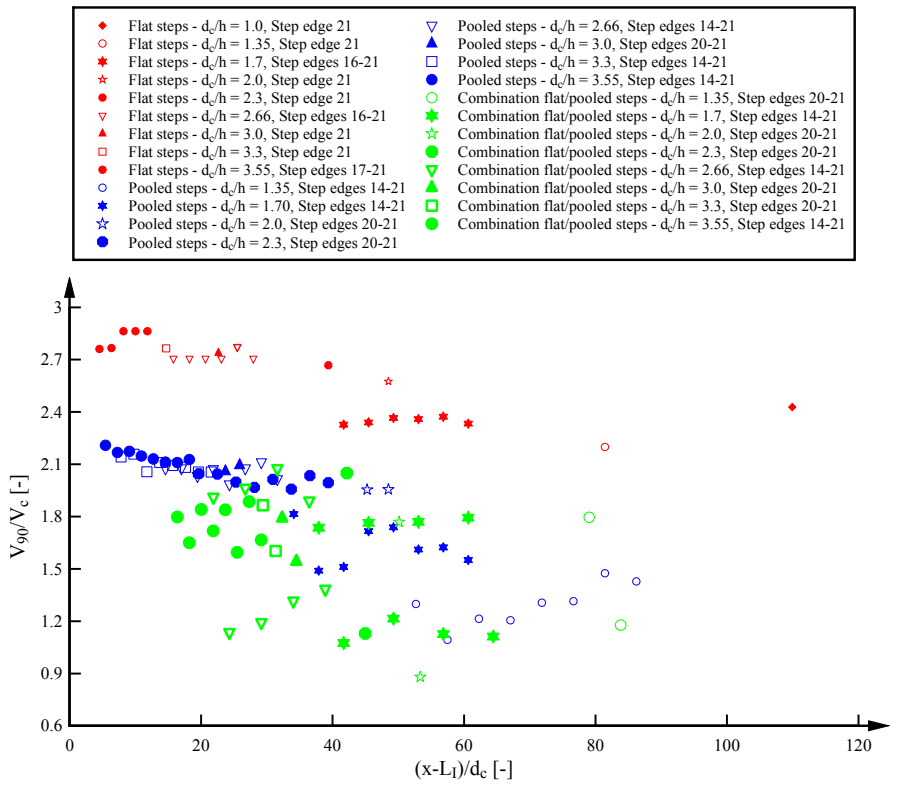

5. ENERGY DISSIPATION AND FLOW RESISTANCE ON THE STEPPED SPILLWAYS

5.1 RESIDUAL HEAD AND ENERGY DISSIPATION

The residual energy and rate of energy dissipation were investigated at the downstream end of the spillways. They were calculated at two successive step edges for the three configurations based upon the detailed air-water flow measurements. The rate of energy dissipation $\Delta H/H_{max}$ quantified the percentage of total energy loss along the stepped spillway, where H_{max} is the upstream total head:

$$H_{max} = \frac{3}{2} \times d_c + H_{dam} \quad (5\text{-}1)$$

with H_{dam} the dam height and d_c the critical flow depth. The total head loss was at every step edge as $\Delta H = H_{max} - H_{res}$, where H_{res} is the residual head estimated as:

$$H_{res} = d \times \cos\theta + \frac{U_w{}^2}{2 \times g} + w \quad (5\text{-}2)$$

where d is the equivalent clear water flow depth, U_w the flow velocity ($U_w = q_w/d$) and w is the weir height.

The rate of energy dissipation for the three configurations is illustrated in Figure 5-1 for the last two step edges as a function of dimensionless drop in elevation between the broad crested weir and the measured step edge Δz_o. The comparison between flat and pooled stepped chute performances showed a larger rate of energy dissipation rate on the pooled step configurations (Fig. 5-1). The largest rate of energy dissipation was observed for the stepped spillway with combination of flat and pooled steps in particle at the largest discharges. For the small discharges, note some data scatter between flat and pooled steps (Fig. 5-1). Altogether the energy dissipation rate for the flat stepped spillway was the lowest of all three configurations for all flow rates.

The results in terms of residual head are presented in Figure 5-2. The data consisted of the dimensionless residual head at the downstream end of the stepped chutes calculated for two consecutive step edges. For the flat stepped spillway the dimensionless residual energy was largest and was nearly independent of the flow rate: i.e., $H_{res}/d_c \approx 3.25$. Similarly the residual head on the pooled stepped spillway was almost constant for all discharges: $H_{res}/d_c \approx 2.25$. The dimensionless residual energy for the stepped spillway with combination of flat and pooled steps showed some data scatter. On average the residual head was smallest for the combined configuration tending to a residual head for the largest flow rates of $H_{res}/d_c \approx 1.7\text{-}1.9$.

Fig. 5-1 Comparison of rate of energy dissipation at two step edges at the downstream end (θ = 8.9°) - Comparison of results for the stepped spillway with flat, pooled and combination of flat and pooled steps and for reanalysed data of THORWARTH (2008)

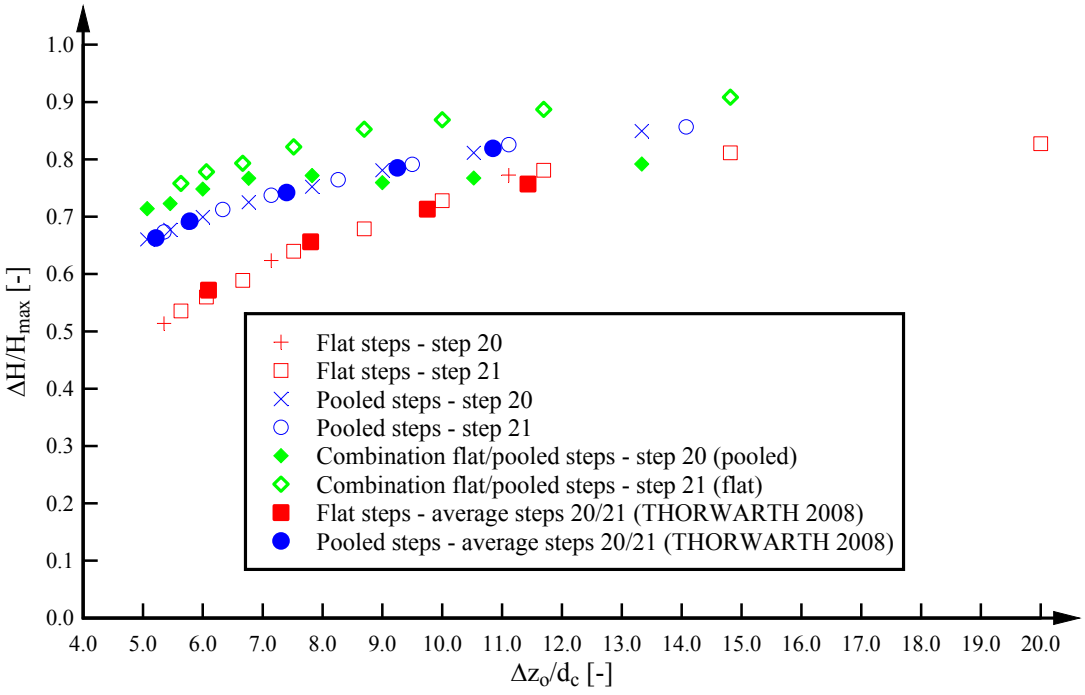

Fig. 5-2 Comparison of dimensionless residual energy at two step edges at the downstream end (θ = 8.9°) - Comparison of results for the stepped spillway with flat, pooled and combination of flat and pooled steps and for reanalysed data of THORWARTH (2008)

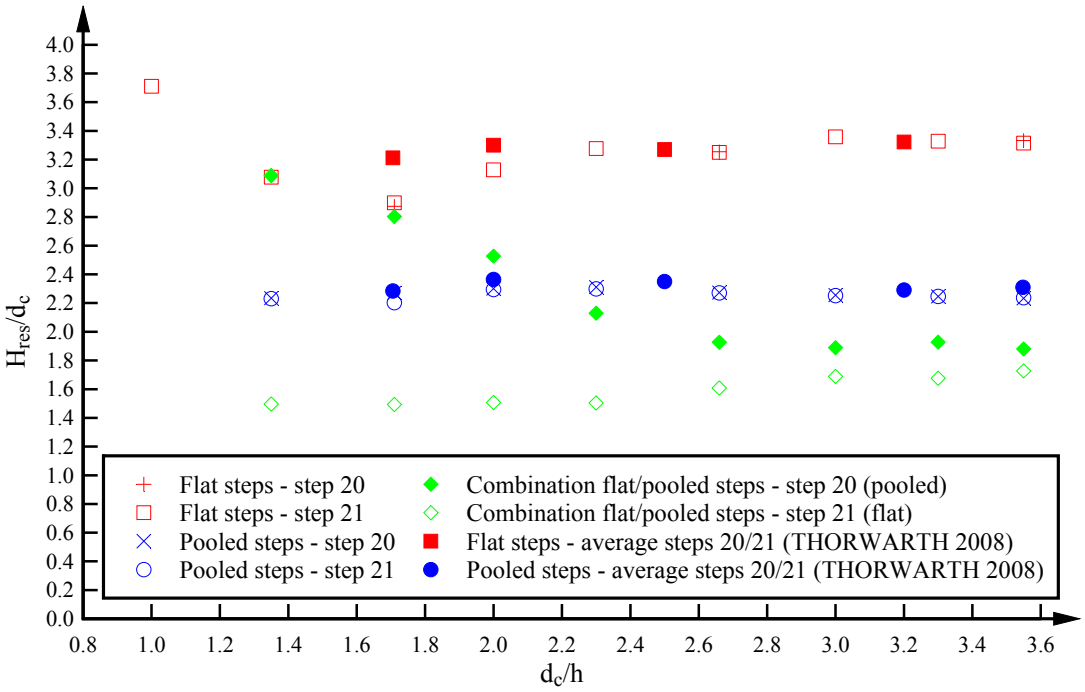

The present data set was compared with some reanalysed data of THORWARTH (2008) on the same stepped spillway facility (θ = 8.9°) with flat and pooled steps. Note that THORWARTH (2008) presented some residual head and the energy dissipation rate calculated based upon the Darcy friction coefficient for two step edges at the downstream end because he assumed a uniform equilibrium flow. Herein, THORWARTH's original void fraction data were re-analysed to estimate the energy dissipation rate and the residual head in the same manner as the current experimental data set. THORWARTH's data are included in Figures 5-1 and 5-2. The results showed a very good agreement between THORWARTH's (2008) reanalysed data and the present data.

5.2 FLOW RESISTANCE

The flow resistance on stepped spillways is characterised by significant form losses caused by the steps (CHANSON 2001). The form drag can be increased by the pool weir at the end of each step. It is common practice to use the Darcy-Weisbach friction factor to quantify the flow resistance in stepped spillway flows (RAJARATNAM 1990, CHANSON 2001). CHANSON et al. (2002) argued that neither the Darcy-Weisbach formula nor the Gauckler-Manning-Strickler formula can be used satisfactory because of the dominant form loss contribution.

In the present study, an uniform equilibrium flow was achieved at the chute downstream end because some small differences of air-water flow properties were observed between successive step edges (e.g. Fig. 4-7). Therefore the Darcy-Weisbach friction factor was calculated to quantify the average shear stress in the gradually-varied flow (e.g. CHANSON 1993):

$$f_e = \frac{8 \times \tau_0}{\rho_w \times U_w^2} = \frac{8 \times g \times S_f \times \left(\int_{y=0}^{Y_{90}} (1-C) dy \right)}{U_w^2} = \frac{8 \times g \times S_f \times d}{U_w^2} \quad (5\text{-}3)$$

where the friction slope equals $S_f = - \partial H / \partial x$, H is the total head, x is the distance in flow direction and U_w is the flow velocity (HENDERSON 1966; CHANSON 2001).

The friction factor was calculated for all experiments and the results are presented in Figure 5-3 as a function of the dimensionless step roughness height. In Figure 5-3, some data of THORWARTH (2008) are added: namely his experimental data on a stepped spillway with flat and pooled steps and 8.9°. Please note that THORWARTH (2008) calculated his friction factors assuming uniform equilibrium flow. For most discharges, the present data and THORWARTH's (2008) friction factor results agreed well (Fig. 5-3). Some small differences might be linked with the gradually varied nature of the air-water flows (FELDER & CHANSON 2009a). Some significantly larger friction factors were observed for the pooled stepped spillway with maximum values for the transition flow regimes (e.g. outlier in the pooled stepped spillway data for large step roughness heights in Fig. 5-

3). Some small values of f_e are visible for the flat stepped spillway (Fig. 5-3).

Fig. 5-3 Comparison of equivalent Darcy friction factors for the stepped spillway with flat, pooled and combination of flat and pooled steps (θ = 8.9°) - Comparison with the data of THORWARTH (2008)

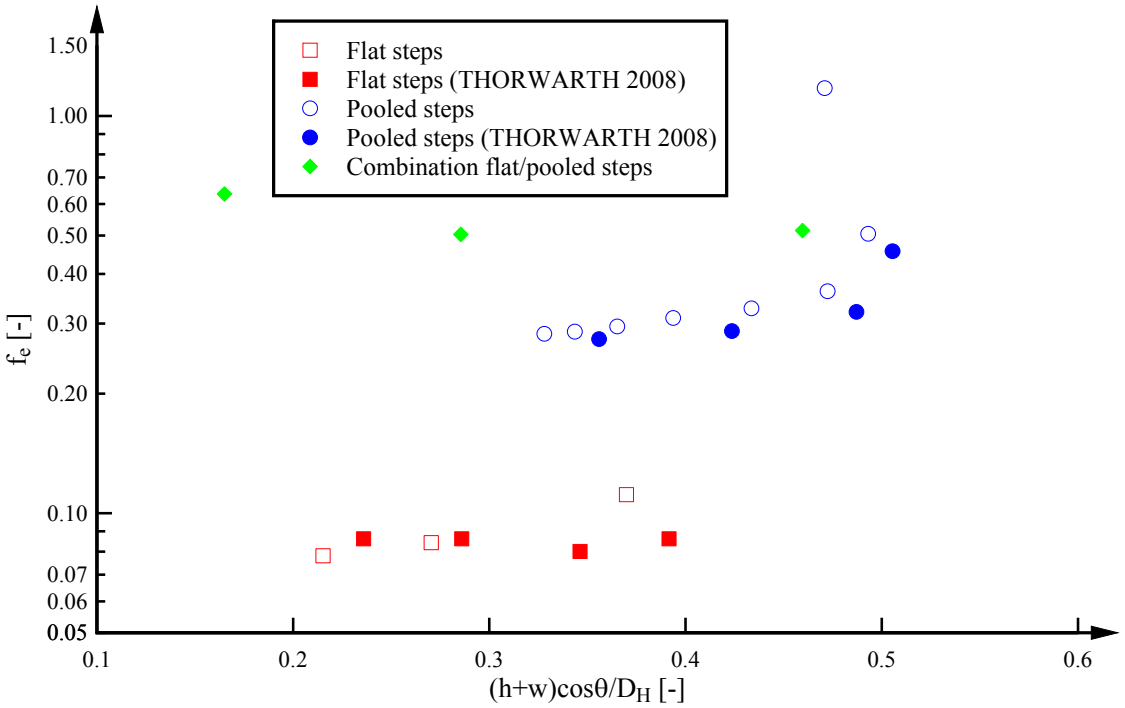

The calculation of the Darcy friction factors for the stepped spillway with combination of flat and pooled steps was more difficult because of the non-uniform nature of the flows caused by the alternation of flat and pooled steps. Figure 5-4 shows some typical longitudinal variation of the total head at the downstream end of the spillway for several consecutive step edges. The data showed that, for the combination of flat and pooled steps, the total head line had a seesaw pattern with larger total head for the flat steps. The total head for the flat and pooled stepped spillways decayed gradually with an almost linear friction slope close to the bed slope sin θ. The Darcy-Weisbach friction factor $\overline{f}_e$ for the stepped spillway with combination of flat and pooled steps was calculated by averaging the friction factors calculated for the flat and pooled steps in this configuration respectively:

$$\overline{f}_e = \frac{8 \times g \times \overline{d} \times \overline{S}_f}{\overline{U}_w^2} \qquad (5\text{-}4)$$

where $\overline{d}$ is the average clear water flow depth, $\overline{S}_f$ the average friction slope for the flat and pooled steps respectively and $\overline{U}$ the average flow velocity. The Darcy-Weisbach friction factors for the

combination of flat and pooled steps are included Figure 5-3 and the results showed the largest flow resistance with the combined pool configuration for all investigated flow rates.

Fig. 5-4 - Total head line at the downstream end of the chute for the stepped spillway with flat, pooled and combination of flat and pooled steps - Flow conditions: $\theta = 8.9°$, $d_c/h = 2.66$, $Q = 0.076$ m^3/s, $Re = 6.03 \times 10^5$

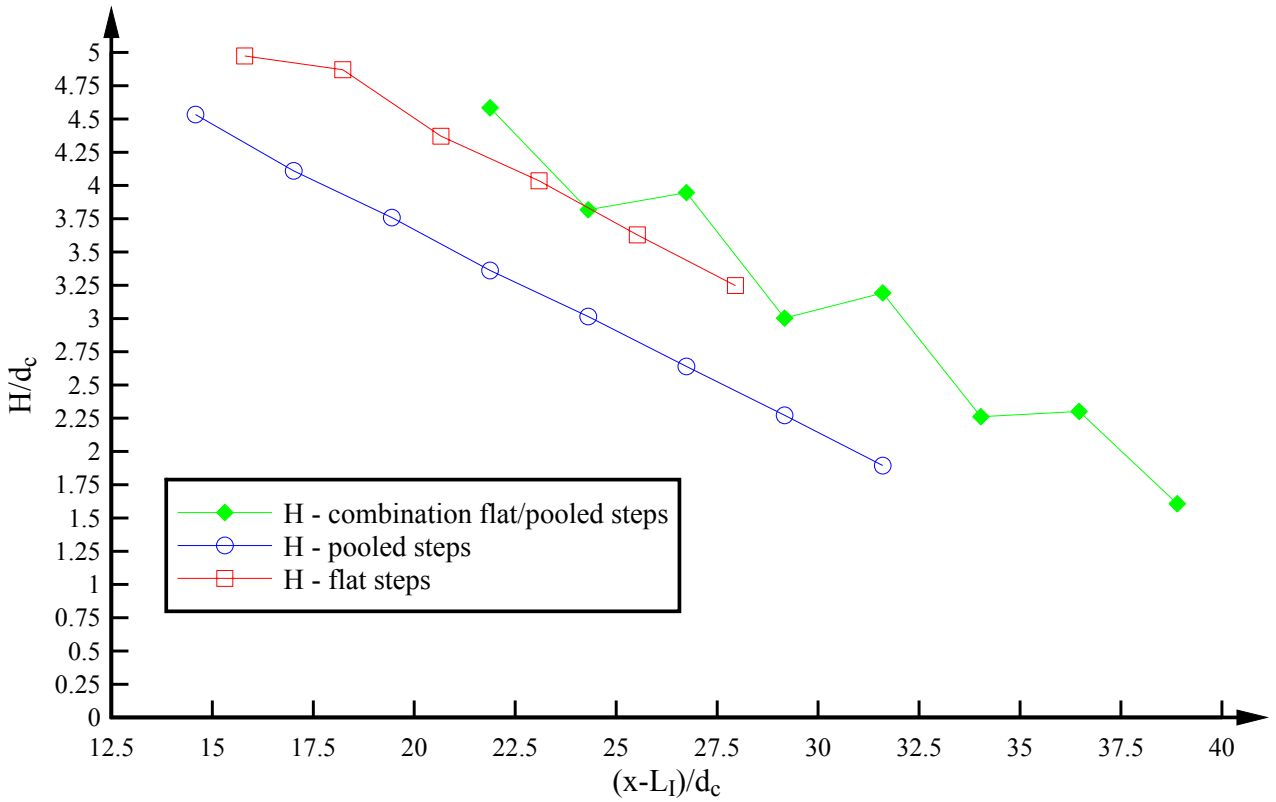

6. CONCLUSION

A physical study was performed on a stepped spillway model with a 8.9° slope and step heights of 0.05 m. Three stepped configurations were tested: these were a flat stepped chute, a pooled step chute (w/h = 1) and a chute with an alternation of flat and pooled steps. Detailed air-water flow measurements were conducted with a double-tip conductivity probe for all three stepped configurations and a comparative analysis was performed for a broad range of discharges 0.02 $m^3/s \leq Q \leq 0.117$ m^3/s corresponding to Reynolds numbers between 1.4×10^5 and 9.3×10^5.

The visual observations showed some typical flow pattern with nappe, transition and skimming flows depending upon the flow rate on the flat stepped spillway. On the pooled stepped spillway configurations, some strong instabilities were observed in the transition flow regime. The self-induced instabilities were associated with instationary cavity recirculation and ejection processes as well as some strong jump waves propagating downstream. For the stepped spillway with combination of flat and pooled steps, no skimming flow regime was achieved within the range of investigated flow rates.

A comparison of air-water flow properties showed some basic differences between the three configurations in terms of void fraction, bubble count rate, interfacial velocity, turbulence intensity and chord size distributions. The void fraction distributions on flat and pooled stepped spillways were overall in agreement, but the combination of flat and pooled steps yielded some stronger aeration for the same flow rate. The interfacial velocity distributions showed largest interfacial velocities for the flat stepped spillway. The turbulence levels were significantly larger on the pooled stepped spillways and it is believed that this was caused by the flow instationarities. The distributions of air bubble and water droplet chord sizes were comparable.

A comparative analysis in terms of the rate of energy dissipation and residual head showed that the largest rate of energy dissipation and the smallest residual head were achieved for the stepped spillway with combination of flat and pooled steps. The largest residual head and smallest energy dissipation rate were observed for the flat stepped spillway. Similarly the Darcy-Weisbach friction factor data showed the smallest values for the flat stepped spillway and the largest friction factors for the pooled stepped spillway configurations.

While the stepped chute configuration with a combination of flat and pooled steps yielded the largest rate of energy dissipation, the geometry may not be regarded as an optimum design. This configuration was characterised by some strong flow instabilities and unsteady flow processes which may be unsuitable for a safe operation of the structure. An incidents on the Sorpe dam pooled stepped spillway was documented and illustrated by CHANSON (2001) and THORWARTH (2008).

7. ACKNOWLEDGEMENTS

The authors thank Dr Mehmet A. KÖKPINAR (Turkey) for his detailed review of the report and valuable comments. They acknowledge the comments of Stefanie LORKE (IWW, RWTH Aachen University, Germany). Some exchange with Dr Marat MIRZOEV (Russia) is acknowledged. The writers thank Professor Holger SCHÜTTRUMPF (IWW, RWTH Aachen University, Germany) for providing access to the experimental facility for the stepped spillway experiments. The first writer acknowledges the financial support through an University of Queensland research scholarship and the Graduate School International Travel Award for undertaking the research at the IWW. The financial support of the Australian Research Council is acknowledged (ARC DP0878922 & DP120100481).

APPENDIX A – PRESENTATION OF AIR-WATER FLOW PROPERTIES FOR THE STEPPED SPILLWAYS

A.1 PRESENTATION

Experiments were conducted on a stepped spillway model equipped with flat steps, pooled steps and a combination of flat and pooled steps for a range of discharges $0.018 < Q < 0.117$ m^3/s. For all three configurations, the air-water flow properties were measured with a double-tip conductivity probe at several step edges downstream of the inception point of free surface aeration. Some basic air-water flow properties were calculated for some typical transition and skimming flow discharges. In this Appendix, the air-water flow properties of void fraction C, bubble count rate F, interfacial velocity V and turbulence levels Tu are presented for all experiments. The flow properties are presented in dimensionless terms. On the left hand side of the figures, the data are presented as a function of y/Y_{90} and on the right hand side as a function of $(y+w)/d_c$. Table A-1 summarises the presented data. Furthermore some characteristic air bubble and water droplet chord size distributions are shown in Figures A-9 to A-14 for several discharges at two consecutive step edges for all three configurations.

Tab. A-1 Summary of compared air-water flow properties and positioning in the following figures (Fig. A-1 to A-8)

C as a function of y/Y_{90}	C as a function of $(y+w)/d_c$
$F \times d_c/V_c$ as a function of y/Y_{90}	$F \times d_c/V_c$ as a function of $(y+w)/d_c$
V/V_c as a function of y/Y_{90}	V/V_c as a function of $(y+w)/d_c$
Tu as a function of y/Y_{90}	Tu as a function of $(y+w)/d_c$

Notes: y: distance normal to the pseudo bottom; Y_{90}: characteristic distance where C = 90%; C: void fraction; F: bubble count rate; d_c: critical flow depth; V_c: critical flow velocity; V: interfacial velocity; Tu: turbulence intensity; w: pool weir height

Fig. A-1 Comparison of dimensionless air-water flow properties on stepped spillway with flat, pooled and combination of flat and pooled steps: θ = 8.9°, d_c/h = 1.35, Q = 0.027 m^3/s, Re = 2.18×10^5

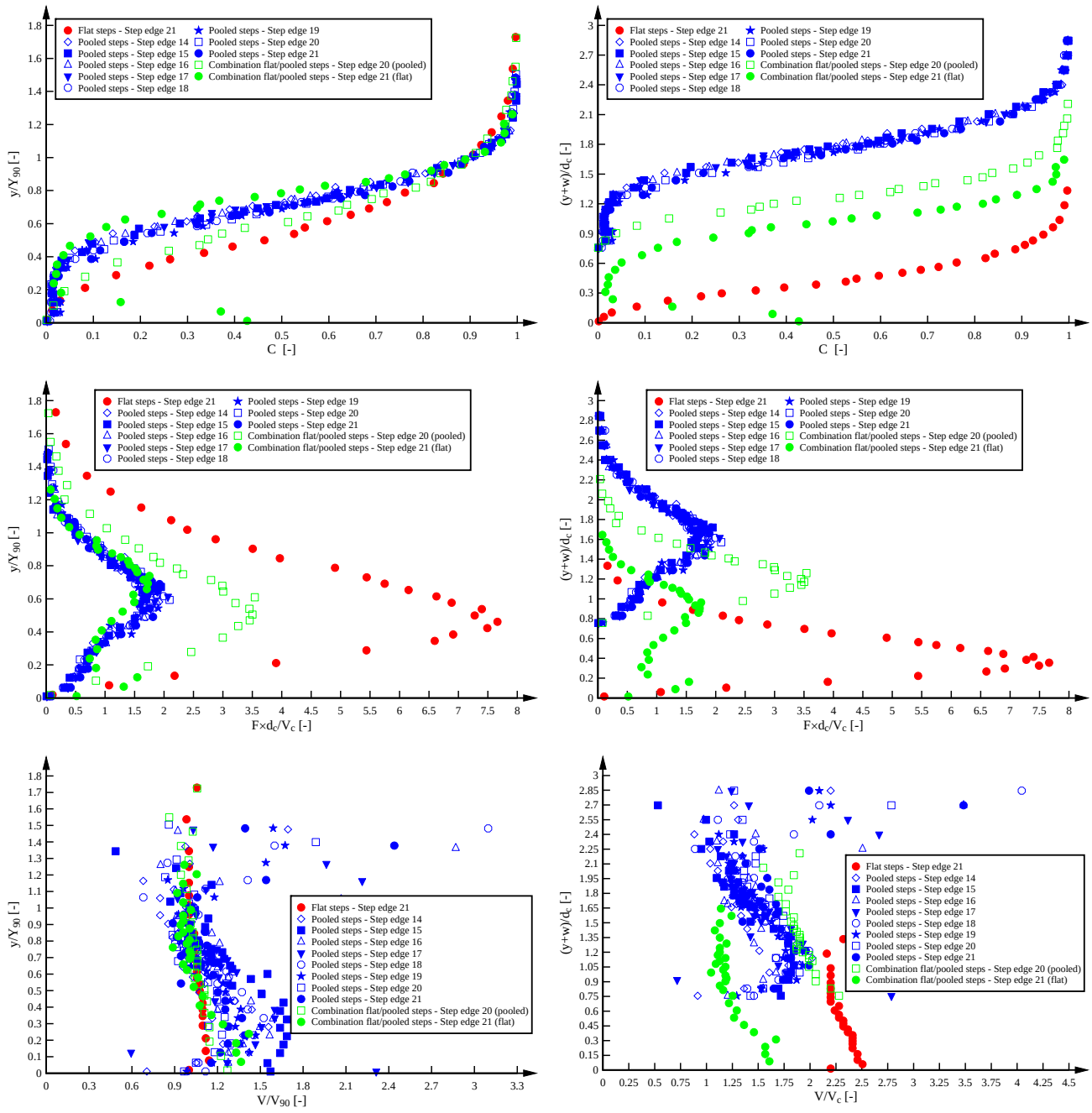

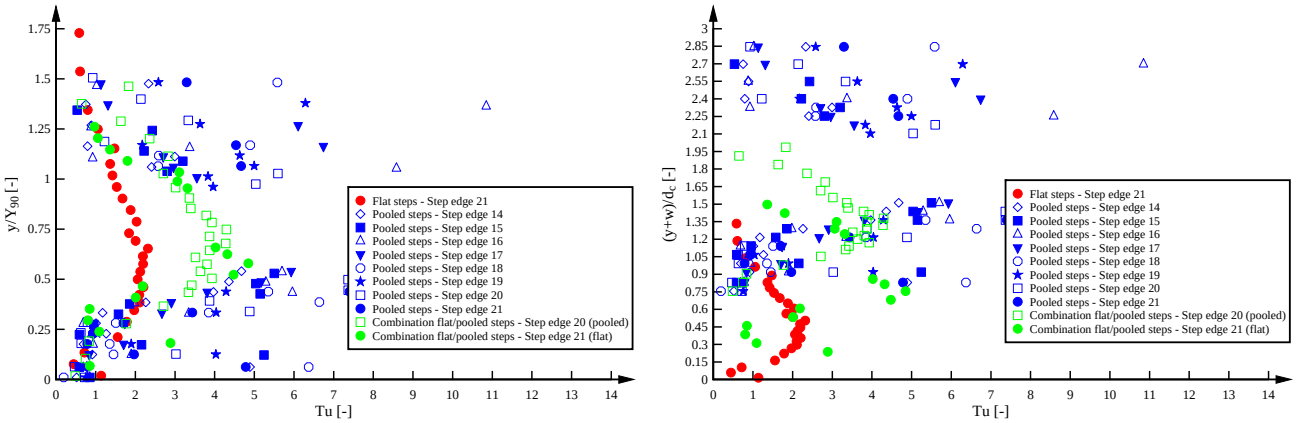

Fig. A-2 Comparison of dimensionless air-water flow properties on stepped spillway with flat, pooled and combination of flat and pooled steps: θ = 8.9°, d_c/h = 1.7, Q = 0.039 m^3/s, Re = 3.10×10^5

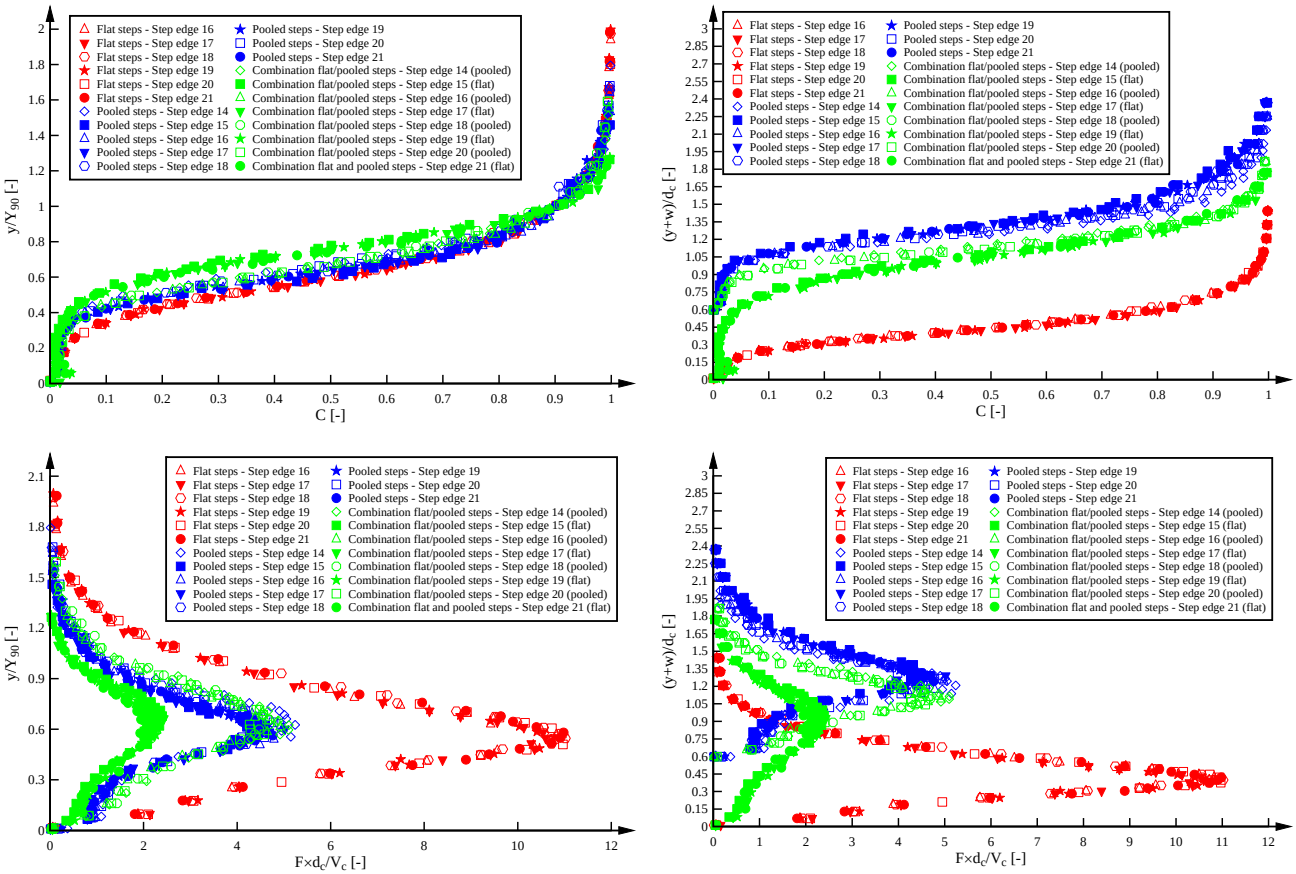

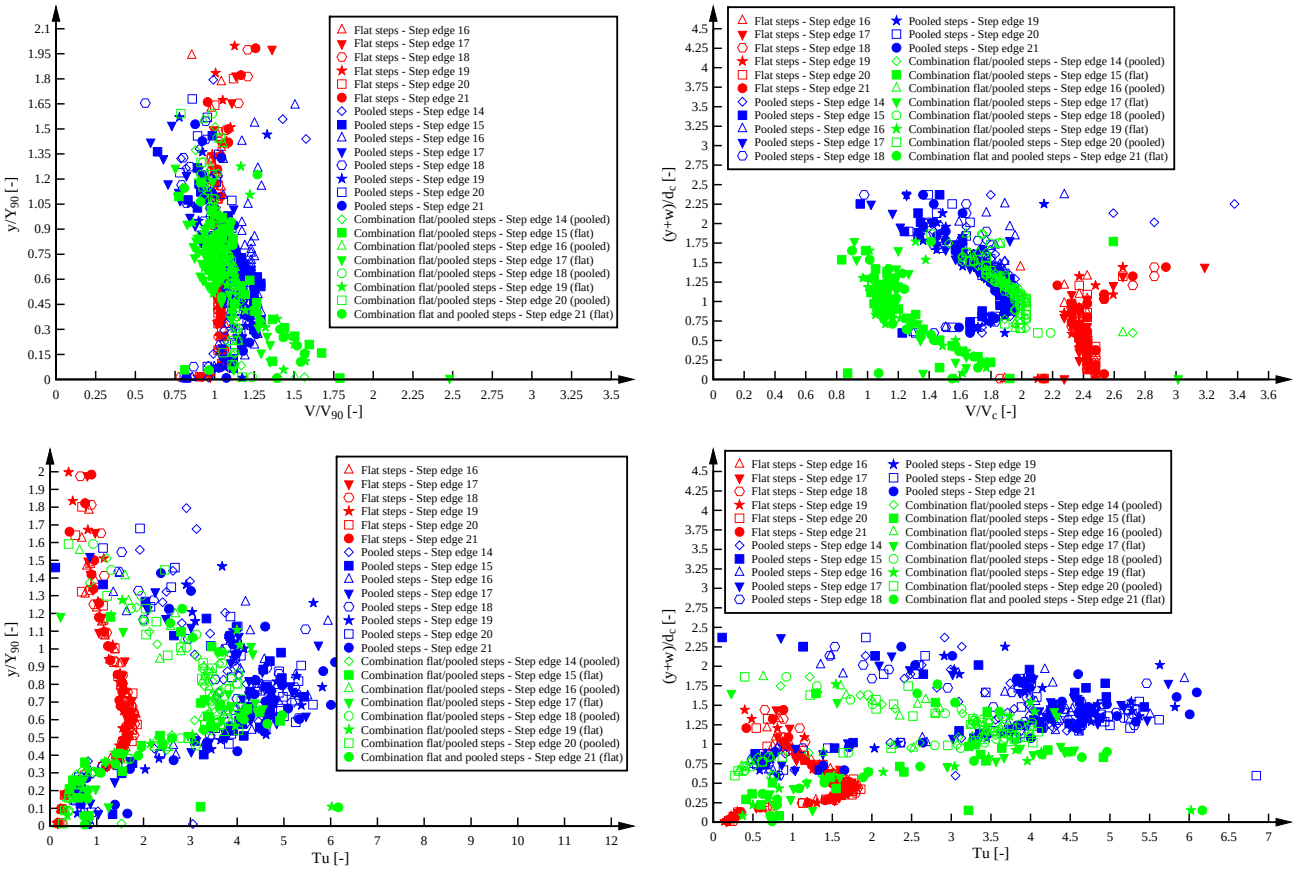

Fig. A-3 Comparison of dimensionless air-water flow properties on stepped spillway with flat, pooled and combination of flat and pooled steps: θ = 8.9°, d_c/h = 2.0, Q = 0.049 m^3/s, Re = 3.93×10^5

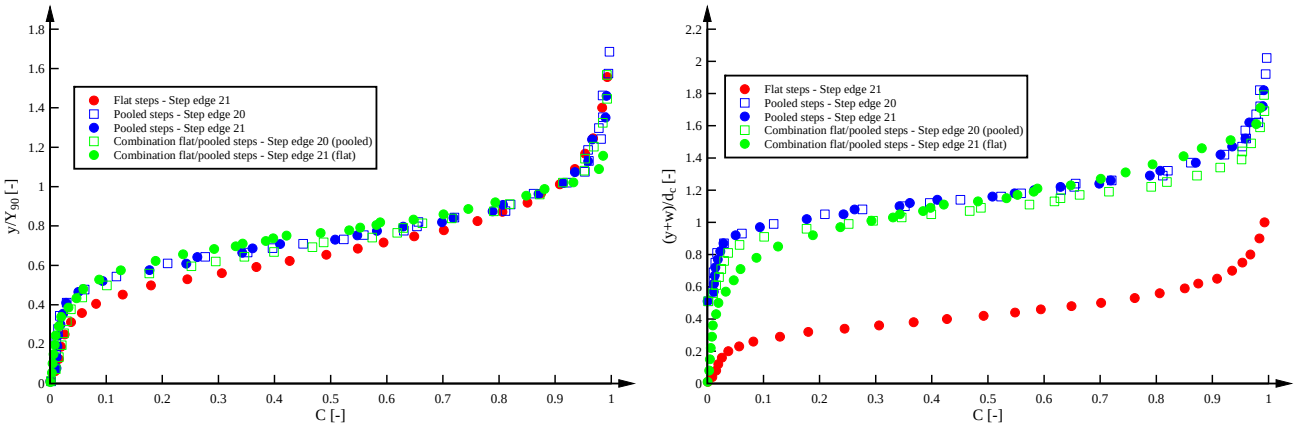

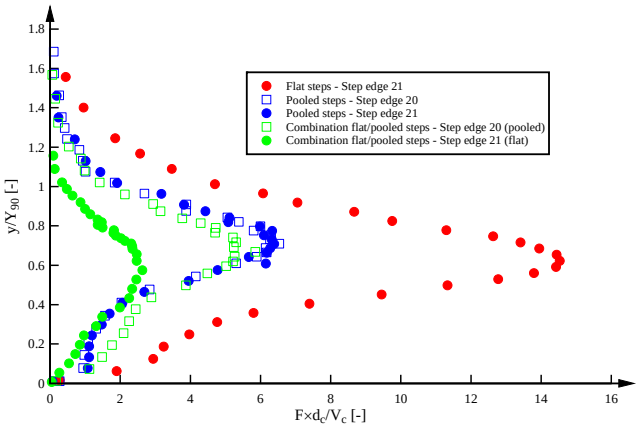
Flat steps - Step edge 21
Pooled steps - Step edge 20
Pooled steps - Step edge 21
Combination flat/pooled steps - Step edge 20 (pooled)
Combination flat/pooled steps - Step edge 21 (flat)
y/Y90 [-]
F×dc/Vc [-]

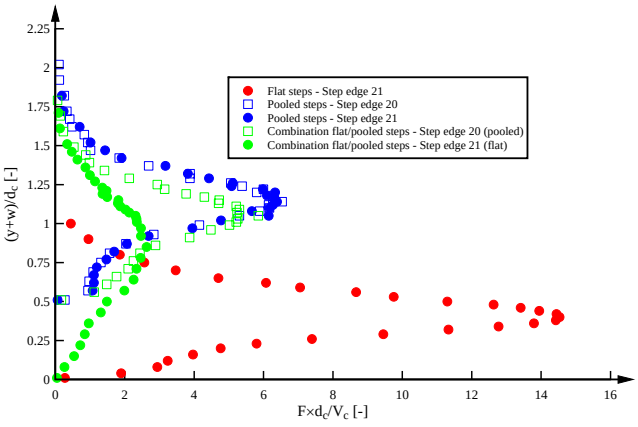
Flat steps - Step edge 21
Pooled steps - Step edge 20
Pooled steps - Step edge 21
Combination flat/pooled steps - Step edge 20 (pooled)
Combination flat/pooled steps - Step edge 21 (flat)
(y+w)/dc [-]
F×dc/Vc [-]

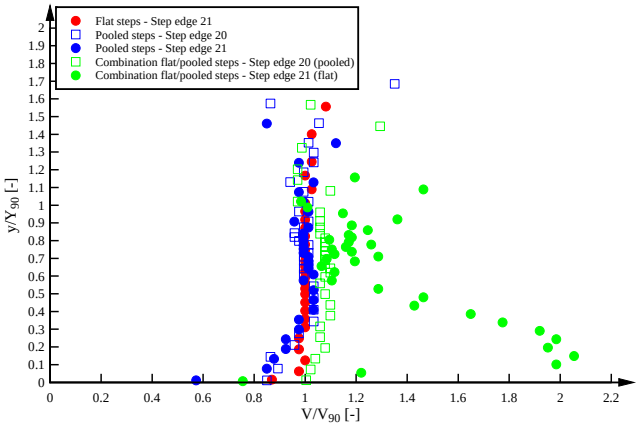
Flat steps - Step edge 21
Pooled steps - Step edge 20
Pooled steps - Step edge 21
Combination flat/pooled steps - Step edge 20 (pooled)
Combination flat/pooled steps - Step edge 21 (flat)
y/Y90 [-]
V/V90 [-]

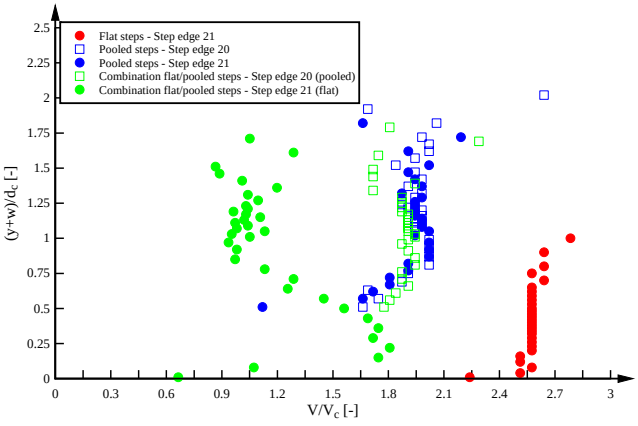
Flat steps - Step edge 21
Pooled steps - Step edge 20
Pooled steps - Step edge 21
Combination flat/pooled steps - Step edge 20 (pooled)
Combination flat/pooled steps - Step edge 21 (flat)
(y+w)/dc [-]
V/Vc [-]

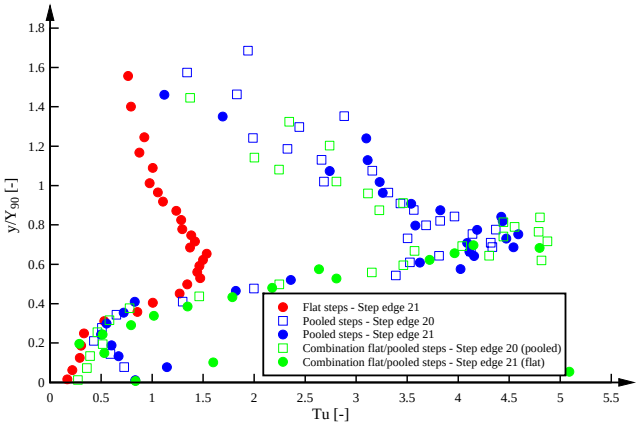
Flat steps - Step edge 21
Pooled steps - Step edge 20
Pooled steps - Step edge 21
Combination flat/pooled steps - Step edge 20 (pooled)
Combination flat/pooled steps - Step edge 21 (flat)
y/Y90 [-]
Tu [-]

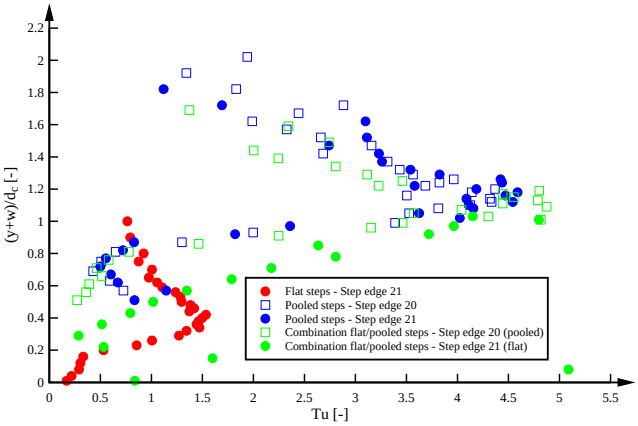
Flat steps - Step edge 21
Pooled steps - Step edge 20
Pooled steps - Step edge 21
Combination flat/pooled steps - Step edge 20 (pooled)
Combination flat/pooled steps - Step edge 21 (flat)
(y+w)/dc [-]
Tu [-]

Fig. A-4 Comparison of dimensionless air-water flow properties on stepped spillway with flat, pooled and combination of flat and pooled steps: θ = 8.9°, d_c/h = 2.3, Q = 0.061 m^3/s, Re = 4.85×10^5

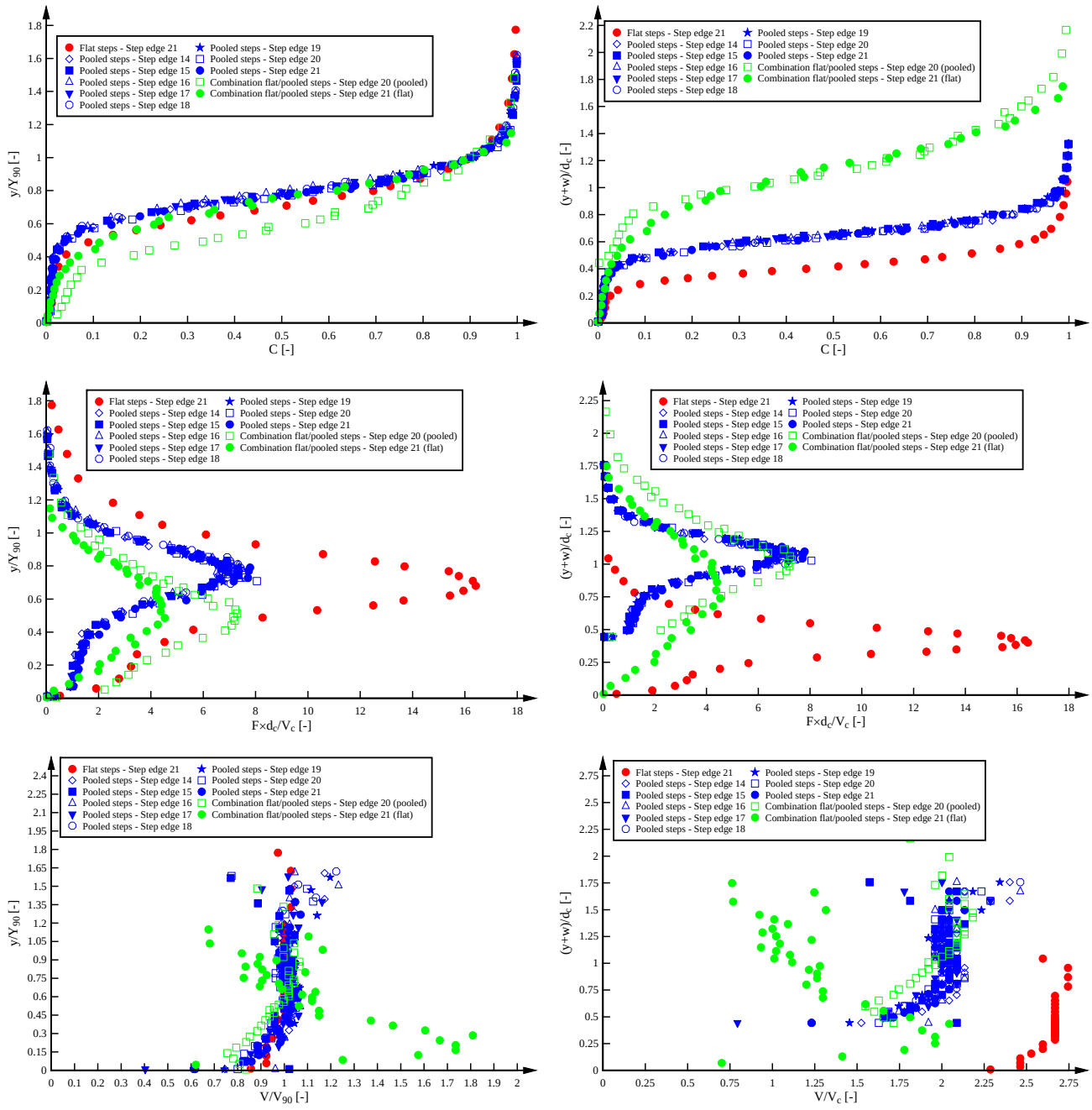

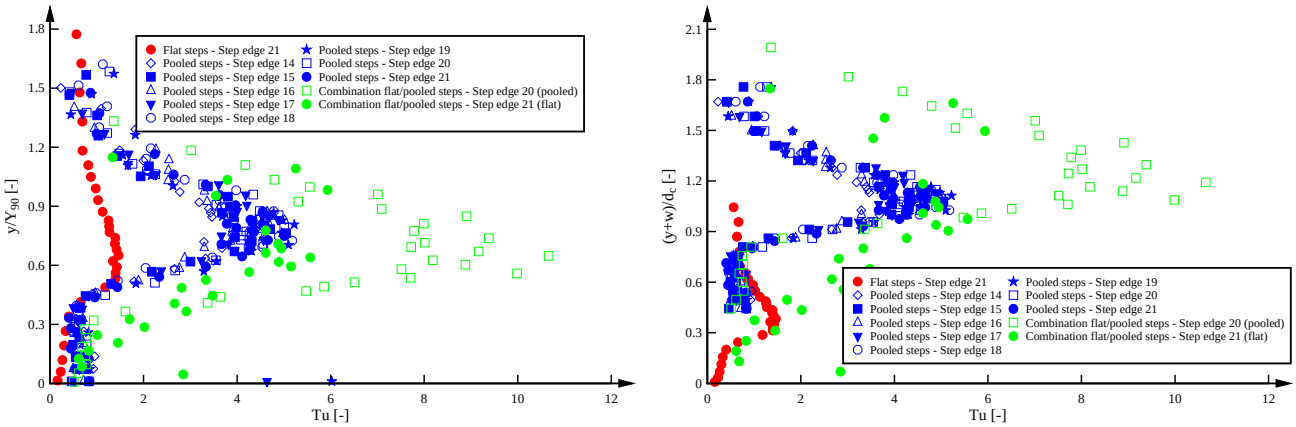

Fig. A-5 Comparison of dimensionless air-water flow properties on stepped spillway with flat, pooled and combination of flat and pooled steps: θ = 8.9°, d_c/h = 2.66, Q = 0.076 m^3/s, Re = 6.03×10^5

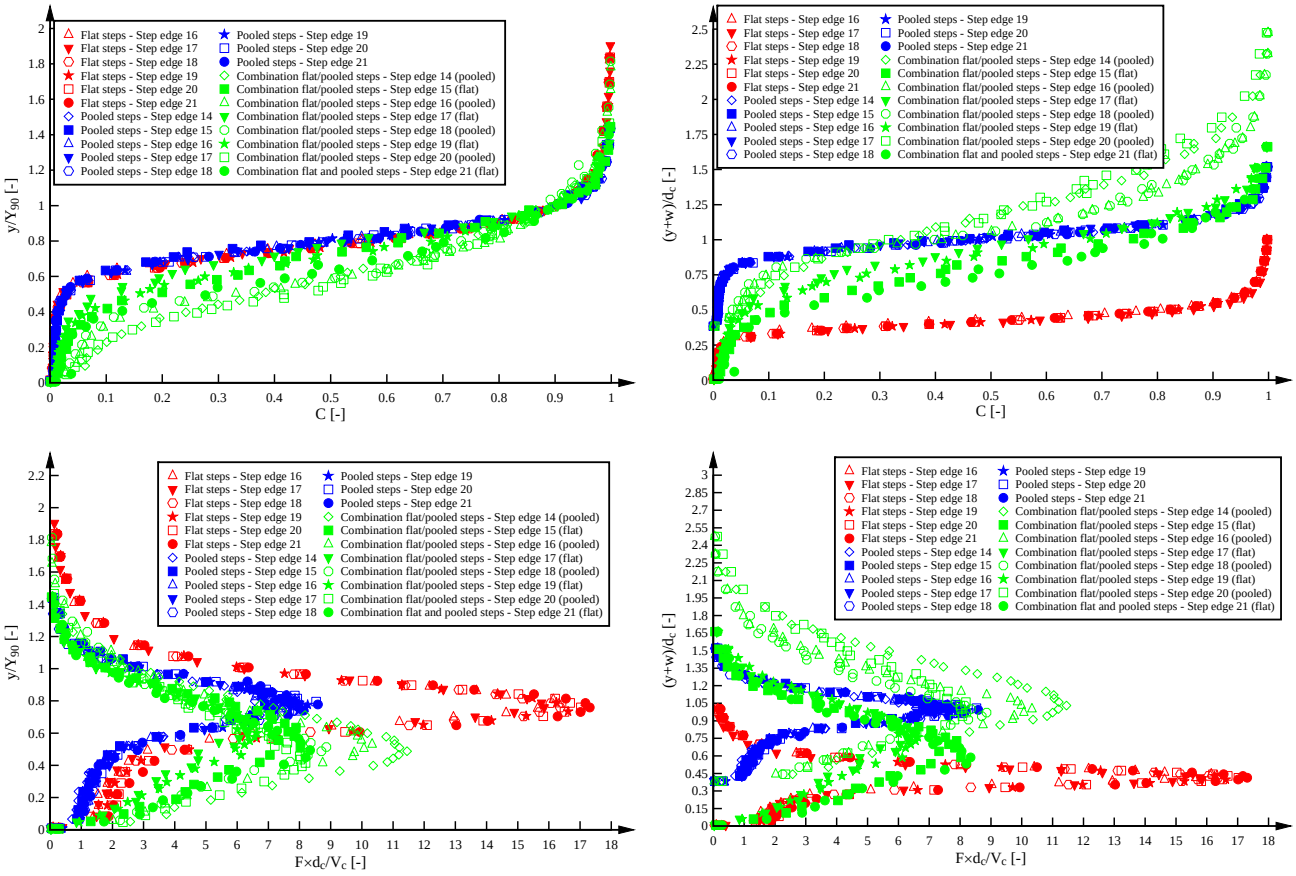

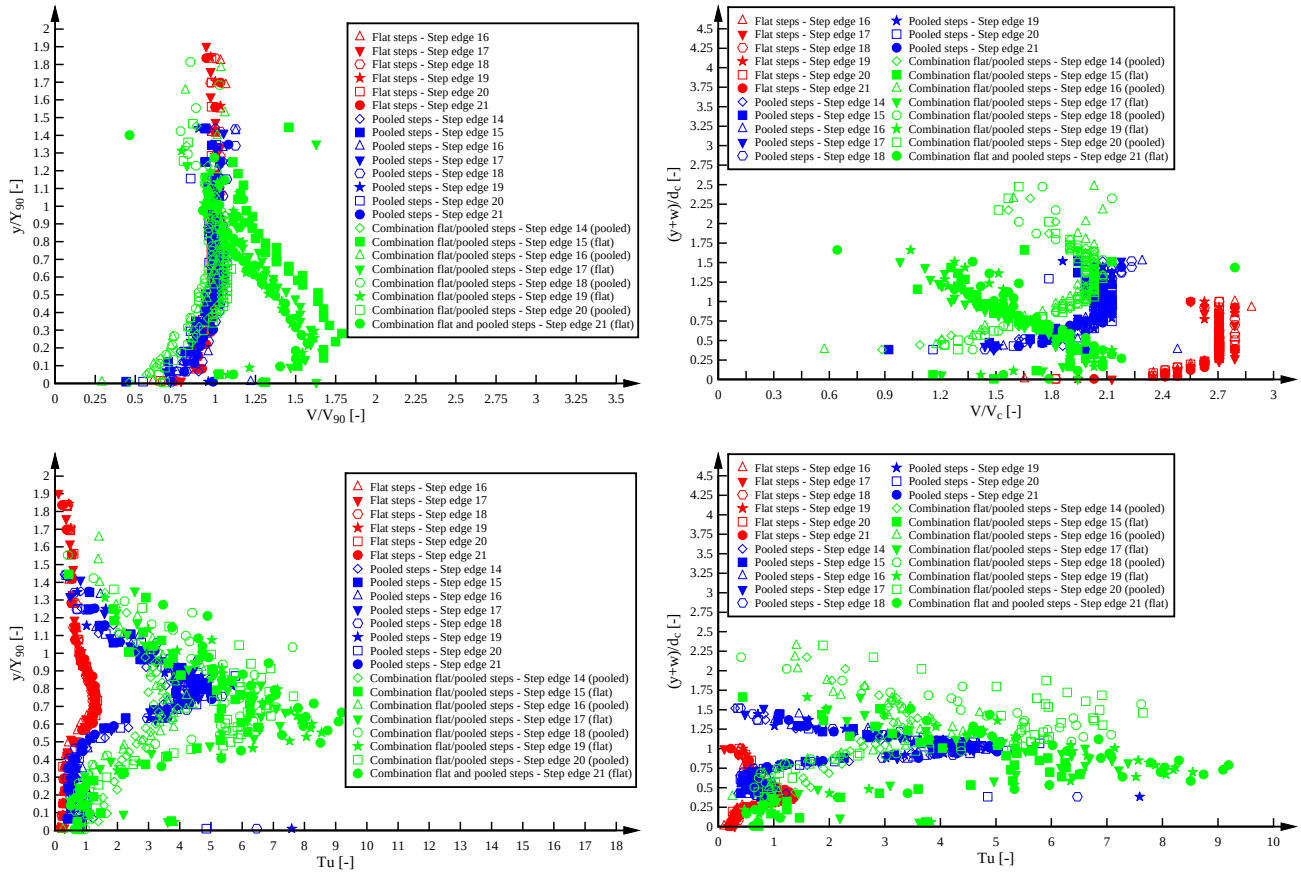

Fig. A-6 Comparison of dimensionless air-water flow properties on stepped spillway with flat, pooled and combination of flat and pooled steps: θ = 8.9°, d_c/h = 3.0, Q = 0.091 m^3/s, Re = 7.23×10^5

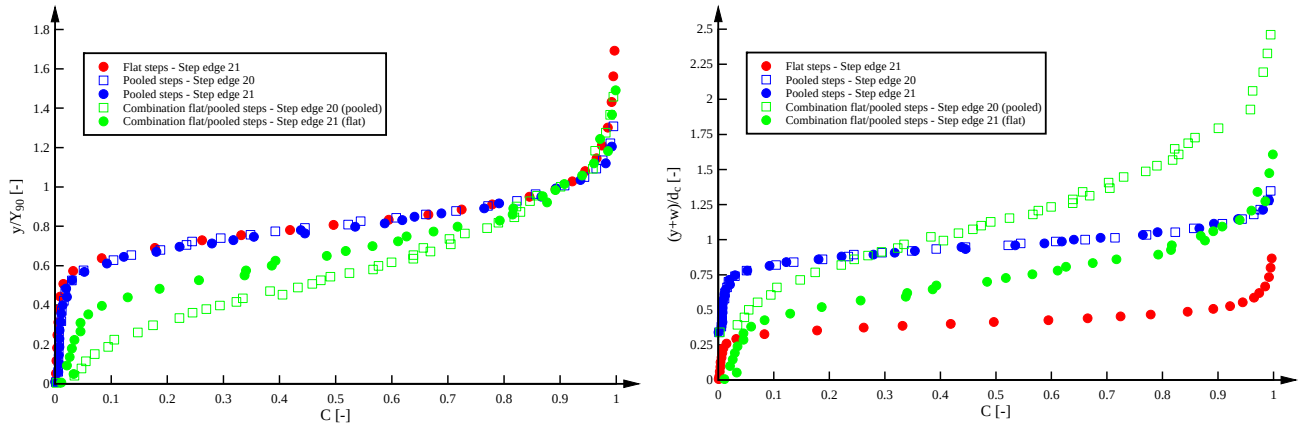

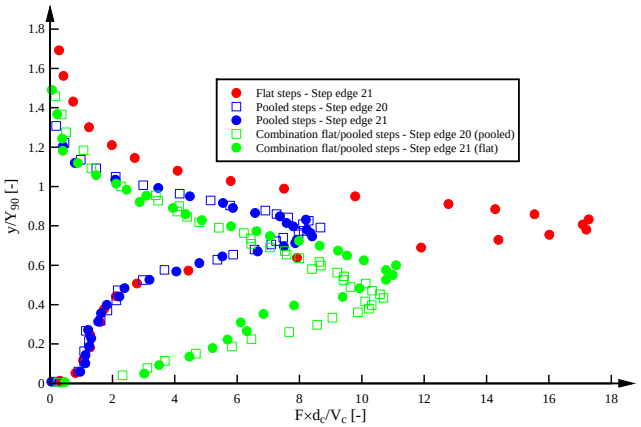
Flat steps - Step edge 21
Pooled steps - Step edge 20
Pooled steps - Step edge 21
Combination flat/pooled steps - Step edge 20 (pooled)
Combination flat/pooled steps - Step edge 21 (flat)
y/Y90 [-]
F×dc/Vc [-]

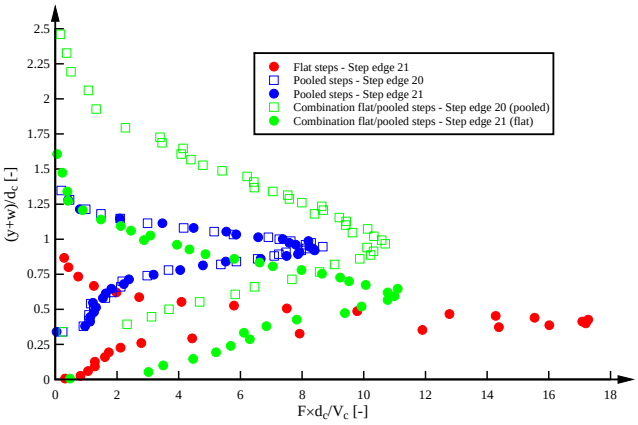
Flat steps - Step edge 21
Pooled steps - Step edge 20
Pooled steps - Step edge 21
Combination flat/pooled steps - Step edge 20 (pooled)
Combination flat/pooled steps - Step edge 21 (flat)
(y+w)/dc [-]
F×dc/Vc [-]

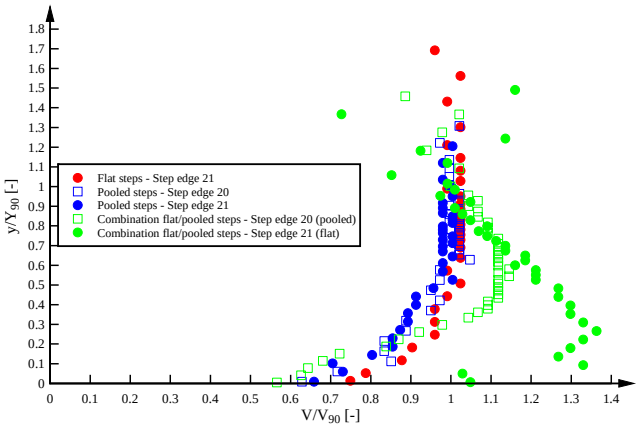
Flat steps - Step edge 21
Pooled steps - Step edge 20
Pooled steps - Step edge 21
Combination flat/pooled steps - Step edge 20 (pooled)
Combination flat/pooled steps - Step edge 21 (flat)
y/Y90 [-]
V/V90 [-]

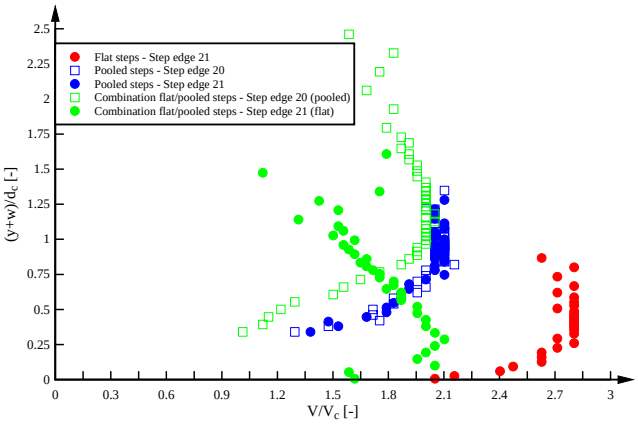
Flat steps - Step edge 21
Pooled steps - Step edge 20
Pooled steps - Step edge 21
Combination flat/pooled steps - Step edge 20 (pooled)
Combination flat/pooled steps - Step edge 21 (flat)
(y+w)/dc [-]
V/Vc [-]

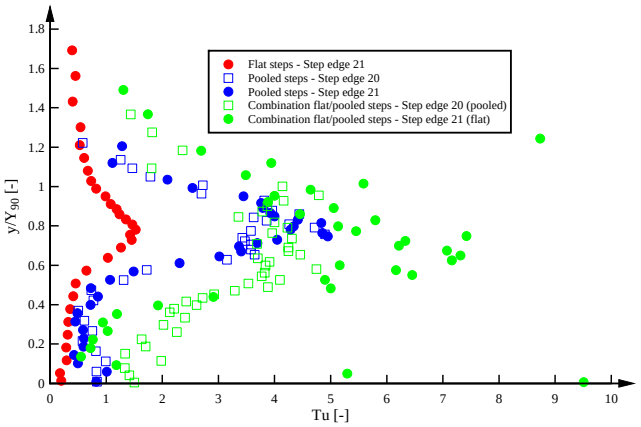
Flat steps - Step edge 21
Pooled steps - Step edge 20
Pooled steps - Step edge 21
Combination flat/pooled steps - Step edge 20 (pooled)
Combination flat/pooled steps - Step edge 21 (flat)
y/Y90 [-]
Tu [-]

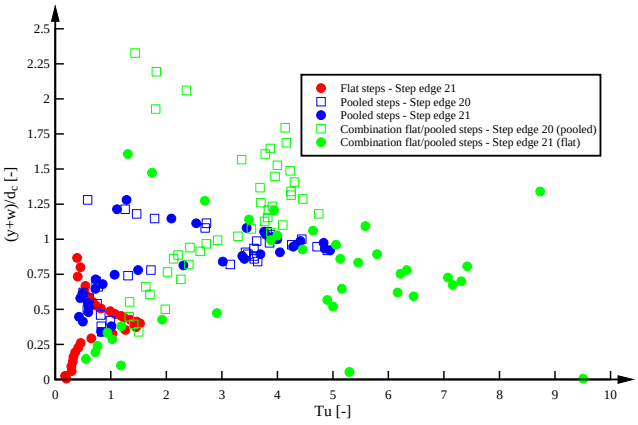
Flat steps - Step edge 21
Pooled steps - Step edge 20
Pooled steps - Step edge 21
Combination flat/pooled steps - Step edge 20 (pooled)
Combination flat/pooled steps - Step edge 21 (flat)
(y+w)/dc [-]
Tu [-]

Fig. A-7 Comparison of dimensionless air-water flow properties on stepped spillway with flat, pooled and combination of flat and pooled steps: θ = 8.9°, d_c/h = 3.3, Q = 0.105 m^3/s, Re = 8.34×10^5

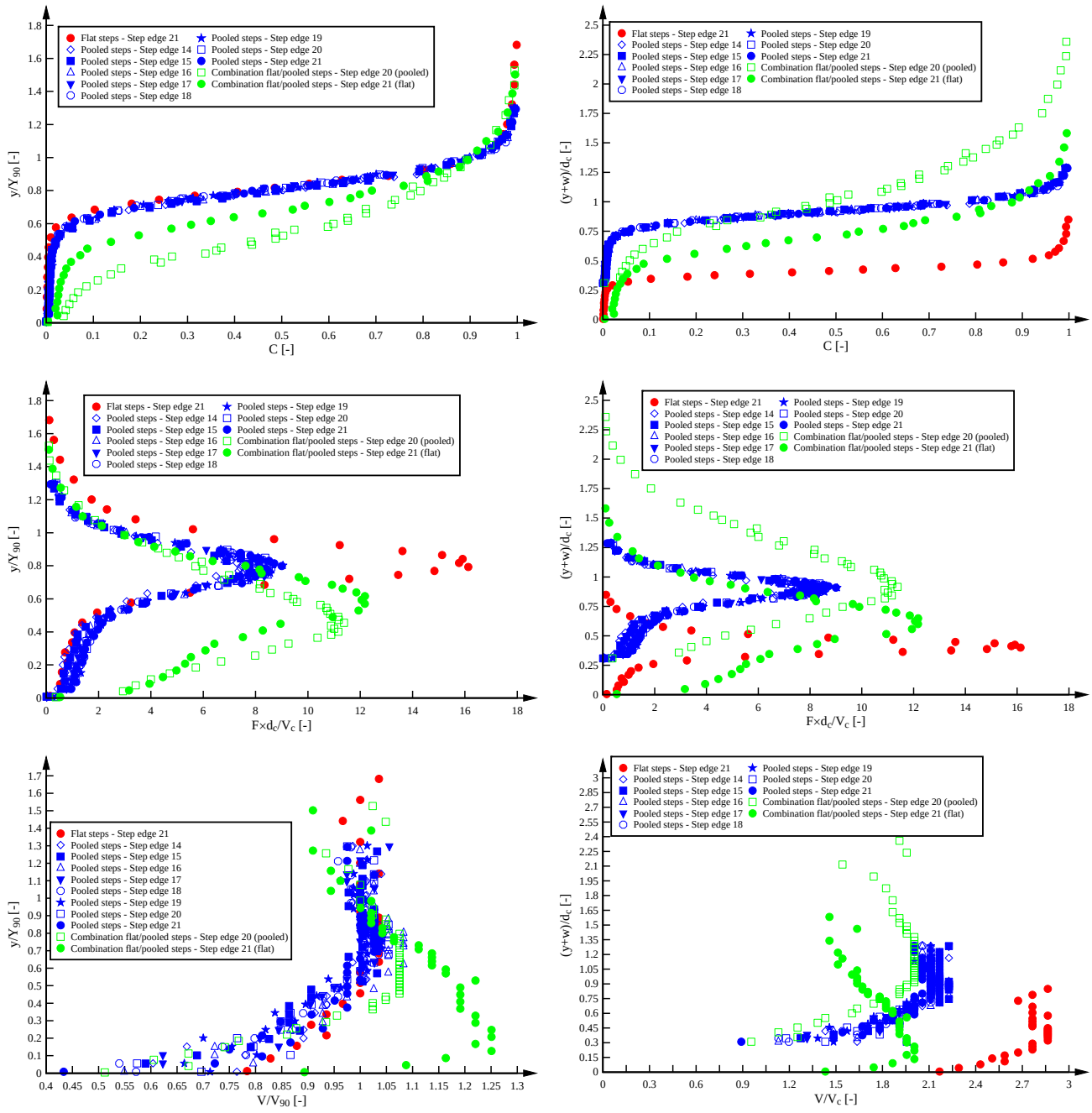

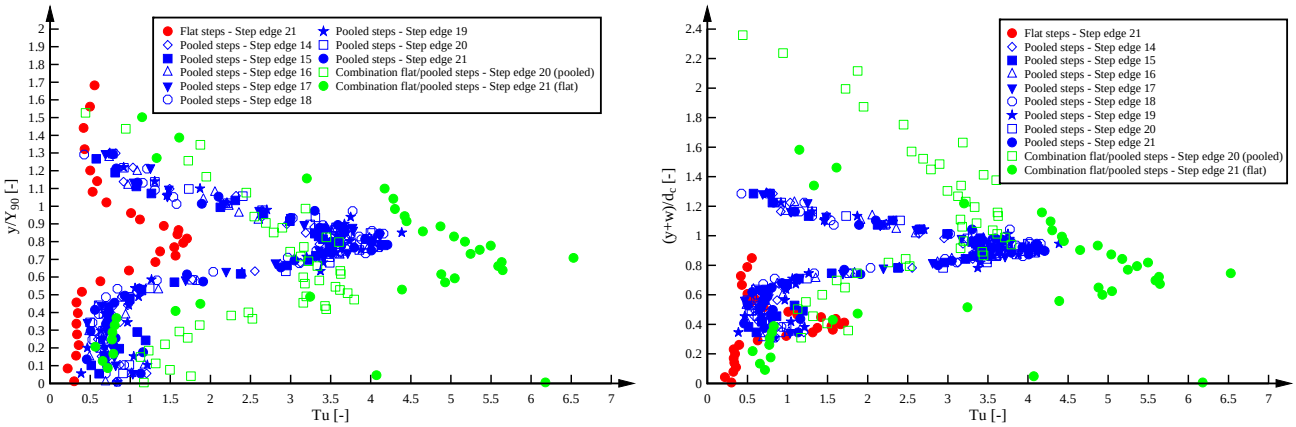

Fig. A-8 Comparison of dimensionless air-water flow properties on stepped spillway with flat, pooled and combination of flat and pooled steps: θ = 8.9°, d_c/h = 3.55, Q = 0.117 m^3/s, Re = 9.30×10^5

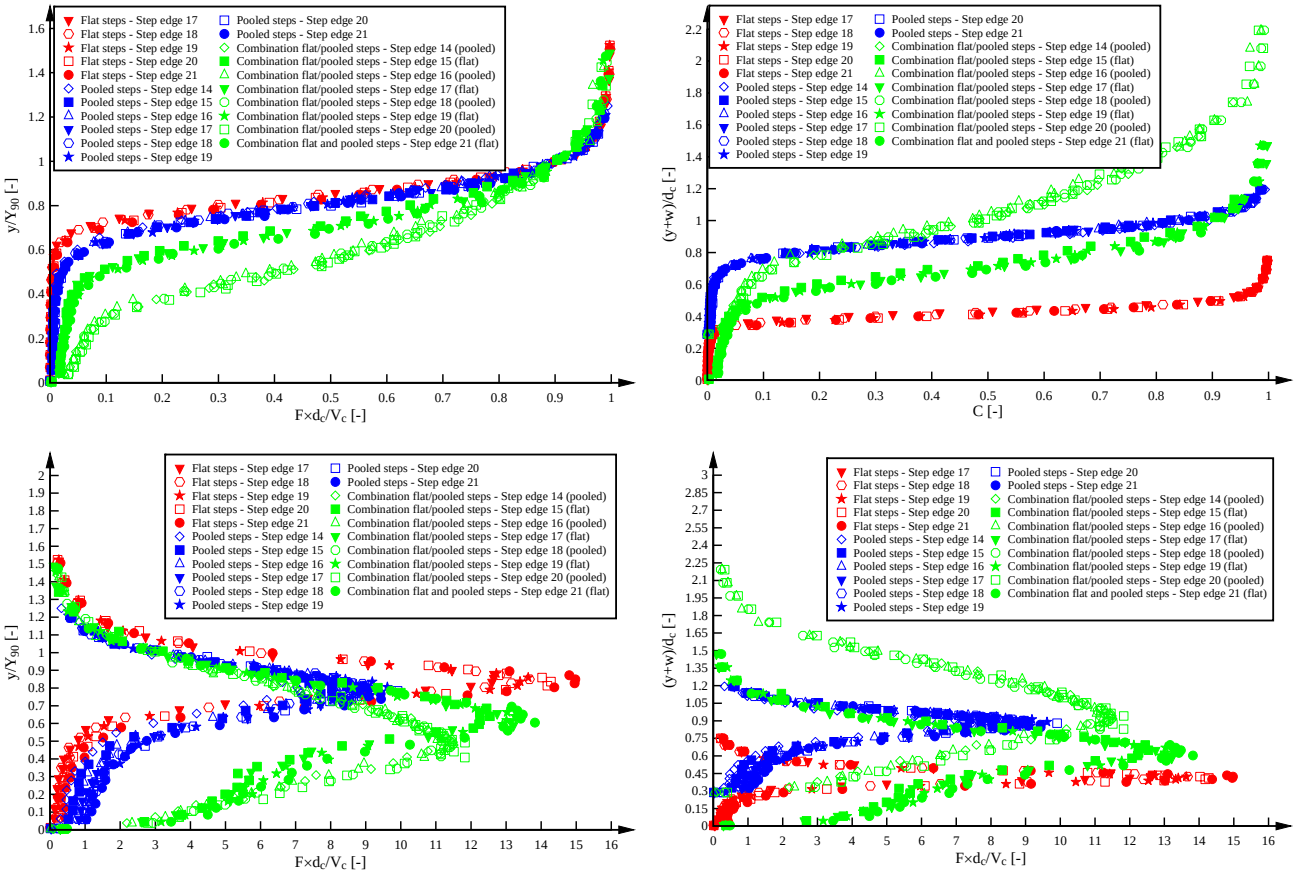

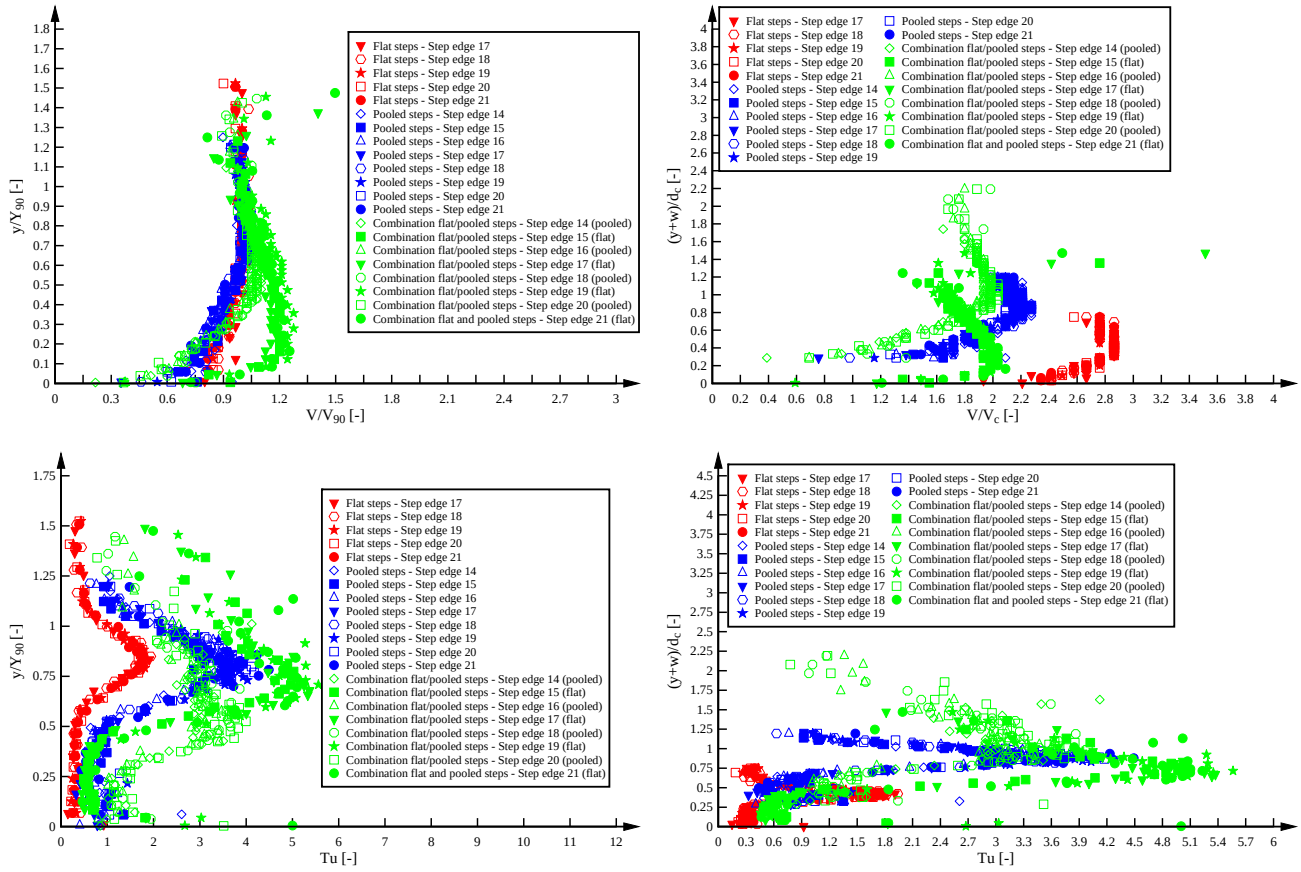

Fig. A-9 Comparison of probability distribution functions of air bubble chord sizes on stepped spillways with flat, pooled and combination of flat and pooled steps: θ = 8.9°, d_c/h = 1.7, Q = 0.039 m^3/s, Re = 3.10×10^5

(A) Step edge 20

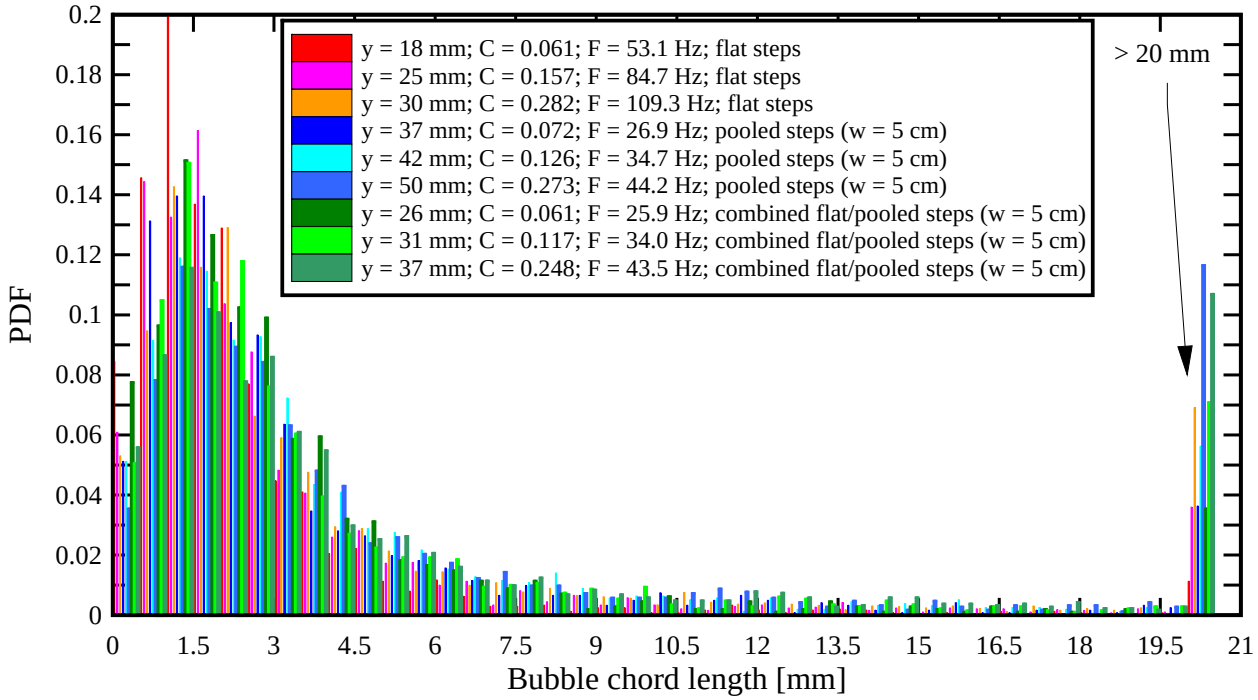

(B) Step edge 21

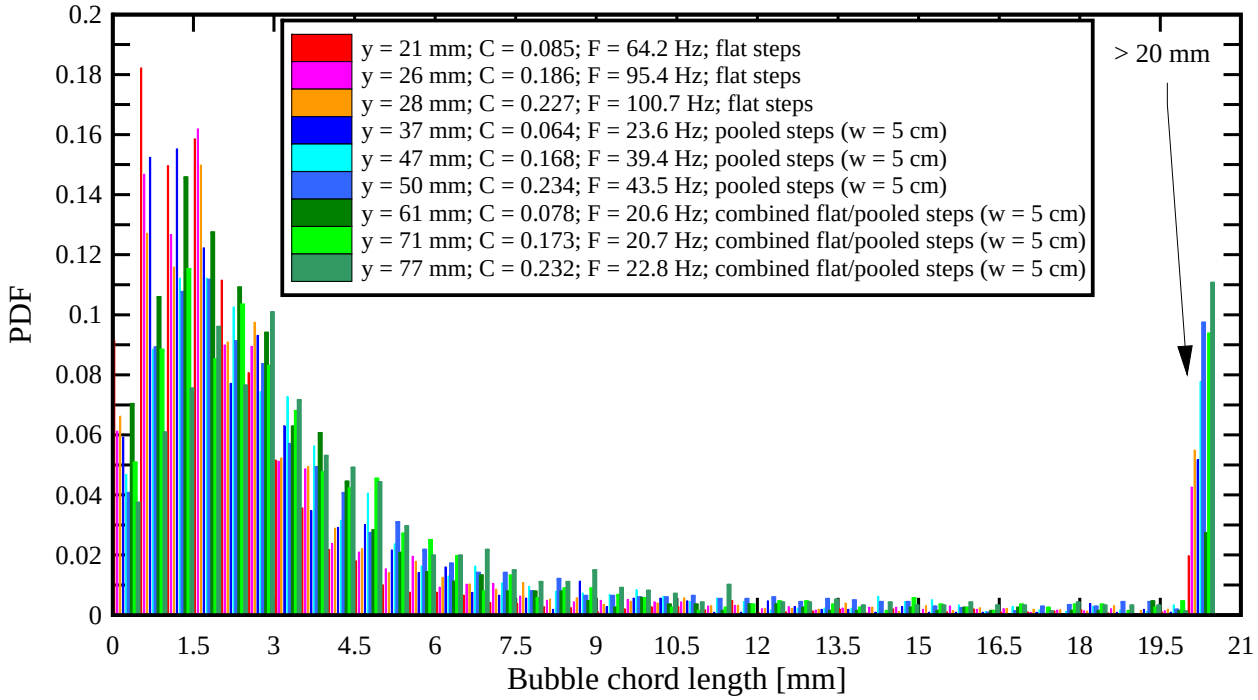

Fig. A-10 Comparison of probability distribution functions of air bubble chord sizes on stepped spillways with flat, pooled and combination of flat and pooled steps: θ = 8.9°, d_c/h = 2.66, Q = 0.076 m^3/s, Re = 6.03×10^5

(A) Step edge 20

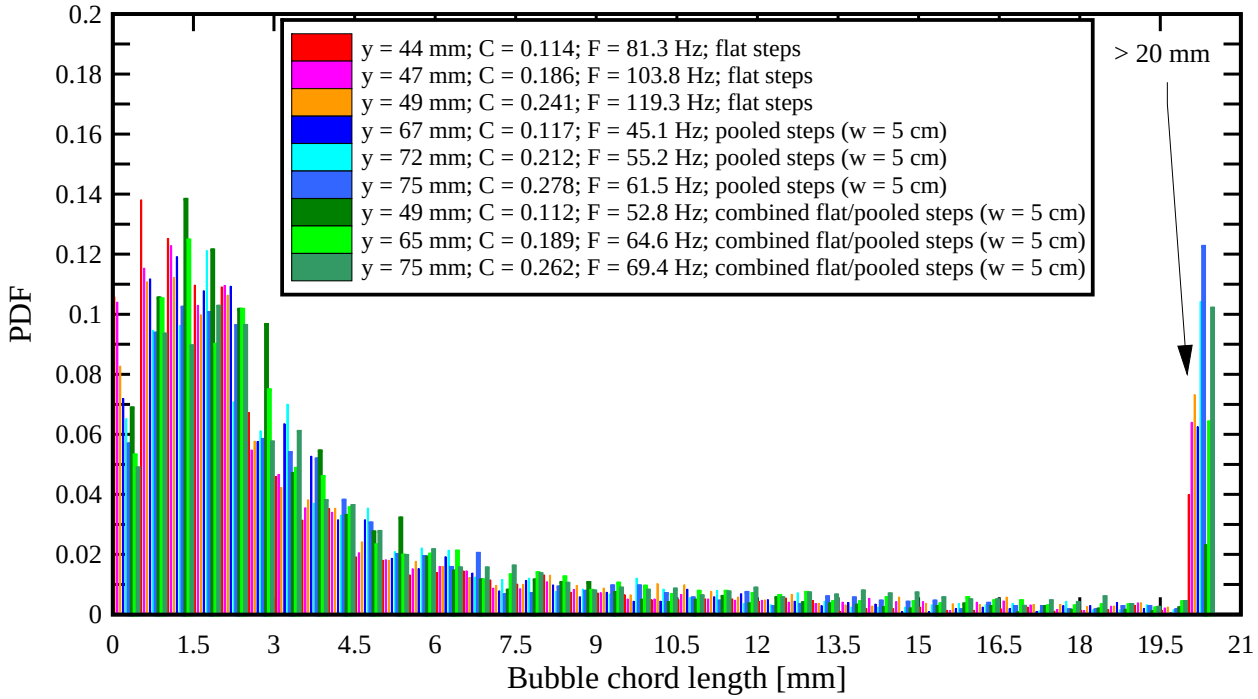

(B) Step edge 21

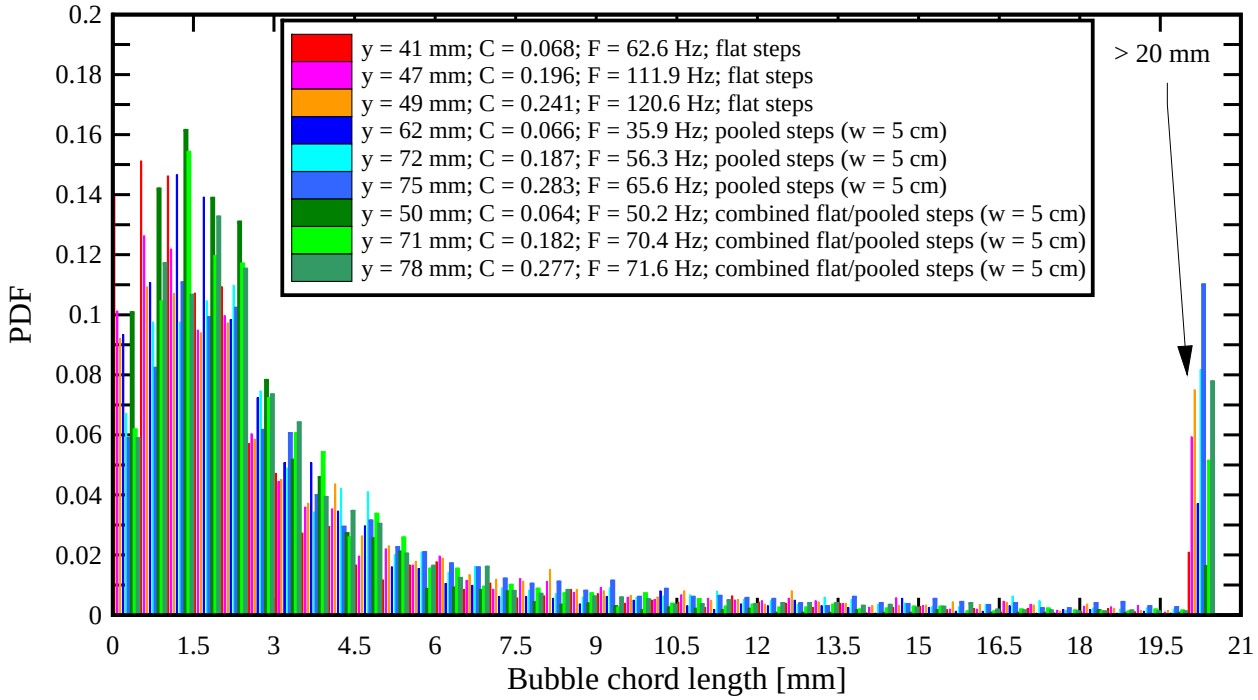

Fig. A-11 Comparison of probability distribution functions of air bubble chord sizes on stepped spillways with flat, pooled and combination of flat and pooled steps: θ = 8.9°, d_c/h = 3.55, Q = 0.117 m^3/s, Re = 9.30×10^5

(A) Step edge 20

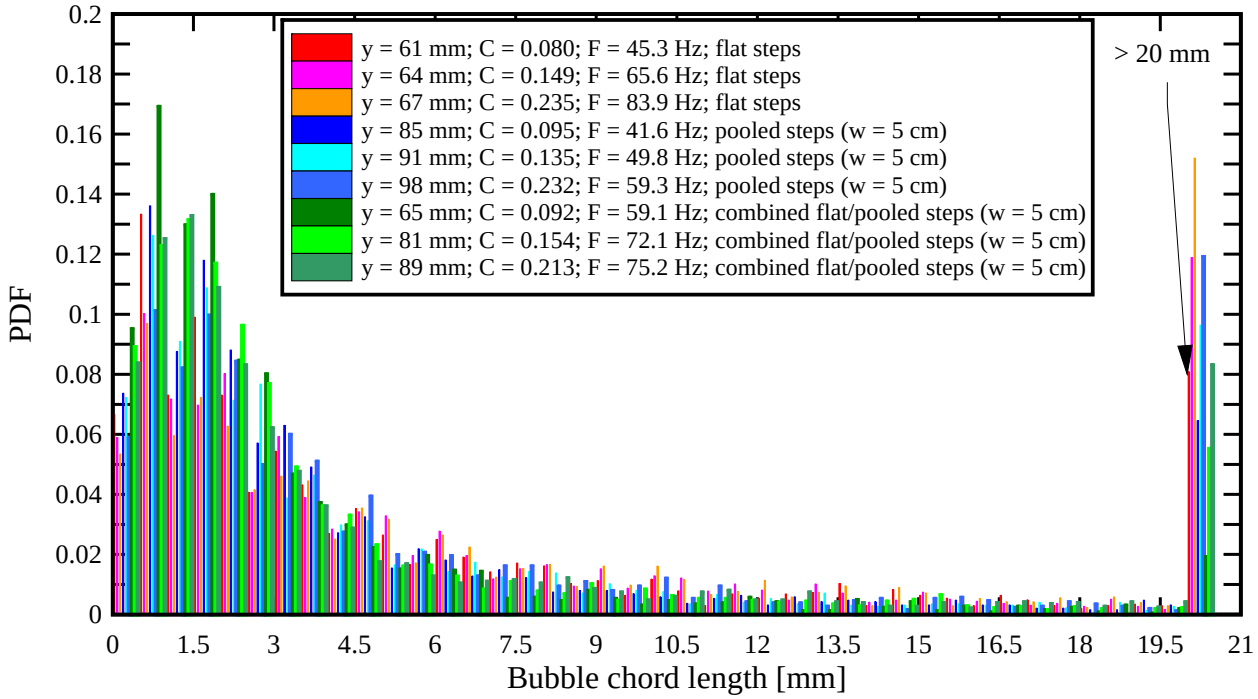

(B) Step edge 21

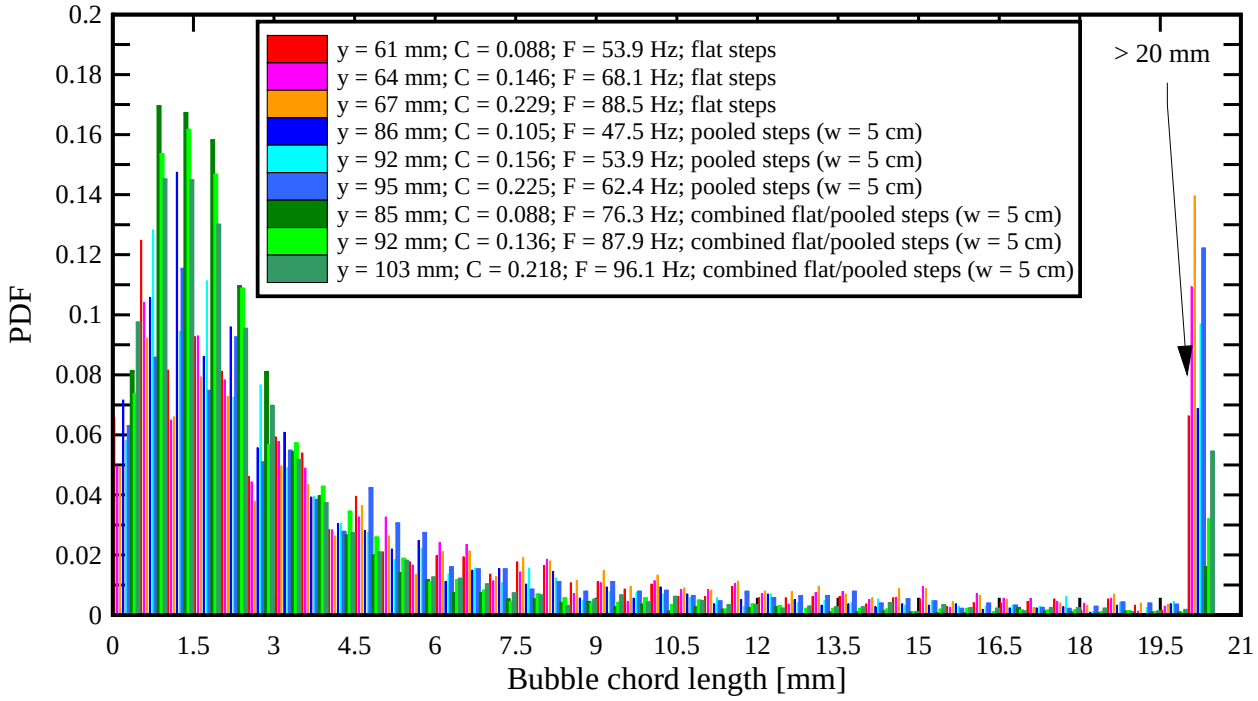

Fig. A-12 Comparison of probability distribution functions of water droplet chord sizes on stepped spillways with flat, pooled and combination of flat and pooled steps: θ = 8.9°, d_c/h = 1.7, Q = 0.039 m^3/s, Re = 3.10×10^5

(A) Step edge 20

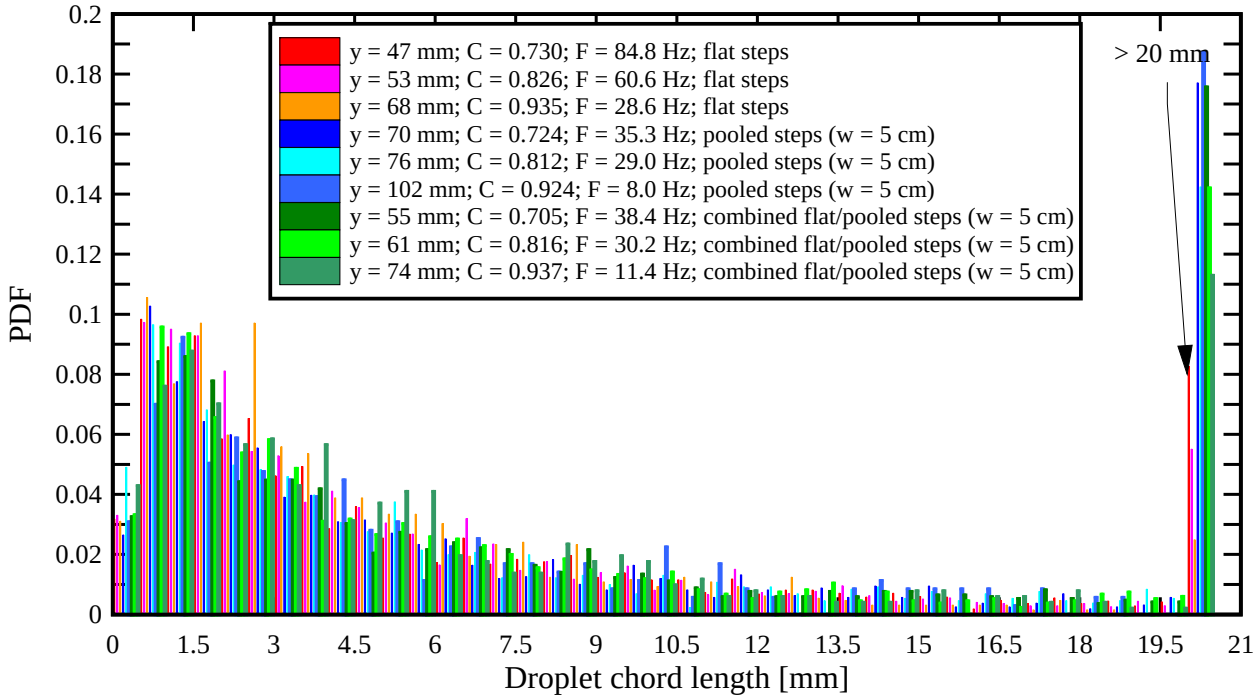

(B) Step edge 21

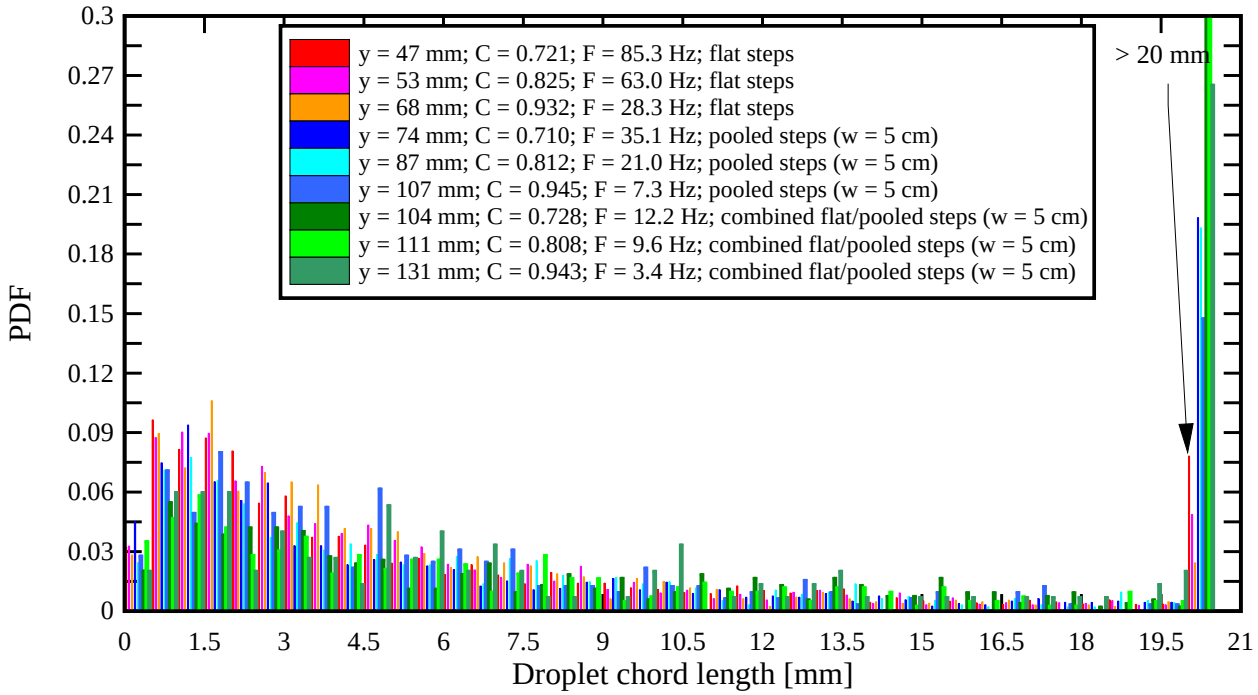

Fig. A-13 Comparison of probability distribution functions of water droplet chord sizes on stepped spillways with flat, pooled and combination of flat and pooled steps: θ = 8.9°, d_c/h = 2.66, Q = 0.076 m^3/s, Re = 6.03×10^5

(A) Step edge 20

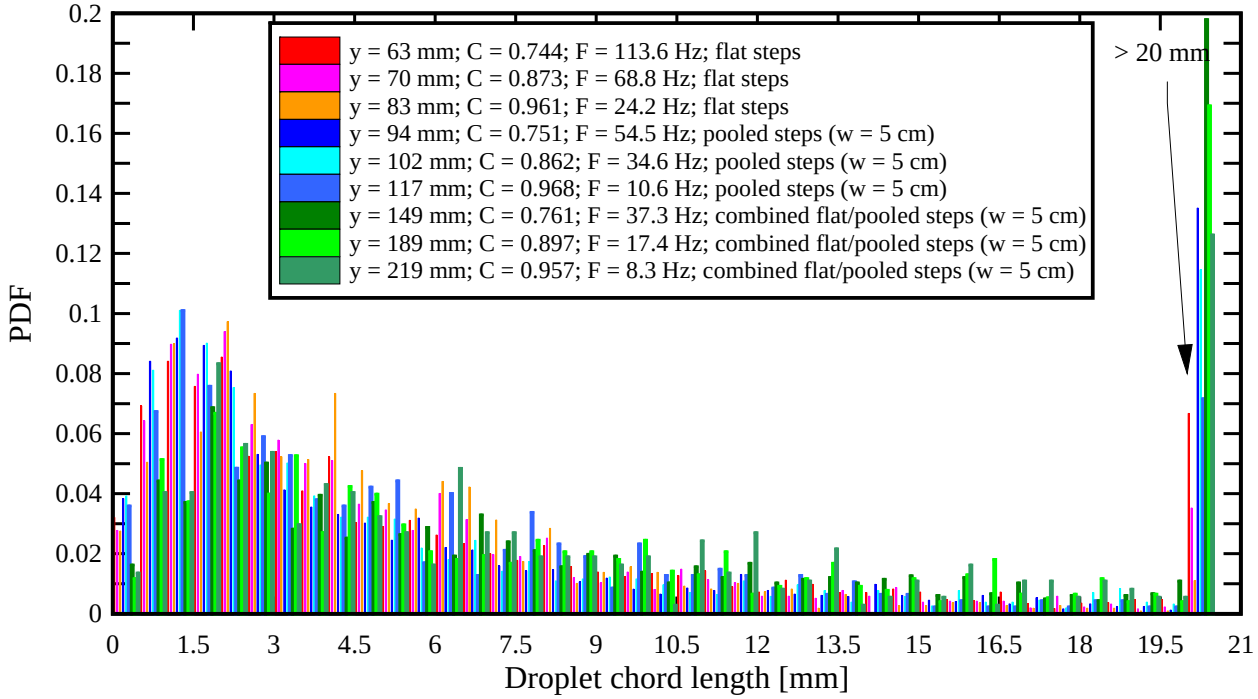

(B) Step edge 21

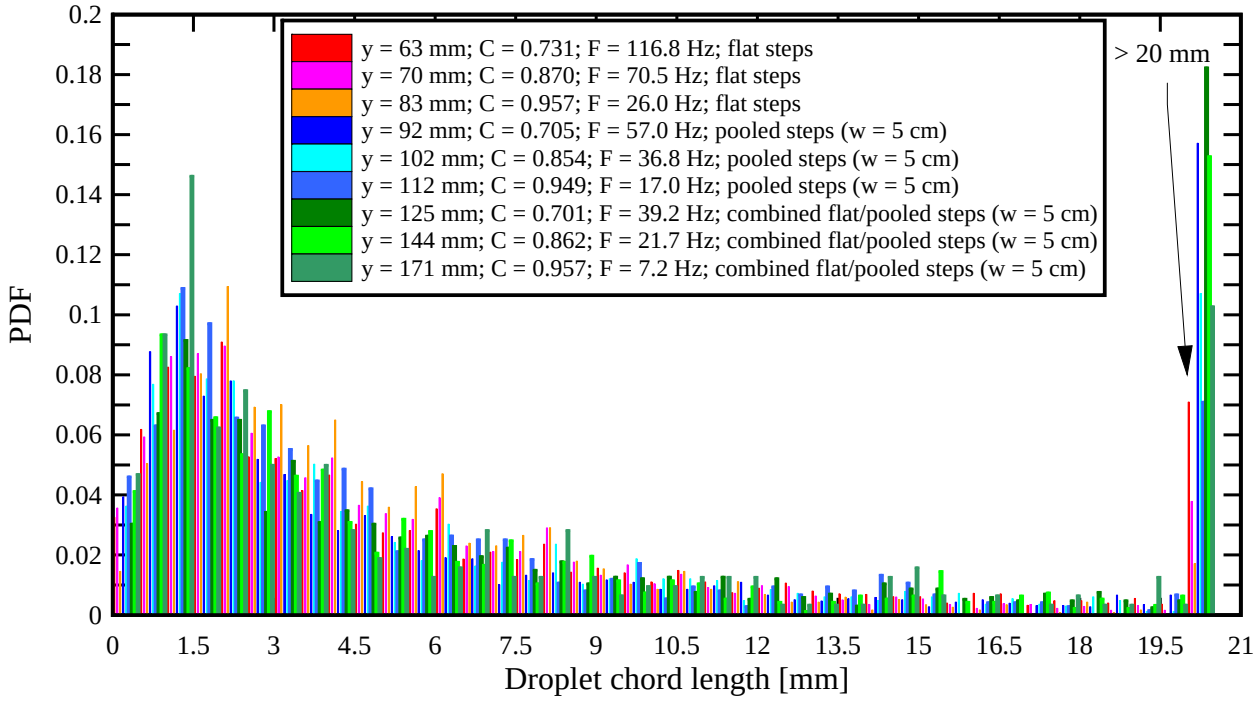

Fig. A-14 Comparison of probability distribution functions of water droplet chord sizes on stepped spillways with flat, pooled and combination of flat and pooled steps: θ = 8.9°, d_c/h = 3.55, Q = 0.117 m^3/s, Re = 9.30×10^5

(A) Step edge 20

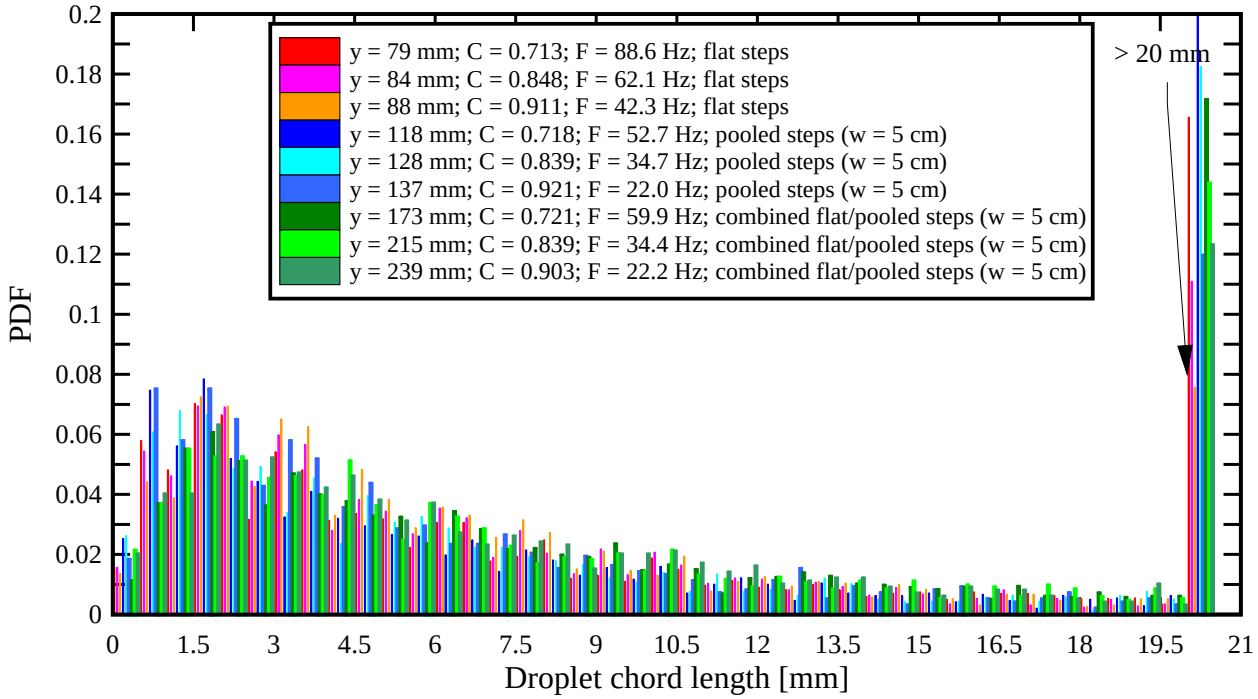

(B) Step edge 21

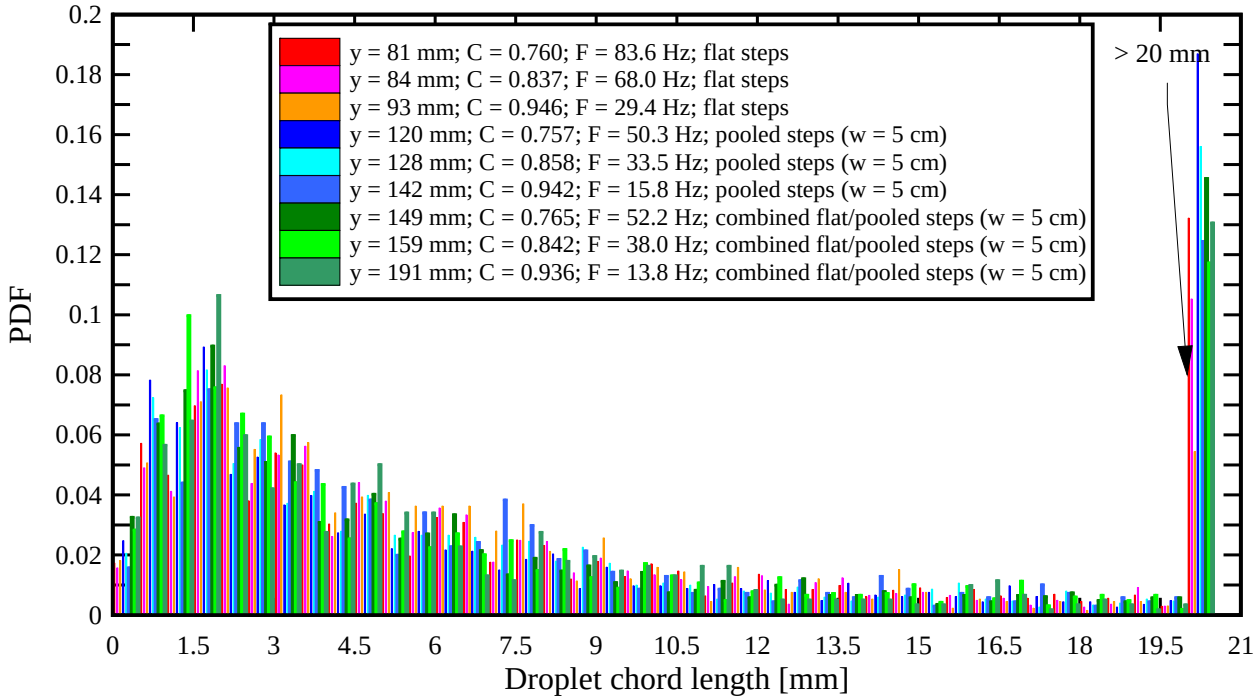

APPENDIX B – PRESENTATION OF CHARACTERISTIC AIR-WATER FLOW PARAMETERS FOR THE STEPPED SPILLWAYS

For all experiments, some characteristic air-water flow parameters were calculated for the stepped spillway configurations with flat, pooled and combination of flat and pooled steps. The characteristic parameters included the depth-averaged void fraction C_{mean}, the characteristic interfacial velocity V_{90}, the mean flow velocity U_w, the equivalent clear water flow depth d, the characteristic depth Y_{90} where the C = 90%, the maximum bubble count rate F_{max} and the maximum turbulence intensity Tu_{max}. The results are presented in Figures B1 to B-7 for all discharges and at all measured step edges for the three configurations. For each figure, the graph (Fig. A) on the left hand side presents the characteristic parameters as functions of the step edges. On the right hand side (Fig. B), the graph shows the parameters as functions of the dimensionless distance from the inception point of air entrainment. For all characteristic air-water flow parameters, some fluctuations are visible from step edge to step edge. The seesaw pattern was characteristic for all stepped spillway configurations and an uniform equilibrium flow was not achieved in the present study. The largest variations of characteristic parameters were observed for the combination of flat and pooled steps. The flat and pooled stepped showed smaller fluctuations around a mean trend.

For the three configurations, the mean void fraction data C_{mean} are shown in Figure B-1. For the smallest flow rates, the flat stepped spillway showed the largest mean air concentration in the transition flow regime. For all configurations, C_{mean} decreased with increasing discharge. For the larger discharges, the largest values of C_{mean} were seen for the stepped spillway with combination of flat and pooled steps.

The characteristic interfacial velocity data V_{90} for the three configurations are illustrated in Figure B-2. The results highlighted that V_{90} was the largest for the flat stepped spillway for all discharges. The stepped spillway with combination of flat and pooled steps exhibited the smallest values of V_{90}, but some strong seesaw pattern from step edge to step edge was observed (Fig. B-2). With increasing flow rate, V_{90} increased for all stepped configurations.

Similar finding were also seen for the flow velocity data U_w as illustrated in dimensionless terms in Figure B-3. The largest velocity was observed on the flat stepped spillway and the smallest for the combination of flat and pooled steps. Conversely, the equivalent clear water flow depth data d yielded the smallest values on the flat stepped spillway and the largest for the combination of flat and pooled steps (Fig. B-4). However some strong fluctuations with longitudinal distance were observed for the combined configuration. The characteristic depth data Y_{90} are presented in Figure B-5. The findings are very close to the observations of the equivalent clear-water flow depth. The smallest values of Y_{90} were seen for the flat stepped spillway and the largest for the combination of

flat and pooled steps. Some strong variations of Y_{90} were clearly visible for the combined stepped spillway (Fig. B-5).

Figure B-6 shows the characteristic maximum bubble count rate data F_{max} for all experiments. The largest number of entrained air bubbles was observed for the flat stepped spillway and the smallest for the pooled stepped spillway. For the smallest flow rates, the results on pooled stepped spillway and combination of flat and pooled steps were similar. For all configurations, some differences in terms of F_{max} were present between successive step edges and the flow was gradually varied.

A comparison of maximum turbulence intensity values highlighted some difference between the pooled stepped spillway configurations and the flat stepped spillway (Fig. B-7). For the pooled stepped spillway and the combination of flat and pooled steps, some very large values of Tu_{max} were seen and the magnitudes for both configurations were similar. The values of Tu_{max} seemed to decrease slightly with increasing discharge. Tu_{max} was significantly smaller for the flat stepped spillway configuration with about constant values for all experiments.

Fig. B-1 Comparison of longitudinal distributions of mean void fraction C_{mean} for the stepped spillway with flat, pooled and combination of flat and pooled steps

(A) Comparison at step edges

(B) Comparison at dimensionless distance from inception point

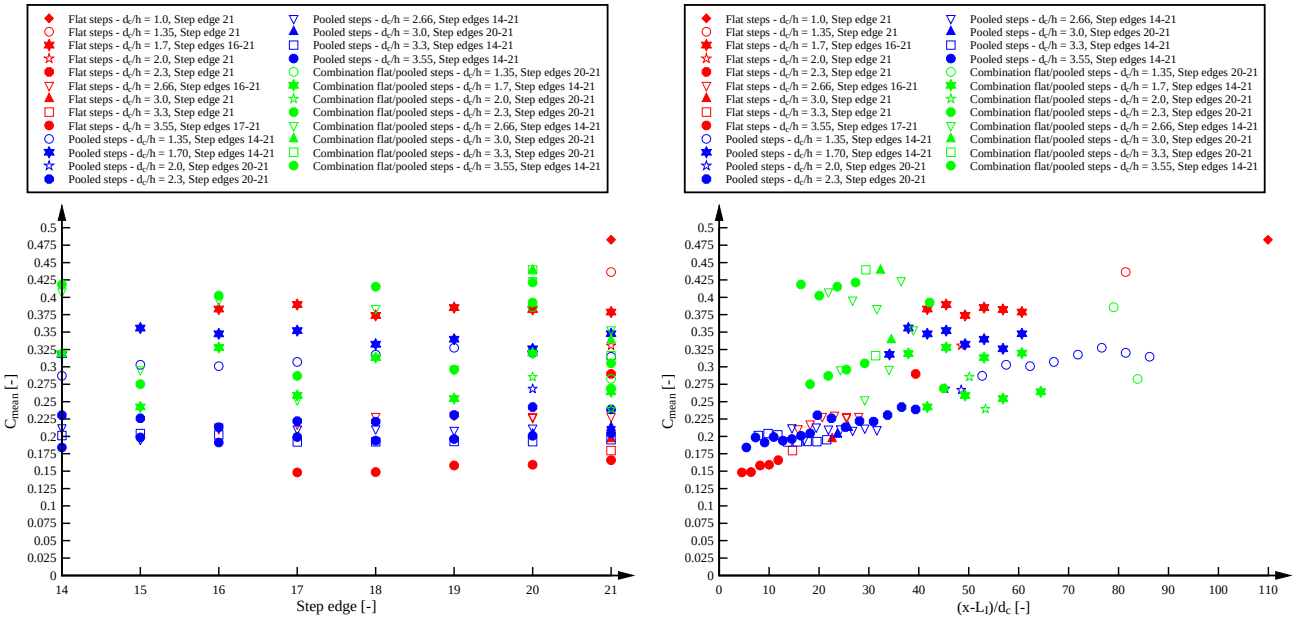

Fig. B-2 Comparison of longitudinal distributions of characteristic interfacial velocity value V_{90}/V_c for the stepped spillway with flat, pooled and combination of flat and pooled steps

(A) Comparison at step edges

(B) Comparison at dimensionless distance from inception point

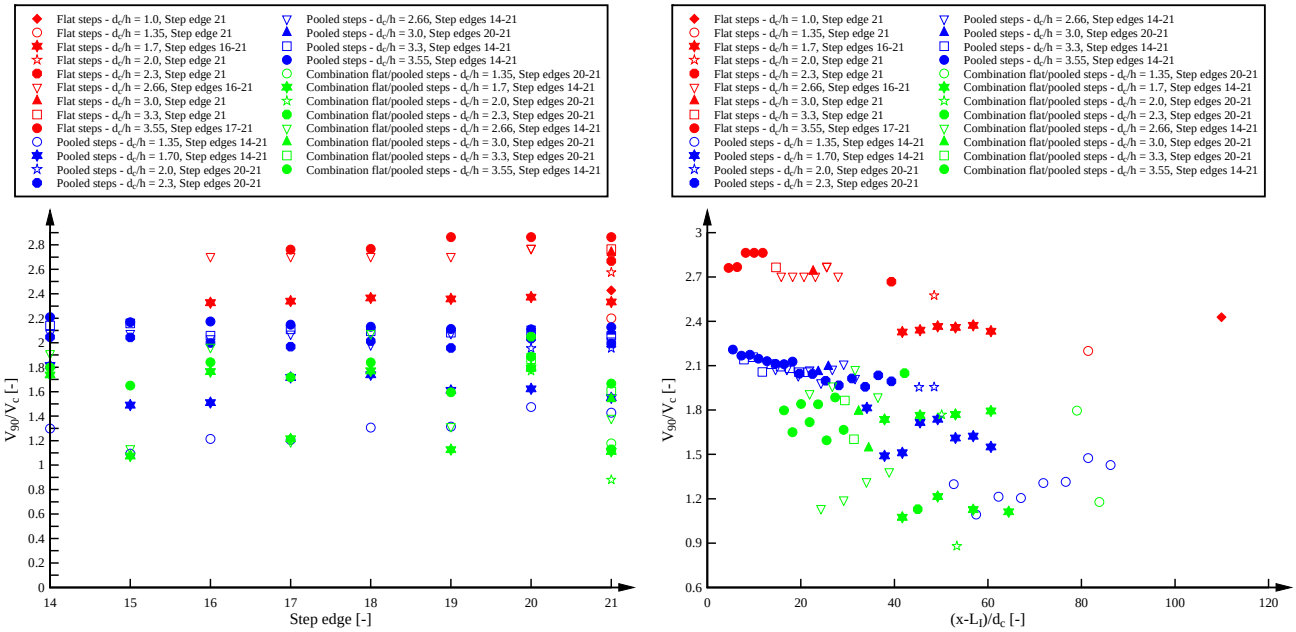

Fig. B-3 Comparison of longitudinal distributions of dimensionless flow velocity U_w/V_c for the stepped spillway with flat, pooled and combination of flat and pooled steps

(A) Comparison at step edges

(B) Comparison at dimensionless distance from inception point

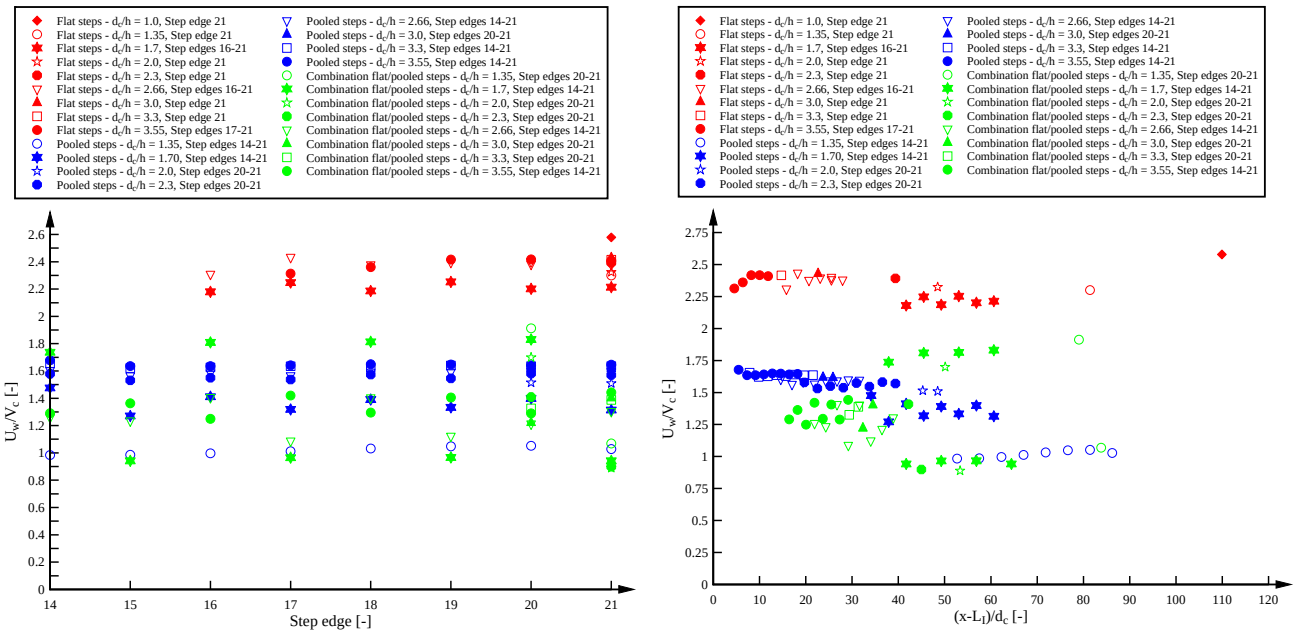

Fig. B-4 Comparison of longitudinal distributions of dimensionless equivalent clear water flow depth d/d_c for the stepped spillway with flat, pooled and combination of flat and pooled steps

(A) Comparison at step edges

(B) Comparison at dimensionless distance from inception point

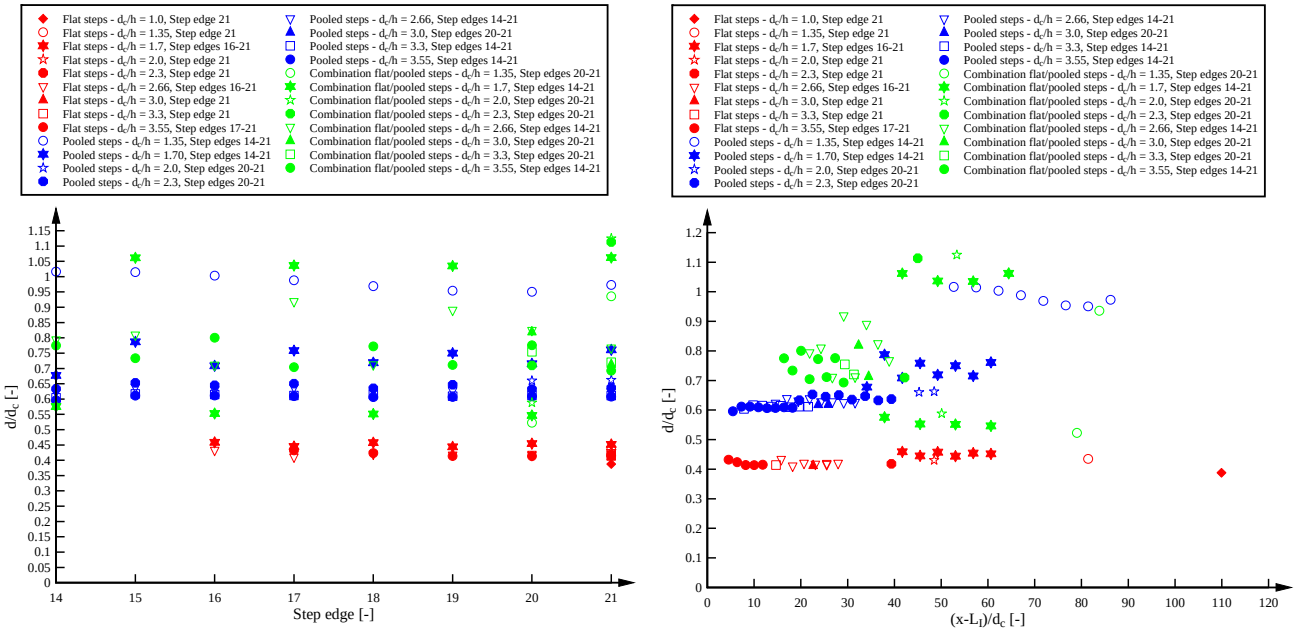

Fig. B-5 Comparison of longitudinal distributions of maximum dimensionless bubble count rate $F_{max} \times d_c/V_c$ for the stepped spillway with flat, pooled and combination of flat and pooled steps

(A) Comparison at step edges

(B) Comparison at dimensionless distance from inception point

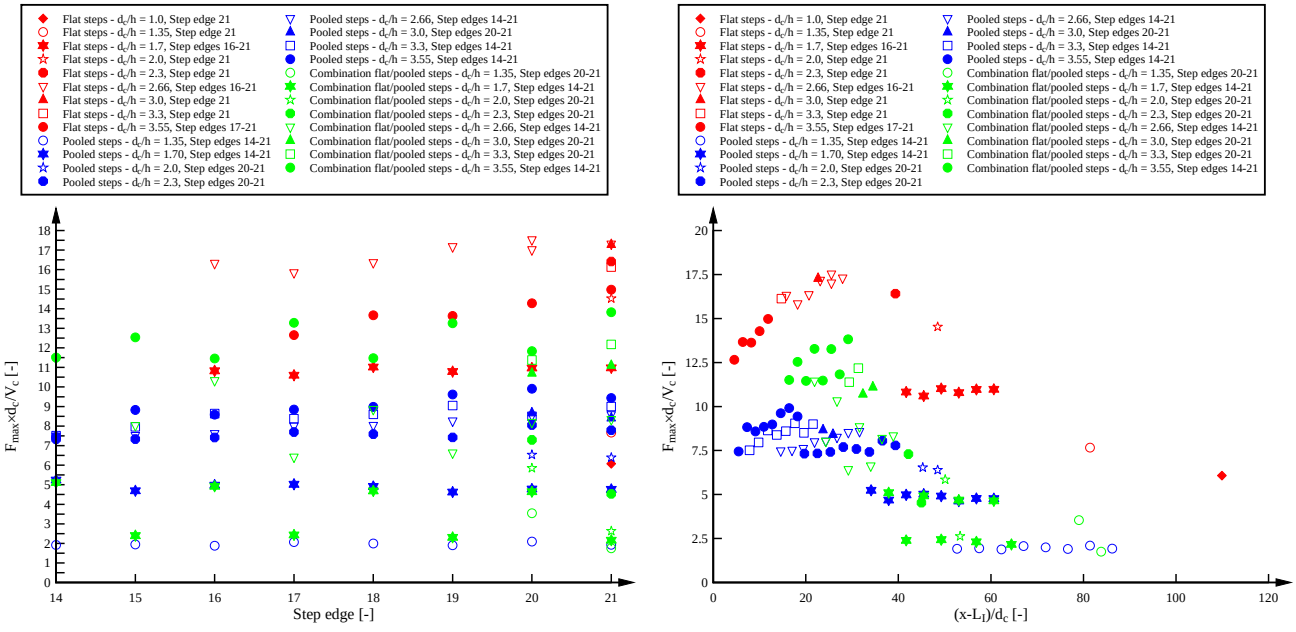

Fig. B-6 Comparison of longitudinal distributions of characteristic flow depth value Y_{90}/d_c for the stepped spillway with flat, pooled and combination of flat and pooled steps

(A) Comparison at step edges

(B) Comparison at dimensionless distance from inception point

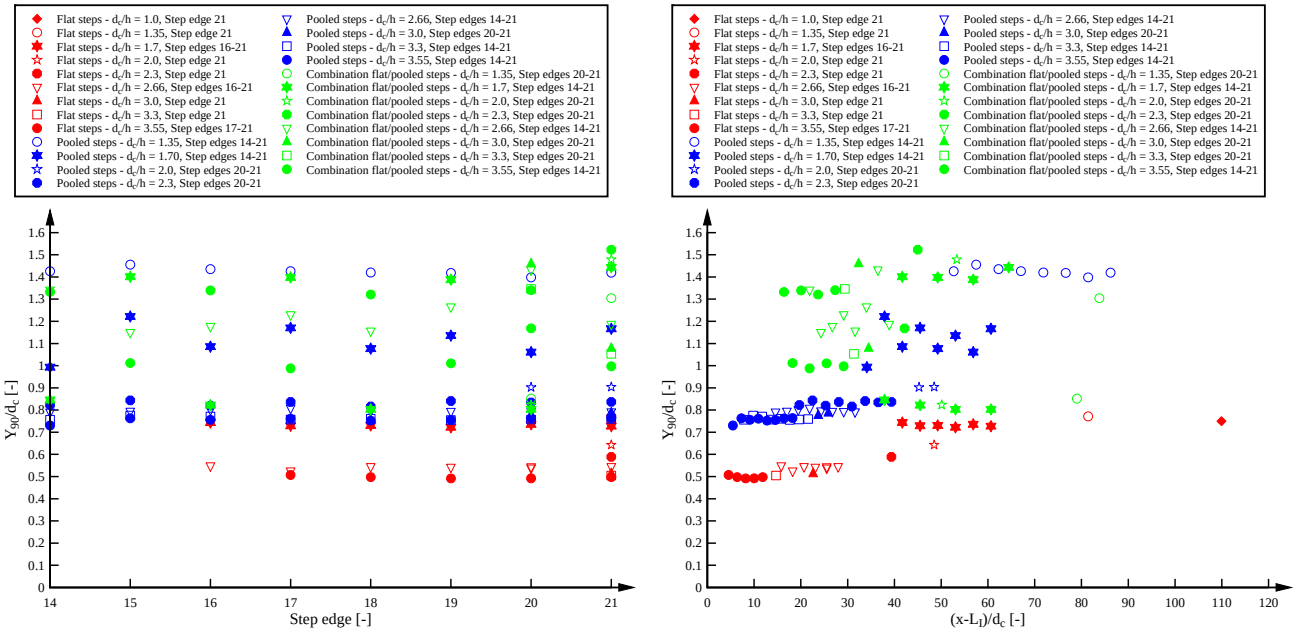

Fig. B-7 Comparison of longitudinal distributions of characteristic maximum turbulence intensity Tu_{max} for the stepped spillway with flat, pooled and combination of flat and pooled steps

(A) Comparison at step edges

(B) Comparison at dimensionless distance from inception point

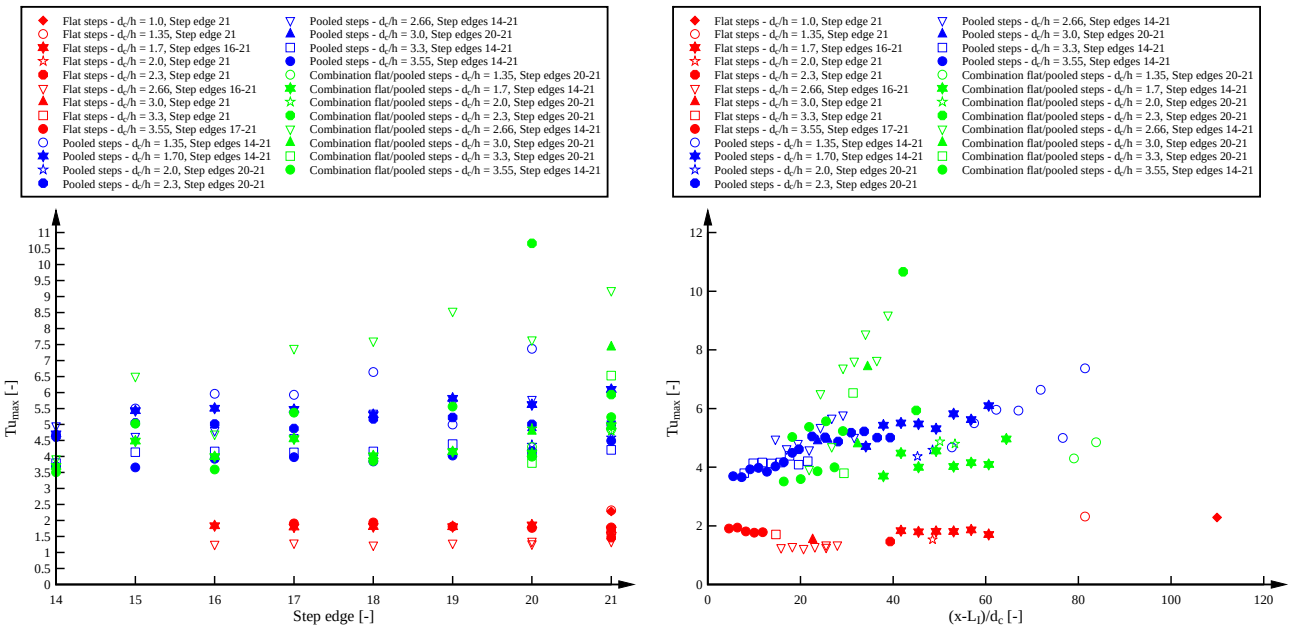

APPENDIX C – COMPARISON OF AIR-WATER FLOW PROPERTIES: SINGLE THRESHOLD TECHNIQUE VERSUS DIFFERENTIATION METHOD

PRESENTATION

The data acquisition system consisted of a LabVIEW^{TM} program designed by the IWW and used in previous studies by THORWATH (2008) and BUNG (2011) at the University of Wuppertal. The LabVIEW^{TM} code had an implemented data analysis code enabling an online analysis of some air-water flow properties such as void fraction, bubble count, and interfacial velocity and bubble chord sizes. The online cross-correlation analysis for the determination of the interfacial velocity was not efficient due to long calculation times. No further air-water flow properties such as the auto- and cross-correlation functions, the turbulence intensities and droplet chord sizes were calculated and printed with the LabVIEW^{TM} software. For these reasons, the LabVIEW^{TM} program was not used for post-processing.

In the present study, the data acquisition system from IWW was therefore solely used for the recording of raw data with sampling durations of 45 s and sampling frequencies of 20 kHz per probe sensor. The raw data were then analysed with a Fortran software designed at UQ and used in previous studies (FELDER & CHANSON 2011a,b,2012; CHACHEREAU & CHANSON, H. 2011). The post-processing software enabled the automated calculation of the full set of air-water flow properties without interference with the data acquisition.

In this Appendix, the results of a separate investigation of the calculation outputs from the LabVIEW^{TM} system and from the Fortran code are compared because there were some subtle differences between the two techniques. The comparison was conducted for the results of an air-water flow measurement on the flat stepped spillway with a double-tip conductivity probe sampling at 40 kHz and for a sampling duration of 10 seconds. The data were recorded for a full cross-section at step edge 20 for one flow rate Q = 0.076 m^3/s (d_c/h = 2.66). The air-water flow properties of void fraction, bubble count rate and interfacial velocity were calculated using THORWARTH's (2008) LabVIEW^{TM} program and the Fortran program respectively. Some results of the microscopic air-water flow property in terms of air bubble chord sizes were also compared. Some characteristic results are discussed at the end of this Appendix.

The calculation of the void fractions and bubble count rates was based upon two different analysis techniques in the two analyses programs. THORWARTH (2008) used a differentiation method for the calculation of the air-water interfaces (CARTELLIER & ACHARD 1991). The differentiation method used the first order difference of the raw voltage signal for the calculation of the air-water interfaces, i.e. of phase changes between water and air. In contrast, the Fortran code used a single-

threshold technique for the calculation of the interfaces. In the single-threshold approach, the PDF analysis of the raw voltage signal lead to a bimodal voltage distribution and the threshold was set at 50% of the differences between the two peaks.

BASIC RESULTS

Both analysis techniques enabled the calculation of the void fraction C and the bubble count rate F. In Figure C-1, the void fraction distributions are presented as a function of y/Y_{90} for both analysis techniques. The results were very close overall. Some small differences are visible in terms of the dimensionless bubble count rate distributions as illustrated in Figure C-2. It appeared that the number of bubbles detected by the LabVIEW^{TM} program was consistently about 10% larger compared to the Fortran program results for $C < 0.95$. In the upper spray region ($C > 0.95$), the data were in close agreement.

The calculation of the interfacial velocity was based upon the cross-correlation analysis of the raw voltage signal for both analysis softwares. The results were therefore in very close agreement as visible in Figure C-3.

Some further characteristic air-water flow parameters are compared in Table C-1 for the two analysis techniques. All parameters were almost identical, but some differences were observed in terms of the maximum bubble count rate F_{max}.

Fig. C-1 Comparison of void fraction distributions calculated with single-threshold technique (Fortran program, Present study) and with differentiation method (LabVIEW™ code from IWW (THORWARTH 2008))

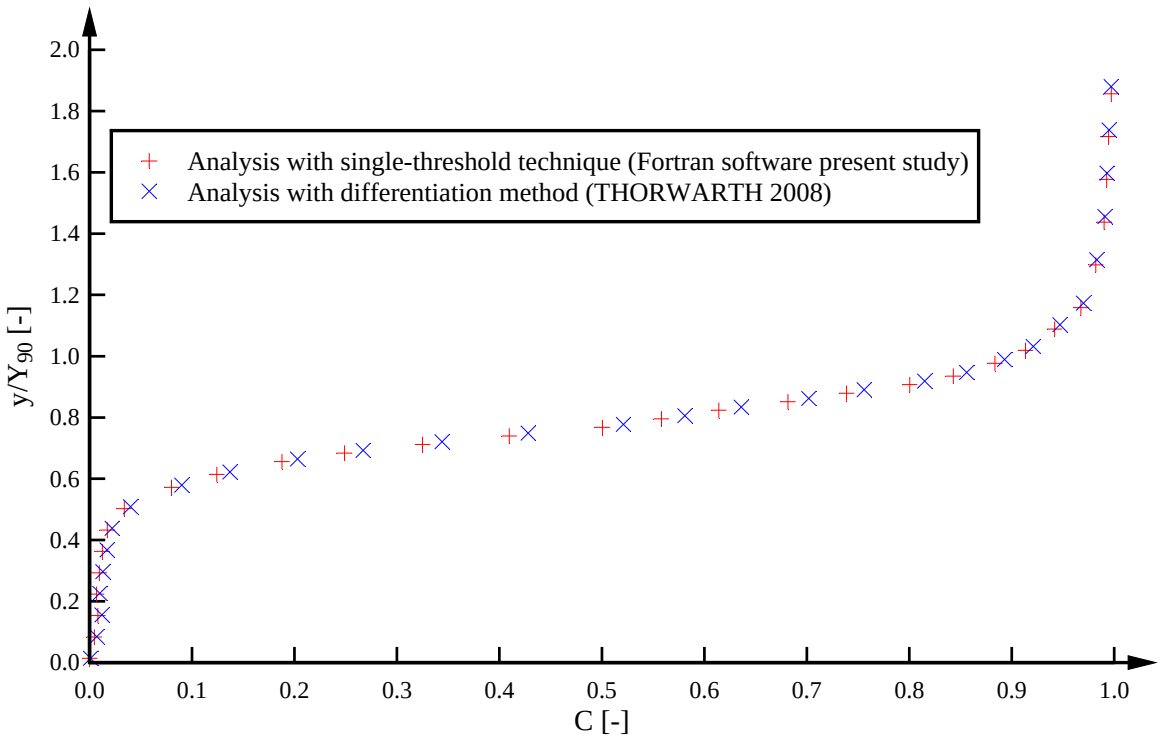

Fig. C-2 Comparison of dimensionless bubble count rate distributions calculated with single-threshold technique (Fortran program, Present study) and with differentiation method (LabVIEW™ code from IWW (THORWARTH 2008))

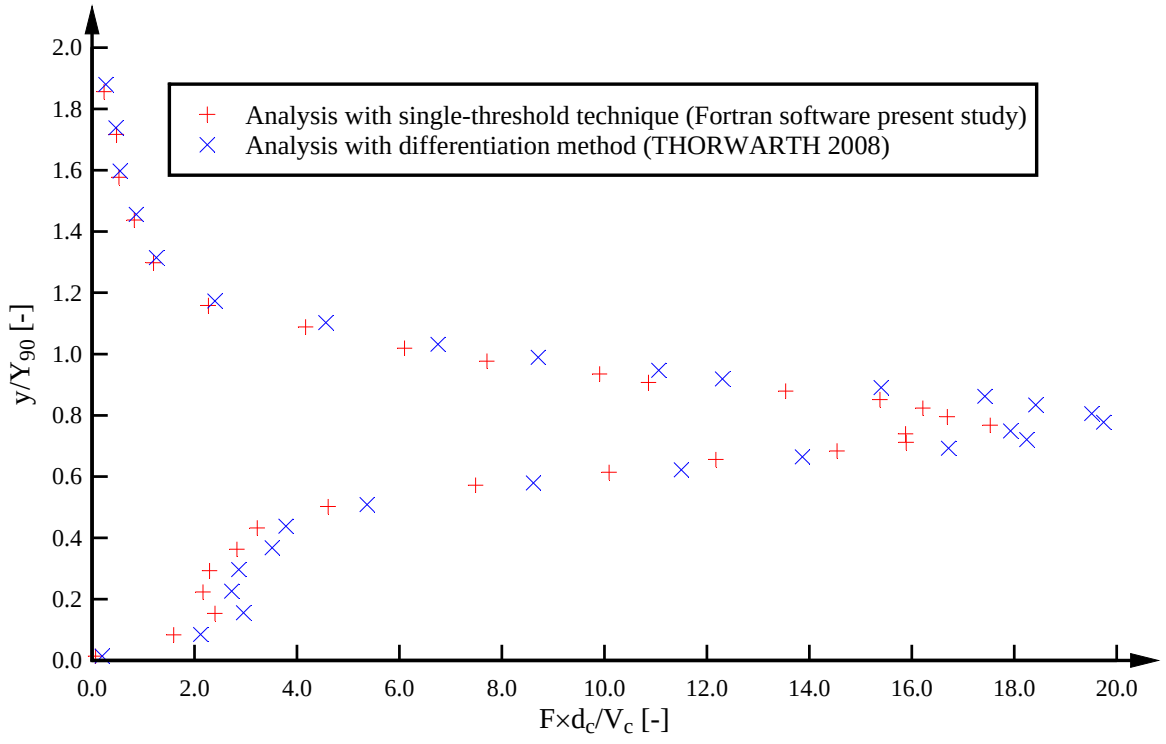

Fig. C-3 Comparison of dimensionless interfacial velocity calculated with Fortran program (Present study) and with LabVIEW^{TM} code from IWW (THORWARTH 2008)

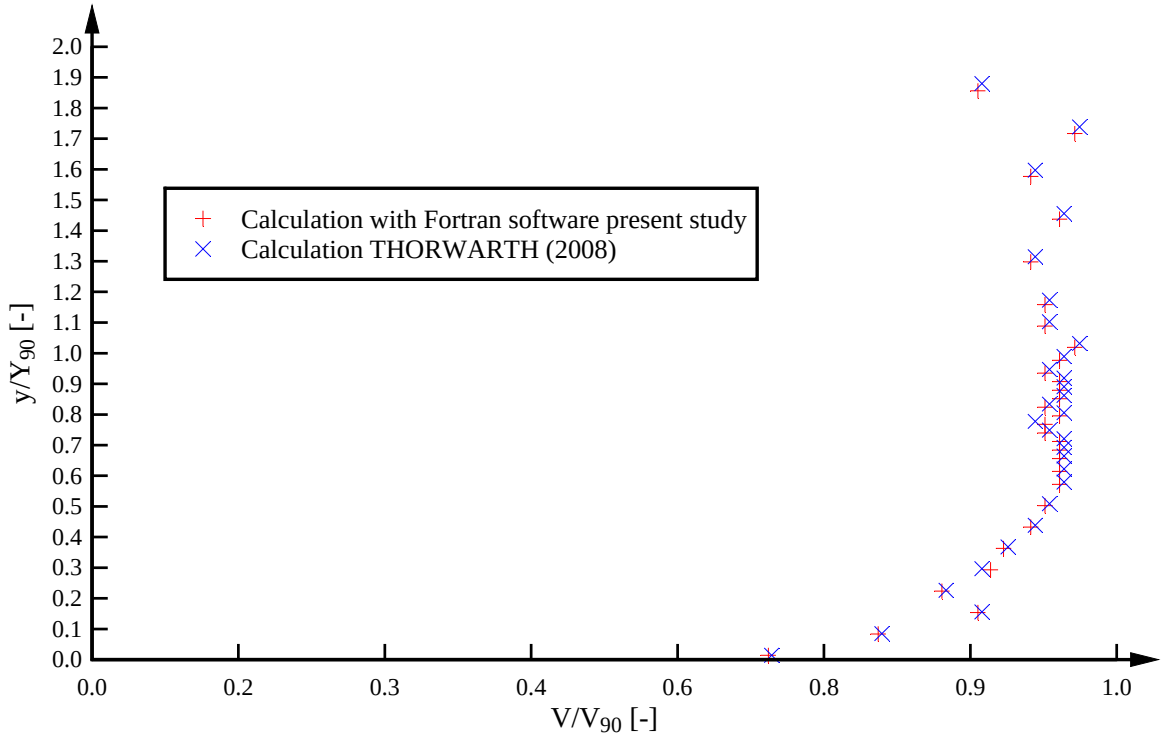

Table C-1 – Summary of characteristic parameters of air-water flow properties on pooled stepped spillway configurations calculated with two different calculation methods/tools

Characteristic parameters	Calculation tools	
	Fortran program (Present study)	LabVIEW^{TM} software (THORWARTH 2008)
(1)	(2)	(3)
C_{mean} [-]	0.227	0.228
F_{max} [Hz]	150.6	169.6
V_{90} [m/s]	3.165	3.151
Y_{90} [mm]	71.65	70.75
U_w [m/s]	2.74	2.78
d [mm]	55.36	54.61

Notes: C_{mean}: mean void fraction; F_{max}: maximum bubble count rate; V_{90}: characteristic interfacial velocity; Y_{90}: characteristic flow depth; U_w: mean flow velocity; d: equivalent clear water flow

DISCUSSION

The differences in terms of bubble frequency seemed to be linked with the different calculation methods (Fig. C-4). In Figure C-4, a short sequence of a typical raw voltage signal and the detection of air-water interfaces is illustrated. In the single-threshold technique, air-water interfaces were detected, when the voltage signal passed the single threshold value (dashed line, Fig. C-4). Some voltage drops and spikes were therefore not detected and did not contribute to the bubble count rate (Fig. C-4). In the differentiation method, on the other hand, a small drop in voltage may be counted as an air bubble (Fig. C-4). Therefore the differentiation method technique tended to yield a larger bubble count rate.

A further air-water flow property was the air bubble chord size probability distribution function (PDF). Some comparative results for the two calculation techniques are presented in Figure C-5. Some small differences in terms of air bubble chord size distributions were seen with a larger number of chord sizes smaller than 1 mm for the Fortran code data. A larger number of chord sizes was observed for the LabVIEW^{TM} calculations in the chord size range of 1.5 to 5 mm (Fig. C-5). It was not possible to verify the calculation method of the air bubble chord sizes in the LabVIEW^{TM} program. The chord size calculation tool implemented in the LabVIEW^{TM} program was never used or published. In other words it was not possible to understand and verify the chord size calculation tool with the LabVIEW^{TM} program.

Fig. C-4 Raw voltage signal and detection of air-bubbles in the single-threshold technique - flow condition: θ = 8.9°, d_c/h = 2.66, Q = 0.076 m^3/s, Re = 6.03×10^5, Step edge 20, y = 51 mm, leading probe

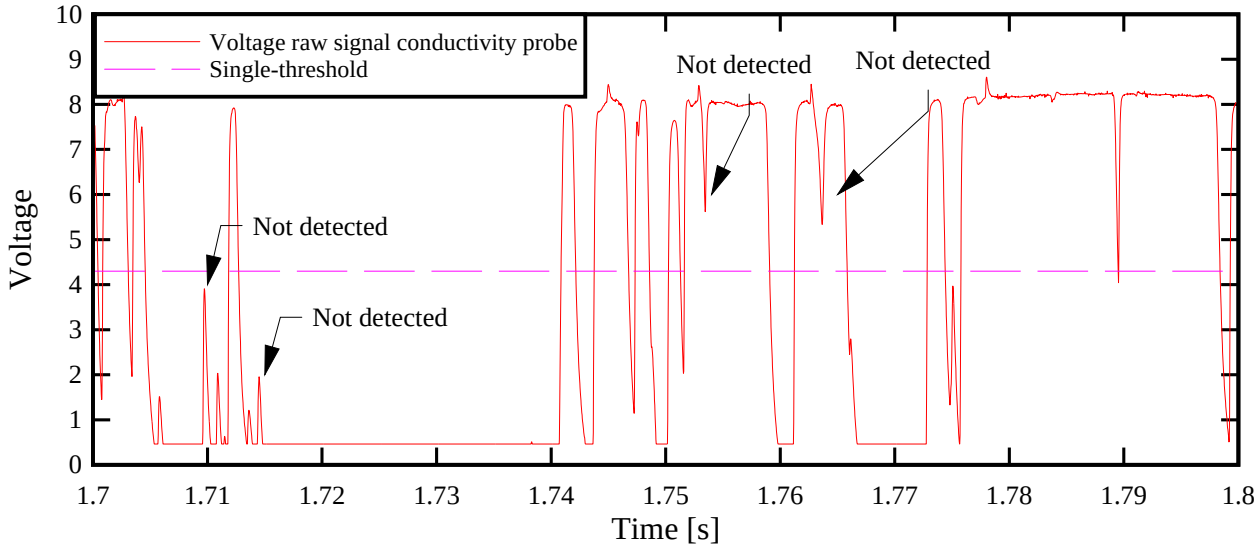

Fig. C-5 Comparison of PDF air-bubble chord size distributions calculated with Fortran program (Present study) and with LabVIEW^{TM} code from IWW (THORWARTH 2008)

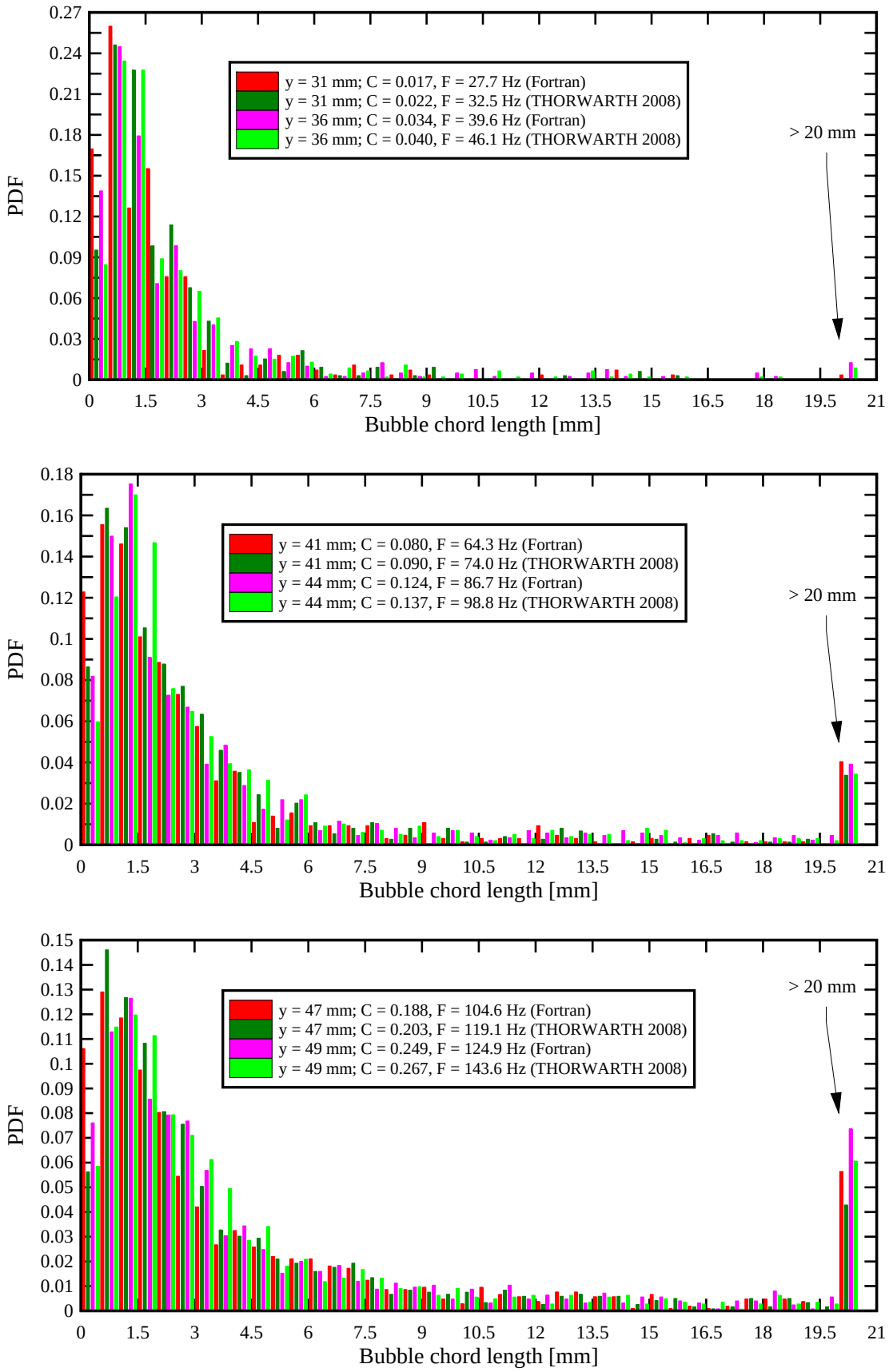

REFERENCES

ANDRÉ, S. (2004). "High velocity aerated flows on stepped chutes with macro-roughness elements." Ph.D. thesis, Laboratoire de Constructions Hydraulics (LCH), EPFL, Lausanne, Switzerland, 272 pages.

BOES, R.M. (2000). "Zweiphasenströmung und Energieumsetzung an Grosskaskaden." ("Two-Phase Flow and Energy Dissipation on Cascades.") Ph.D. thesis, VAW-ETH, Zürich, Switzerland (in German). (also Mitteilungen der Versuchsanstalt für Wasserbau, Hydrologie and Glaziologie, ETH-Zürich, Switzerland, No. 166).

BUNG, D.B. (2009). "Zur selbstbelüfteten Gerinneströmung auf Kaskaden mit gemäßigter Neigung." Ph.D. thesis, Lehr- und Forschungsgebiet Wasserwirtschaft und Wasserbau, Bergische Universitaet Wuppertal, Germany (in German).

BUNG, D.B. (2011). "Developing flow in skimming flow regime on embankment stepped spillways. " Jl of Hydraulic Research, Vol. 49, No 5, pp. 639-648.

CARTELLIER, A. and ACHARD, J.L. (1991): "Local phase detection probes in fluid/fluid two-phase flows." Rev. Sci. Instrum., Volume 62, No. 2, pp. 279-303.

CHACHEREAU, Y. and CHANSON, H. (2011). "Bubbly Flow Measurements in Hydraulic Jumps with Small Inflow Froude Numbers." International Journal of Multiphase Flow, Vol. 37, No. 6, pp. 555-564 (DOI: 10.1016/j.ijmultiphaseflow.2011.03.012).

CHAMANI, M.R. and RAJARATNAM, N. (1999). "Characteristics of Skimming Flow over Stepped Spillways." Journal of Hydraulic Engineering, ASCE, Vol. 125, No. 4, pp. 361-368.

CHANSON, H. (1993). "Flow Resistance in High Velocity Supercritical Flows." Australian Civil Engineering Transactions, Vol. CE35, No. 2, pp. 141-149.

CHANSON, H. (1995). "Hydraulic Design of Stepped Cascades, Channels, Weirs and Spillways." Pergamon, Oxford, UK, Jan., 292 pages (ISBN 0-08-041918-6).

CHANSON, H. (2001). "The Hydraulics of Stepped Chutes and Spillways." Balkema, Lisse, The Netherlands (ISBN 90 5809 352 2).

CHANSON, H. and CAROSI, G. (2007). "Turbulent time and length scale measurements in high velocity open channel flows." Experiments in Fluids Vol. 42, No. 3, pp. 385-401.

CHANSON, H. and TOOMBES, L. (1997). "Energy Dissipation in Stepped Waterway." Proc. 27th IAHR Biennial Congress, San Francisco, USA, Vol. D, F.M. HOLLY Jr. and A. ALSAFFAR Ed., pp. 595-600.

CHANSON, H. and TOOMBES, L. (2002). "Air-Water Flows down Stepped chutes: Turbulence and Flow Structure Observations." International Journal of Multiphase Flow, Vol. 28, No. 11, pp. 1737-1761.

CHANSON, H. and TOOMBES, L. (2004). "Hydraulics of stepped chutes: The transition flow." Journal of Hydraulic Research, Vol. 42, No. 1, pp. 43-54.

CHANSON, H., YASUDA, Y. and OHTSU, I. (2002). "Flow Resistance in Skimming Flows and its Modelling." Canadian Journal of Civil Engineering, Vol. 29, No. 6, pp. 809-819.

CHENG, X.J., CHEN, Y.C. and LUO, L. (2006). "Numerical simulation of air-water two-phase flow over stepped spillways." Science in China Series E-Technological Sciences, Vol. 49, No. 6, pp. 674-684.

FELDER, S., and CHANSON, H. (2009a). "Energy dissipation, flow resistance and gas-liquid interfacial area in skimming flows on moderate-slope stepped spillways." Environmental Fluid Mechanics, Vol. 9, No. 4, pp. 427-441.

FELDER, S. and CHANSON, H. (2009b). "Turbulence, Dynamic Similarity and Scale Effects in High-Velocity Free-Surface Flows above a Stepped Chute." Experiments in Fluids, Vol. 47, No. 1, pp. 1-18.

FELDER, S. and CHANSON, H. (2011a). "Air-Water Flow Properties in Step Cavity down a Stepped Chute." International Journal of Multiphase Flow, Vol. 37, No. 7, pp. 732–745 (DOI: 10.1016/j.ijmultiphaseflow.2011.02.009).

FELDER, S. and CHANSON, H. (2011b). "Energy Dissipation down a Stepped Spillway with Non-Uniform Step Heights." Journal of Hydraulic Engineering, ASCE, Vol. 137, No. 11, pp. 1543-1548 (DOI 10.1061/(ASCE)HY.1943-7900.0000455).

FELDER, S. and CHANSON, H. (2012). "Air-Water Flow Measurements in Instationary Free-Surface Flows: a Triple Decomposition Technique." Hydraulic Model Report No. CH85/12, School of Civil Engineering, The University of Queensland, Brisbane, Australia (ISBN 9781742720494).

HENDERSON, F.M. (1966). "Open Channel Flow." MacMillan Company, New York, USA, 522 pages (ISBN 0-02-353510-5).

HORNER, M.W. (1969). "An Analysis of Flow on Cascades of Steps." Ph.D. thesis, University of Birmingham, UK, 357 pages.

KÖKPINAR, M.A. (2004). "Flow over a Stepped Chute with and without Macro-Roughness Elements." Canadian Journal of Civil Engineering, Vol. 31, No. 5, pp. 880-891.

MATOS, J (2001). "Onset of Skimming Flow on Stepped Spillways. Discussion" Journal of Hydraulic Engineering, ASCE, Vol. 127, No. 6, pp. 519-521.

MEIRELES, I.; BOMBARDELLI, F. and MATOS, J. (2009). "Experimental testing and numerical simulation of the non-aerated skimming flow over steeply sloping stepped spillways." 33rd IAHR Congress, Vancouver, Canada, pp. 1972-1979.

OHTSU, I. and YASUDA, Y. (1997). "Characteristics of Flow Conditions on Stepped Channels." Proc. 27th IAHR Biennial Congress, San Francisco, USA, Theme D, pp. 583-588.

PEYRAS, L.; ROYET, P. and DEGOUTTE, G. (1992). "Flow and Energy Dissipation over Stepped Gabion Weirs." Journal of Hydraulic Engineering, ASCE, Vol. 118, No. 5, pp. 707-717.

QIAN, Z.D., HU, X.Q., HUAI, W.X. and AMADOR, A. (2009). "Numerical simulation and analysis of water flow over stepped spillways." Science in China Series E-Technological Sciences, Vol. 52, No. 7, pp. 1958-1965.

RAJARATNAM, N. (1990). "Skimming Flow in Stepped Spillways." Jl of Hydraulic Engineering, ASCE, Vol. 116, No. 4, pp. 587-591.

THORWARTH, J. (2008). "Hydraulisches Verhalten der Treppengerinne mit eingetieften Stufen – Selbstinduzierte Abflussinstationaritäten und Energiedissipation." ("Hydraulics of Pooled Stepped Spillways – Self-induced Unsteady Flow and Energy Dissipation.") Ph.D. thesis, University of Aachen, Germany (in German).

THORWARTH, J. and KOENGETER, J. (2006). "Physical Model Test on a Stepped Chute with Pooled Steps – Investigation of Flow Resistance and Flow Instabilities." In: Recent Developments on Hydraulic Structures: From Hybrid Modelling to Operation and Repairs; Cuidad Guayana, Venezuela, October 2006 [International symposium on Hydraulic Structures] / Ed. by Arturo MARCANO et al., Caracas, Venezuela: Venezuelan Society of Hydraulic Engineering, pp. 477-486 (ISBN 980-12-2177-1).

TOOMBES, L. (2002). "Experimental Study of Air-Water Flow Properties on Low-Gradient Stepped Cascades." Ph.D. thesis, Dept. of Civil Engineering, University of Queensland, Australia.

TOOMBES, L. and CHANSON, H. (2008a). "Flow Patterns in Nappe Flow Regime down Low Gradient Stepped Chutes." Journal of Hydraulic Research, IAHR, Vol. 46, No. 1, pp. 4-14.

TOOMBES, L. and CHANSON, H. (2008b). "Interfacial Aeration and Bubble Count Rate Distributions in a Supercritical Flow Past a Backward-Facing Step." International Journal of Multiphase Flow, Vol. 34, No. 5, pp. 427-436 (doi.org/10.1016/j.ijmultiphaseflow.2008.01.005).

Bibliography

CAROSI, G. and CHANSON, H. (2006). "Air-Water Time and Length Scales in Skimming Flows on a Stepped Spillway. Application to the Spray Characterisation." Report No. CH59/06, Div. of Civil Engineering, The University of Queensland, Brisbane, Australia, July, 142 pages (ISBN 1864998601).

FELDER, S. and CHANSON, H. (2008). "Turbulence and Turbulent Length and Time Scales in Skimming Flows on a Stepped Spillway. Dynamic Similarity, Physical Modelling and Scale Effects." Report No. CH64/07, Hydraulic Model Report CH series, Division of Civil Engineering, The University of Queensland, Brisbane, Australia, March, 217 pages (ISBN 9781864998870).

GONZALEZ, C.A. (2005). "An Experimental Study of Free-Surface Aeration on Embankment Stepped Chutes." Ph.D. thesis, Department of Civil Engineering, The University of Queensland, Brisbane, Australia.

Internet bibliography

Research papers in hydraulic engineering (open access)	{http://espace.library.uq.edu.au/list/author_id/193/}
Air entrainment on chute and stepped spillways	{http://www.uq.edu.au/~e2hchans/self_aer.html}
Embankment overflow stepped spillways: earth dam spillways with precast concrete blocks	{http://www.uq.edu.au/~e2hchans/over_st.html}

Bibliographic reference of the Report CH86/12

The Hydraulic Model research report series CH is a refereed publication published by the School of Civil Engineering at the University of Queensland, Brisbane, Australia.

The bibliographic reference of the present report is:

FELDER, S., FROMM, C., and CHANSON, H. (2012). "Air Entrainment and Energy Dissipation on a 8.9° Slope Stepped Spillway with Flat and Pooled Steps." *Hydraulic Model Report No. CH86/12*, School of Civil Engineering, The University of Queensland, Brisbane, Australia, 80 pages (ISBN 9781742720531).

The Report CH86/12 is available, in the present form, as a PDF file on the Internet at UQeSpace:

http://espace.library.uq.edu.au/

It is listed at:

http://espace.library.uq.edu.au/list/author_id/193/

HYDRAULIC MODEL RESEARCH REPORT CH

The Hydraulic Model Report CH series is published by the School of Civil Engineering at the University of Queensland. Orders of any reprint(s) of the Hydraulic Model Reports should be addressed to the School Secretary.

School Secretary, School of Civil Engineering, The University of Queensland
Brisbane 4072, Australia - Tel.: (61 7) 3365 3619 - Fax : (61 7) 3365 4599
Url: http://www.eng.uq.edu.au/civil/ Email: hodciveng@uq.edu.au

Report CH	**Unit price**	Quantity	**Total price**
CHANSON, H., and WANG, H. (2012). "Unsteady Discharge Calibration of a Large V-Notch Weir." *Hydraulic Model Report No. CH88/12*, School of Civil Engineering, The University of Queensland, Brisbane, Australia, 50 pages & 4 movies (ISBN 9781742720579).	AUD$60.00		
FELDER, S., GUENTHER, P., and CHANSON, H. (2012). "Air-Water Flow Properties and Energy Dissipation on Stepped Spillways: a Physical Study of Several Pooled Stepped Configurations." *Hydraulic Model Report No. CH87/12*, School of Civil Engineering, The University of Queensland, Brisbane, Australia, 225 pages (ISBN 9781742720555).	AUD$60.00		
FELDER, S., FROMM, C., and CHANSON, H. (2012). "Air Entrainment and Energy Dissipation on a 8.9° Slope Stepped Spillway with Flat and Pooled Steps." *Hydraulic Model Report No. CH86/12*, School of Civil Engineering, The University of Queensland, Brisbane, Australia, 80 pages (ISBN 9781742720531).	AUD$60.00		
FELDER, S., and CHANSON, H. (2012). "Air-Water Flow Measurements in Instationary Free-Surface Flows: a Triple Decomposition Technique." *Hydraulic Model Report No. CH85/12*, School of Civil Engineering, The University of Queensland, Brisbane, Australia, 142 pages (ISBN 9781742720494).	AUD$60.00		
REICHSTETTER, M., and CHANSON, H. (2011). "Physical and Numerical Modelling of Negative Surges in Open Channels." *Hydraulic Model Report No. CH84/11*, School of Civil Engineering, The University of Queensland, Brisbane, Australia, 82 pages (ISBN 9781742720388).	AUD$60.00		
BROWN, R., CHANSON, H., McINTOSH, D., and MADHANI, J. (2011). "Turbulent Velocity and Suspended Sediment Concentration Measurements in an Urban Environment of the Brisbane River Flood Plain at Gardens Point on 12-13 January 2011." *Hydraulic Model Report No. CH83/11*, School of Civil Engineering, The University of Queensland, Brisbane, Australia, 120 pages (ISBN 9781742720272).	AUD$60.00		
CHANSON, H. "The 2010-2011 Floods in Queensland (Australia): Photographic Observations, Comments and Personal Experience." *Hydraulic Model Report No. CH82/11*, School of Civil Engineering, The University of Queensland, Brisbane, Australia, 127 pages (ISBN 9781742720234).	AUD$60.00		
MOUAZE, D., CHANSON, H., and SIMON, B. (2010). "Field Measurements in the Tidal Bore of the Sélune River in the Bay of Mont Saint Michel (September 2010)." *Hydraulic Model Report No. CH81/10*, School of Civil Engineering, The University of Queensland, Brisbane, Australia, 72 pages (ISBN 9781742720210).	AUD$60.00		

JANSSEN, R., and CHANSON, H. (2010). "Hydraulic Structures: Useful Water Harvesting Systems or Relics." *Proceedings of the Third International Junior Researcher and Engineer Workshop on Hydraulic Structures (IJREWHS'10)*, 2-3 May 2010, Edinburgh, Scotland, R. JANSSEN and H. CHANSON (Eds), Hydraulic Model Report CH80/10, School of Civil Engineering, The University of Queensland, Brisbane, Australia, 211 pages (ISBN 9781742720159).	AUD$60.00		
CHANSON, H., LUBIN, P., SIMON, B., and REUNGOAT, D. (2010). "Turbulence and Sediment Processes in the Tidal Bore of the Garonne River: First Observations." *Hydraulic Model Report No. CH79/10*, School of Civil Engineering, The University of Queensland, Brisbane, Australia, 97 pages (ISBN 9781742720104).	AUD$60.00		
CHACHEREAU, Y., and CHANSON, H., (2010). "Free-Surface Turbulent Fluctuations and Air-Water Flow Measurements in Hydraulics Jumps with Small Inflow Froude Numbers." *Hydraulic Model Report No. CH78/10*, School of Civil Engineering, The University of Queensland, Brisbane, Australia, 133 pages (ISBN 9781742720036).	AUD$60.00		
CHANSON, H., BROWN, R., and TREVETHAN, M. (2010). " Turbulence Measurements in a Small Subtropical Estuary under King Tide Conditions." *Hydraulic Model Report No. CH77/10*, School of Civil Engineering, The University of Queensland, Brisbane, Australia, 82 pages (ISBN 9781864999969).	AUD$60.00		
DOCHERTY, N.J., and CHANSON, H. (2010). "Characterisation of Unsteady Turbulence in Breaking Tidal Bores including the Effects of Bed Roughness." *Hydraulic Model Report No. CH76/10*, School of Civil Engineering, The University of Queensland, Brisbane, Australia, 112 pages (ISBN 9781864999884).	AUD$60.00		
CHANSON, H. (2009). "Advective Diffusion of Air Bubbles in Hydraulic Jumps with Large Froude Numbers: an Experimental Study." *Hydraulic Model Report No. CH75/09*, School of Civil Engineering, The University of Queensland, Brisbane, Australia, 89 pages & 3 videos (ISBN 9781864999730).	AUD$60.00		
CHANSON, H. (2009). "An Experimental Study of Tidal Bore Propagation: the Impact of Bridge Piers and Channel Constriction." *Hydraulic Model Report No. CH74/09*, School of Civil Engineering, The University of Queensland, Brisbane, Australia, 110 pages and 5 movies (ISBN 9781864999600).	AUD$60.00		
CHANSON, H. (2008). "Jean-Baptiste Charles Joseph BÉLANGER (1790-1874), the Backwater Equation and the Bélanger Equation." *Hydraulic Model Report No. CH69/08*, Div. of Civil Engineering, The University of Queensland, Brisbane, Australia, 40 pages (ISBN 9781864999211).	AUD$60.00		
GOURLAY, M.R., and HACKER, J. (2008). "Reef-Top Currents in Vicinity of Heron Island Boat Harbour, Great Barrier Reef, Australia: 2. Specific Influences of Tides Meteorological Events and Waves." *Hydraulic Model Report No. CH73/08*, Div. of Civil Engineering, The University of Queensland, Brisbane, Australia, 331 pages (ISBN 9781864999365).	AUD$60.00		
GOURLAY, M.R., and HACKER, J. (2008). "Reef Top Currents in Vicinity of Heron Island Boat Harbour Great Barrier Reef, Australia: 1. Overall influence of Tides, Winds, and Waves." *Hydraulic Model Report CH72/08*, Div. of Civil Engineering, The University of Queensland, Brisbane, Australia, 201 pages (ISBN 9781864999358).	AUD$60.00		
LARRARTE, F., and CHANSON, H. (2008). "Experiences and Challenges in Sewers: Measurements and Hydrodynamics." *Proceedings of the International Meeting on Measurements and Hydraulics of Sewers*, Summer School GEMCEA/LCPC, 19-21 Aug. 2008, Bouguenais, Hydraulic Model Report No. CH70/08, Div. of Civil Engineering, The University of Queensland, Brisbane, Australia (ISBN 9781864999280).	AUD$60.00		

CHANSON, H. (2008). "Photographic Observations of Tidal Bores (Mascarets) in France." *Hydraulic Model Report No. CH71/08*, Div. of Civil Engineering, The University of Queensland, Brisbane, Australia, 104 pages, 1 movie and 2 audio files (ISBN 9781864999303).	AUD$60.00		
CHANSON, H. (2008). "Turbulence in Positive Surges and Tidal Bores. Effects of Bed Roughness and Adverse Bed Slopes." *Hydraulic Model Report No. CH68/08*, Div. of Civil Engineering, The University of Queensland, Brisbane, Australia, 121 pages & 5 movie files (ISBN 9781864999198)	AUD$70.00		
FURUYAMA, S., and CHANSON, H. (2008). "A Numerical Study of Open Channel Flow Hydrodynamics and Turbulence of the Tidal Bore and Dam-Break Flows." *Report No. CH66/08*, Div. of Civil Engineering, The University of Queensland, Brisbane, Australia, May, 88 pages (ISBN 9781864999068).	AUD$60.00		
GUARD, P., MACPHERSON, K., and MOHOUPT, J. (2008). "A Field Investigation into the Groundwater Dynamics of Raine Island." *Report No. CH67/08*, Div. of Civil Engineering, The University of Queensland, Brisbane, Australia, February, 21 pages (ISBN 9781864999075).	AUD$40.00		
FELDER, S., and CHANSON, H. (2008). "Turbulence and Turbulent Length and Time Scales in Skimming Flows on a Stepped Spillway. Dynamic Similarity, Physical Modelling and Scale Effects." *Report No. CH64/07*, Div. of Civil Engineering, The University of Queensland, Brisbane, Australia, March, 217 pages (ISBN 9781864998870).	AUD$60.00		
TREVETHAN, M., CHANSON, H., and BROWN, R.J. (2007). "Turbulence and Turbulent Flux Events in a Small Subtropical Estuary." Report No. CH65/07, Div. of Civil Engineering, The University of Queensland, Brisbane, Australia, November, 67 pages (ISBN 9781864998993)	AUD$60.00		
MURZYN, F., and CHANSON, H. (2007). "Free Surface, Bubbly flow and Turbulence Measurements in Hydraulic Jumps." *Report CH63/07*, Div. of Civil Engineering, The University of Queensland, Brisbane, Australia, August, 116 pages (ISBN 9781864998917).	AUD$60.00		
KUCUKALI, S., and CHANSON, H. (2007). "Turbulence in Hydraulic Jumps: Experimental Measurements." *Report No. CH62/07*, Div. of Civil Engineering, The University of Queensland, Brisbane, Australia, July, 96 pages (ISBN 9781864998825).	AUD$60.00		
CHANSON, H., TAKEUCHI, M, and TREVETHAN, M. (2006). "Using Turbidity and Acoustic Backscatter Intensity as Surrogate Measures of Suspended Sediment Concentration. Application to a Sub-Tropical Estuary (Eprapah Creek)." *Report No. CH60/06*, Div. of Civil Engineering, The University of Queensland, Brisbane, Australia, July, 142 pages (ISBN 1864998628).	AUD$60.00		
CAROSI, G., and CHANSON, H. (2006). "Air-Water Time and Length Scales in Skimming Flows on a Stepped Spillway. Application to the Spray Characterisation." *Report No. CH59/06*, Div. of Civil Engineering, The University of Queensland, Brisbane, Australia, July (ISBN 1864998601).	AUD$60.00		
TREVETHAN, M., CHANSON, H., and BROWN, R. (2006). "Two Series of Detailed Turbulence Measurements in a Small Sub-Tropical Estuarine System." *Report No. CH58/06*, Div. of Civil Engineering, The University of Queensland, Brisbane, Australia, Mar. (ISBN 1864998520).	AUD$60.00		
KOCH, C., and CHANSON, H. (2005). "An Experimental Study of Tidal Bores and Positive Surges: Hydrodynamics and Turbulence of the Bore Front." *Report No. CH56/05*, Dept. of Civil Engineering, The University of Queensland, Brisbane, Australia, July (ISBN 1864998245).	AUD$60.00		
CHANSON, H. (2005). "Applications of the Saint-Venant Equations and Method of Characteristics to the Dam Break Wave Problem." *Report No. CH55/05*, Dept. of Civil Engineering, The University of Queensland, Brisbane, Australia, May (ISBN 1864997966).	AUD$60.00		

CHANSON, H., COUSSOT, P., JARNY, S., and TOQUER, L. (2004). "A Study of Dam Break Wave of Thixotropic Fluid: Bentonite Surges down an Inclined plane." *Report No. CH54/04*, Dept. of Civil Engineering, The University of Queensland, Brisbane, Australia, June, 90 pages (ISBN 1864997710).	AUD$60.00		
CHANSON, H. (2003). "A Hydraulic, Environmental and Ecological Assessment of a Sub-tropical Stream in Eastern Australia: Eprapah Creek, Victoria Point QLD on 4 April 2003." *Report No. CH52/03*, Dept. of Civil Engineering, The University of Queensland, Brisbane, Australia, June, 189 pages (ISBN 1864997044).	AUD$90.00		
CHANSON, H. (2003). "Sudden Flood Release down a Stepped Cascade. Unsteady Air-Water Flow Measurements. Applications to Wave Run-up, Flash Flood and Dam Break Wave." *Report CH51/03*, Dept of Civil Eng., Univ. of Queensland, Brisbane, Australia, 142 pages (ISBN 1864996552).	AUD$60.00		
CHANSON, H,. (2002). "An Experimental Study of Roman Dropshaft Operation : Hydraulics, Two-Phase Flow, Acoustics." *Report CH50/02*, Dept of Civil Eng., Univ. of Queensland, Brisbane, Australia, 99 pages (ISBN 1864996544).	AUD$60.00		
CHANSON, H., and BRATTBERG, T. (1997). "Experimental Investigations of Air Bubble Entrainment in Developing Shear Layers." *Report CH48/97*, Dept. of Civil Engineering, University of Queensland, Australia, Oct., 309 pages (ISBN 0 86776 748 0).	AUD$90.00		
CHANSON, H. (1996). "Some Hydraulic Aspects during Overflow above Inflatable Flexible Membrane Dam." *Report CH47/96*, Dept. of Civil Engineering, University of Queensland, Australia, May, 60 pages (ISBN 0 86776 644 1).	AUD$60.00		
CHANSON, H. (1995). "Flow Characteristics of Undular Hydraulic Jumps. Comparison with Near-Critical Flows." *Report CH45/95*, Dept. of Civil Engineering, University of Queensland, Australia, June, 202 pages (ISBN 0 86776 612 3).	AUD$60.00		
CHANSON, H. (1995). "Air Bubble Entrainment in Free-surface Turbulent Flows. Experimental Investigations." *Report CH46/95*, Dept. of Civil Engineering, University of Queensland, Australia, June, 368 pages (ISBN 0 86776 611 5).	AUD$80.00		
CHANSON, H. (1994). "Hydraulic Design of Stepped Channels and Spillways." *Report CH43/94*, Dept. of Civil Engineering, University of Queensland, Australia, Feb., 169 pages (ISBN 0 86776 560 7).	AUD$60.00		
POSTAGE & HANDLING (per report)	AUD$10.00		
GRAND TOTAL			

OTHER HYDRAULIC RESEARCH REPORTS

Reports/Theses	Unit price	Quantity	Total price
TREVETHAN, M. (2008). "A Fundamental Study of Turbulence and Turbulent Mixing in a Small Subtropical Estuary." Ph.D. thesis, Div. of Civil Engineering, The University of Queensland, 342 pages.	AUD$100.00		
GONZALEZ, C.A. (2005). "An Experimental Study of Free-Surface Aeration on Embankment Stepped Chutes." *Ph.D. thesis*, Dept of Civil Engineering, The University of Queensland, Brisbane, Australia, 240 pages.	AUD$80.00		

TOOMBES, L. (2002). "Experimental Study of Air-Water Flow Properties on Low-Gradient Stepped Cascades." *Ph.D. thesis*, Dept of Civil Engineering, The University of Queensland, Brisbane, Australia.	AUD$100.00		
CHANSON, H. (1988). "A Study of Air Entrainment and Aeration Devices on a Spillway Model." *Ph.D. thesis*, University of Canterbury, New Zealand.	AUD$60.00		
POSTAGE & HANDLING (per report)	AUD$10.00		
GRAND TOTAL			

CIVIL ENGINEERING RESEARCH REPORT CE

The Civil Engineering Research Report CE series is published by the School of Civil Engineering at the University of Queensland. Orders of any of the Civil Engineering Research Report CE should be addressed to the School Secretary.

School Secretary, School of Civil Engineering, The University of Queensland
Brisbane 4072, Australia
Tel.: (61 7) 3365 3619 Fax : (61 7) 3365 4599
Url: http://www.eng.uq.edu.au/civil/ Email: hodciveng@uq.edu.au

Recent Research Report CE	Unit price	Quantity	Total price
CALLAGHAN, D.P., NIELSEN, P., and CARTWRIGHT, N. (2006). "Data and Analysis Report: Manihiki and Rakahanga, Northern Cook Islands - For February and October/November 2004 Research Trips." *Research Report CE161*, Division of Civil Engineering, The University of Queensland (ISBN No. 1864998318).	AUD$10.00		
GONZALEZ, C.A., TAKAHASHI, M., and CHANSON, H. (2005). "Effects of Step Roughness in Skimming Flows: an Experimental Study." *Research Report No. CE160*, Dept. of Civil Engineering, The University of Queensland, Brisbane, Australia, July (ISBN 1864998105).	AUD$10.00		
CHANSON, H., and TOOMBES, L. (2001). "Experimental Investigations of Air Entrainment in Transition and Skimming Flows down a Stepped Chute. Application to Embankment Overflow Stepped Spillways." *Research Report No. CE158*, Dept. of Civil Engineering, The University of Queensland, Brisbane, Australia, July, 74 pages (ISBN 1 864995297).	AUD$10.00		
HANDLING (per order)	AUD$10.00		
GRAND TOTAL			

Note: Prices include postages and processing.

PAYMENT INFORMATION

1- VISA Card

Name on the card :	
Visa card number :	
Expiry date :	
Amount :	AUD$ .....

2- Cheque/remittance payable to: THE UNIVERSITY OF QUEENSLAND and crossed "Not Negotiable".

N.B. For overseas buyers, cheque payable in Australian Dollars drawn on an office in Australia of a bank operating in Australia, payable to: THE UNIVERSITY OF QUEENSLAND and crossed "Not Negotiable".

Orders of any Research Report should be addressed to the School Secretary.

School Secretary, School of Civil Engineering, The University of Queensland
Brisbane 4072, Australia - Tel.: (61 7) 3365 3619 - Fax : (61 7) 3365 4599
Url: http://www.eng.uq.edu.au/civil/ Email: hodciveng@uq.edu.au